Cyprus
University of
Technology

Faculty of Engineering
and Technology

Doctoral Dissertation

**Toward nearly Zero Energy Buildings through Electrical
Storage and Mathematical Optimization**

Giorgos S. Georgiou

Limassol, November 2020

CYPRUS UNIVERSITY OF TECHNOLOGY

FACULTY OF ENGINEERING AND TECHNOLOGY

DEPARTMENT OF ELECTRICAL ENGINEERING AND COMPUTER
ENGINEERING AND INFORMATICS

Doctoral Dissertation

Toward nearly Zero Energy Buildings through Electrical Storage and Mathematical Optimization

Giorgos S. Georgiou

Limassol, November 2020

Approval Form

Doctoral Dissertation

Toward nearly Zero Energy Buildings through Electrical Storage and Mathematical Optimization

Presented by

Giorgos S. Georgiou

Supervisor: Department of Electrical Engineering, Computer Engineering and Informatics, Paul Christodoulides, Assistant Professor

Signature _____

Chair of the committee: Department of Electrical Engineering, Computer Engineering and Informatics, Christakis Damianou, Professor

Signature _____

Member of the committee: Department of Mechanical Engineering and Materials Science and Engineering, Soteris A. Kalogirou, Professor (co-supervisor)

Signature _____

Member of the committee: Department of Electrical and Computer Engineering, University of Cyprus, George E. Georghiou, Professor

Signature _____

Cyprus University of Technology

Limassol, November 2020

Copyrights

ABSTRACT

With the nearly Zero Energy Buildings (nZEBs) EU Directive (2010/31/EU) currently in force, all new buildings shall simultaneously reduce their primary energy consumption (energy from utility grids) and increase their energy share from Renewable Energy Sources (RES). Based on the fact that nZEBs are commonly addressed during their design and construction phase, this Thesis proposes a novel mathematical optimization approach, which attempts to maintain a low import and export energy profile (i.e., net grid electrical energy), daily, in an adaptive manner, and hence, allowing the building to further reduce its primary energy consumption throughout the year. For this purpose, a Linear Programming (LP) model is developed for allowing the battery's optimum daily dispatch. The LP model is assisted by tools such as Artificial Neural Networks (ANN) for forecasting the next day's hourly load consumption and Photovoltaic (PV) generation, and Genetic Algorithm (GA) for optimally driving LP and maintaining the building's daily net grid electrical energy as close to zero as possible (i.e., nearly zero). Moreover, for addressing the non-linear and complex nature of the battery the proven freeware System Advisor Model (SAM) of National Renewable Energy Laboratory (NREL) is integrated with the proposed approach. Using real data of PV generation and load consumption of a building, in Cyprus, the obtained results show that the daily hourly profile of the import and export energies is smoothed and flattened; thus, achieving, a nearly zero grid energy of the building. The results suggest that this method is superior than a conventional rule-based battery dispatch and can lead to the reduction of the annual aggregated grid usage by 53% and to the increase of the building's RES share by 60%, when compared to a no storage scenario. Finally, the proposed approach further decreases the primary energy consumption of the building, when compared to the no storage scenario and a battery dispatch approach driven by a conventional rule-based algorithm. Based on these findings, the proposed paradigm provides a tool contributing to the enhancement of the daily building's energy consumption; thus, supporting the nZEB philosophy, in addition to the design measures taken for nZEBs so far.

TABLE OF CONTENTS

LIST OF TABLES

LIST OF FIGURES

LIST OF ABBREVIATIONS

AI   Artificial Intelligence

ANN   Artificial Neural Network

BEM   Building Energy Management

BESS   Battery Energy Storage System

CP   Convex Programming

DP   Dynamic Programming

DSM   Demand Side Management

FPGA   Field Programmable Gate Array

GA   Genetic Algorithm

GHI   Global Horizontal Irradiation

LP   Linear Programming

MCA   Minimum Cut Algorithm

MILP   Mixed-Integer Linear Optimization or Programming

MINLP   Mixed-Integer Non-Linear Optimization or Programming

MPC   Model Predictive Control

nRMSE   Normalized Root Mean Squared Error

NPV   Net Present Value

nZEBs   nearly Zero Energy Buildings

NREL   National Renewable Energy Laboratory

PMV   Predicted Mean Vote

PoA   Plane of Array

PSO   Particle Swarm Optimization

PV   Photovoltaic

QP   Quadratic Programming

REG   Renewable Energy Generation

RES   Renewable Energy Sources

SAM   System Advisor Model

1 Introduction

Buildings are responsible for the 20% and 40% of the total energy consumption across the globe and the EU, respectively. The EU Proposal 2016/0381 (COD) [1], states that approximately 75% of existing buildings are energy inefficient and approximately only 1% of those buildings undergo a renovation for upgrading their energy efficiency. Consequently, the 2010/31/EU Directive introduced nearly Zero Energy Buildings (nZEBs) as buildings of high energy efficiency with very low primary energy needs and, simultaneously, covering their low energy needs with integrated (or nearby) Renewable Energy Sources (RES) as much as possible. The Directive requires now (2020 onwards) that each new building shall comply and be a nZEB.
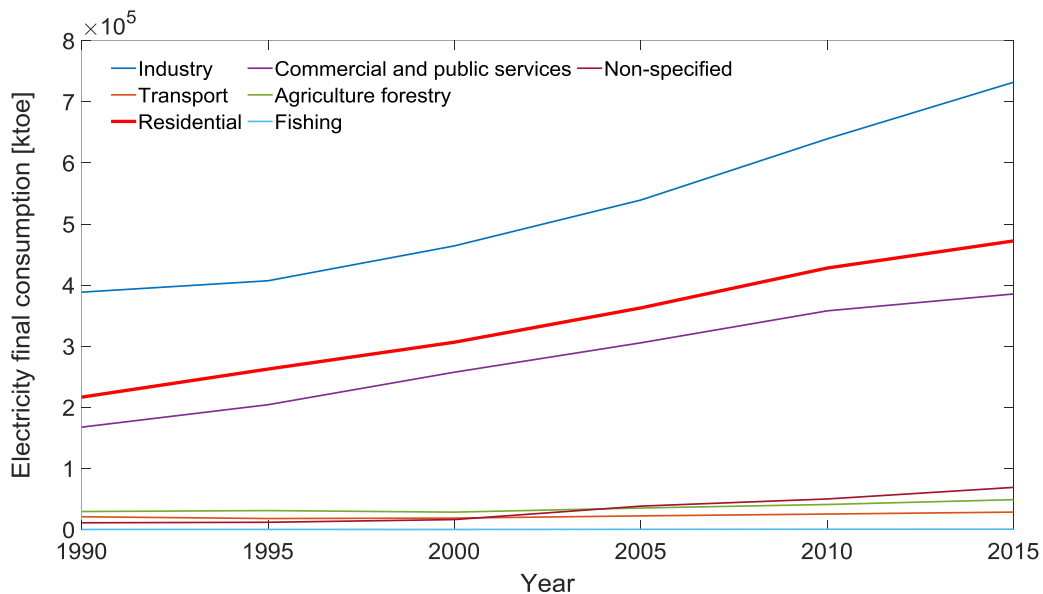
Figure 1: Global Electricity final consumption by sector [2]

Further to the high energy consumption levels in buildings, Figure 1 highlights the high share and the trend increase of electricity final energy consumption in the residential sector, within the global energy system. With such an increasing trend of electricity share in a building's total energy mix (e.g. transition from natural gas heating systems to heat pumps) and the non-neglected total energy consumption of buildings, it is therefore vital to concentrate on the buildings' electrical energy management further to common passive energy efficiency measures, such as thermal insulation, building orientation, PV

system sizing and so on. Such passive approaches are widely adopted and used, but can only be applied and utilized for designing and constructing nZEBs only. It is known that in general, while a building is in operation, its energy consumption levels are strongly related to human behaviour and RES stochasticity and, hence, significant deviations between the measured and pre-estimated energy consumption levels may be present. Therefore, energy efficiency measures utilized during the construction of a building may not be adequate for supporting the nZEB concept while the building is in operation.

Based on the above fact, for supporting an nZEB while in operation and be in line with the relevant EU Directive, the energy exchange between the building itself and the utility grid should be minimized, on a daily basis, and be as close to zero as possible. With this way, it is possible to maintain its annual primary energy consumption to low energy levels, as required by the aforementioned Directive. For instance, a nZEB daily energy profile, from an electrical point of view, should minimize both the import and export energies and cover its needs by the energy generated from the integrated RES, during the whole day. Such a phenomenon, for the sake of this Thesis, will be called as the daily nearly zeroing of the net-grid electrical energy.

For achieving the daily nearly zeroing of a building's net-grid electrical energy, Building Energy Management (BEM), which can be achieved utilizing storage and Renewable Energy Sources (RES), is essential. In this context, mathematical optimization (mostly Convex Optimization) is a proven method and is utilized for achieving lower energy targets. Convex Optimization is considered an ideal method for BEM schemes as it gives global solutions, compared to other techniques such as Heuristic Optimization.

Within this context and as it will be shown in the next Chapter, literature shows that the majority of existing methods focus on themes such as minimizing the daily operational and energy costs, (peak) loads, user discomfort levels, annual CO_2 emissions and user economic benefits. Although such studies contribute toward lower energy use from utility grids, they are beyond the nZEB philosophy as clearly identified above. Moreover, as Lu et al. [3] mentions, there is a lack of methods for designing and controlling nZEBs during their operation, due to the complexity and stochasticity of both Renewable Energy Generation (REG) and energy consumption, as well as difficulties concerning energy storage. This phenomenon was also verified and reported by Ipsos and Navigant [4], who mentioned the low adoption of nZEBs in the EU.

Therefore, one may conclude that there is still a need for a method, that is in line with the nZEB Directive and literally integrating a criterion related to the nearly zeroing of the building's net-grid energy, within the optimization problem.

In summary: (i) Buildings are associated with high energy consumption levels; (ii) electricity consumption continually increases its share of the final energy consumption in buildings; (iii) nZEBs are becoming more attractive in EU and are mainly addressed at the design and construction phase; (iv) according to the author's best knowledge, all studies utilizing mathematical optimization and storage in buildings mainly focus on themes not in line with the nZEB EU Directive, as mentioned above. Consequently, this Thesis proposes a novel method, which utilizes the energy coming from the building integrated PV and – based on a nearly zero net-grid energy criterion accommodated within the optimization problem – the battery's daily operation is optimally decided, in order to achieve a low annual primary energy consumption throughout the year. Hence, the proposed method contributes to the conservation of an nZEB's low energy consumption, while in operation.

Such a target is achieved through Convex Optimization combined with adopted tools such as Artificial Neural Networks (ANN), Genetic Algorithm (GA) and a realistic dispatch software known as System Advisor Model (SAM) developed from National Renewable Energy Laboratory (NREL). According to the author's best knowledge, the proposed approach and its consequent contribution was not attempted before in the literature.

More specifically, the dispatch problem is modelled as a Linear Programming (LP) problem – a Convex (global) Optimization method – and through the utilization of ANN, GA and SAM the battery is optimally dispatched throughout the day. Thus, the daily net-grid energy profile of the building is smoothed, flattened and remains close to the desired zero net-grid energy, according to the studied scenario. As a result, the import and export energies, throughout the day are minimized, giving an even lower annual primary energy consumption, compared to the no storage scenario and a conventional rule-based battery dispatch technique. The applied approach proves to be appropriate for the further enhancement of the nZEB concept for buildings also not necessarily built within the rules of the EU Directive for nZEBs nor having a high energy certificate.

The methodology regarding the chosen approach is as follows. Since the daily nearly zeroing of the building's electrical energy requires global optimization and input parameters need to be known *a priori*, the proposed methodology utilizes ANNs, which provide the hourly forecast for both the PV generation and load consumption of the next day. Based on the forecasts and the daily nearly zero net-grid energy criterion used, GA searches for the optimum parameters (objective function weights) of LP. The LP then, based on the parameters provided by the GA, runs the dispatch problem and decides, in an adaptive manner, the optimum battery charge and discharge energies, throughout the day. Finally, the battery dispatch resulting from LP is then imported in SAM, which accounts for the non-linear and complex battery behaviour and contributes to giving the final and realistic energy dispatch – another novel feature of the proposed methodology – with the outcome of the dispatch containing the optimum battery charge/discharge energies, import/export energies and battery storage level, throughout the day. Finally, the uncertainties in both PV generation and load consumption are handled with the model continually recalculating the battery dispatch at every time-step (hour) of the optimization horizon (day), based on the current measurements of PV and load. As a result, the energy balance between PV, load, battery and grid is maintained and the battery operates within its physical limits. It should be noted here that the novelty of this Research is not designated by each individual model presented hereafter, but by the proposed holistic integration of the developed LP model and the three tools (ANN, GA and SAM) utilized.

In the sequel of this Thesis, Chapter 2 presents a literature review in fields relevant to the problem under investigation, that is BEM through storage and Convex Optimization. Hence, the existing gap in literature is identified from the different studies reviewed showing the absence of such an approach. For further reading regarding nZEBs, Convex Optimization and ANNs, relevant background material can be found in Appendix I.

Following the literature review, Chapter 3 presents the proposed approach and methodology beginning with a brief overview of the holistic integrated model, which is then followed by an explanation of the general methodology used in MATLAB for developing LP problems along with the presentation of the complete LP model developed here in matrix form and implemented in MATLAB. Following the mathematical presentation and explanation of the proposed LP model, intermediate results of a base study, when the proposed LP model is applied, are shown, for

demonstrating the LP behaviour and enabling the reader to have a better understanding of the model. The needs for adoption and utilization of a heuristic optimization approach (GA) as well as a forecasting tool (ANN) are then presented, and finally the holistic integration of the LP, GA, ANN and SAM and how the complete model behaves are demonstrated.

In Chapter 4, using real data of PV generation and load consumption from a building in Cyprus, the approach is tested and cross-validated showing the achievement of the daily nearly zeroing of the building's net-grid energy and its reduced primary energy consumption (from an electrical point of view). Moreover, a potential application of the proposed method is described.

The main conclusions drawn by this study as well as the potential future work are finally outlined in Chapters 5 and 6, respectively.

2   Literature Review for Building Energy Management [1]

As mentioned in the Introduction, the achievement of the nearly zeroing of a building's daily net-grid energy requires energy management and thus global optimization. To this end, the sequel of this Chapter focuses on the field of managing (dispatching) the energy profile in a building through Convex Optimization. The different studies reviewed are grouped according to the Convex Optimization used such as LP, Mixed Integer (Non) Linear Programming (MI(N)LP) and Quadradic Programming (QP). The approach of each study is presented and summarized with their aim/contribution categorized and discussed in the end. Finally, this review aims to present the state-of-art in BEM and identify the existing gap in literature regarding methods that can be applied in a building's daily operation and further contribute to the decrease of the primary energy consumption, as required by the nZEB EU directive.

2.1   Building Energy Management using Convex Optimization

Energy optimization in buildings, using convex optimization, attracted the academic interest, in recent years, mainly due to the high consumption levels in buildings. Many researchers found that convex optimization regarding the energy costs minimization can be superior than common rule-based and heuristic optimization techniques.

In general, the dispatch problem, which is simply the conservation of the energy balance between load and different energy sources such as grid, RES and storage, is modelled as an optimization problem. The optimization problem is composed by an objective function (aka cost function) and different constraints that represent the physical nature of the problem under investigation. For instance, the objective function may represent the minimization of the daily electricity buying cost, while the energy balance as well as battery limitations constitute the problem's constraints. The problem in this case might be linearly (LP, MILP) or non-linearly (MINLP, QP) modelled – depending on the problem's nature – and is solved with main target either to minimize or maximize the objective function.

The configuration presented in Figure 2 represents an electrical system consisting of RES, storage, grid and load. For a dispatch problem the equivalent optimization

---

[1] Material from published paper [82]

problem here is to optimally dispatch the different energy sources (e.g. PV and battery) and/or loads (e.g. electrical appliances, HVACs and so on) for minimizing the objective function at the point of common coupling. In the sequel of this Chapter, the different studies reviewed are grouped based on the optimization method utilized, with the main features and contribution of the studies being highlighted.
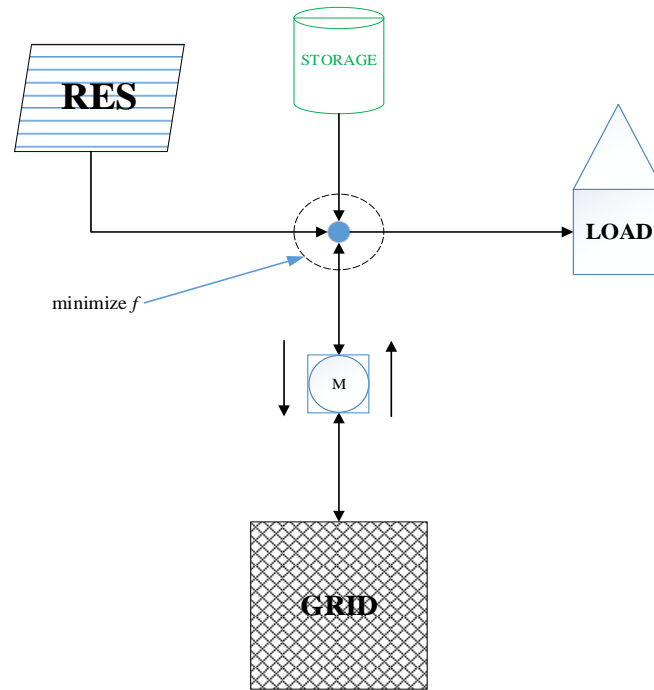
Figure 2: Equivalent optimization network diagram

Linear Programming

Figueiredo and Martins [5] demonstrated a method for optimizing the production of the RES, based on the generation costs of different sources such as PV, Biomass, Wind and Oil. The optimization is achieved through an LP formulation and targets the minimization of the operational cost. Moreover, Demand Side Management (DSM), Building Automation System and Energy Production System Management interact with each other, so as to enable the control of the load and the management of the RES production. Storage and on-site renewables are also considered into the optimization problem. Nottrott et al. [6] presented an LP routine for reducing the net-peak load with the aid of a grid-connected PV and a battery system, in an optimized manner. Forecasted data of both the load profile and the PV output, on a 24-hour basis and a 15-

minute interval, are taken as inputs to the main algorithm, which decides the optimum scheduling of the battery during the peak periods. Hanna et al. [7] further improved the model presented in [6], so as to address the uncertainties of forecasting in both solar radiation and load demand of the building, using LP. The output dispatch scheme was updated based on the pre-calculated net error forecast between the forecasted and measured PV output and load demand. This allowed the model to be more practical and applicable in real life situations, with an improved performance avoiding also conservative dispatch schemes. Chen et al. [8] developed an LP model for scheduling the battery and appliance operation in a building. The problem is modelled using deterministic LP and load, and PV uncertainties are modelled through a pre-selected adaptation variable. PV and battery operational and maintenance costs are integrated within the objective function for optimally coordinating the electrical appliances. By considering the renewable generation and storage, the financial expenses of the building are reduced, based on a time-varying electricity pricing scheme. Youn and Cho [9] used LP for scheduling the battery, based on gaussian and binomial distributions of load and on-site generation, respectively. The main aim of the study was to maximize storage revenues and hence, user benefits, based on electricity buying and generation operational costs. Georgiou et al. [10] made a first attempt to use a hybrid optimization approach using LP in combination with GA for optimally dispatching a battery in a building having PV installed. The objective function integrated the import and export energies, the battery charging and discharging energies and the storage level, which are normalized, weighted and summed. The main aim of the study was to find the optimum values of the LP weights through GA, based on the daily PV and consumption data and hence, minimize the grid import and export energies.

Further to the studies reviewed above, which is a selection aiming at explaining the basic applications of mathematical optimization within the BEM, Table 1 presents more studies found in the literature, concerning the LP scheme. The table – as well as Tables 2 and 3 for MILP and QP, respectively – show the different parameters considered in the optimization, such as appliance scheduling (load dispatch), grid usage, energy storage dispatch, on-site generation utilization, energy prices consideration and prediction, with the latter shown only in case the study presented a model for forecasting generation and/or load consumption.

Table 1: Studies related to LP energy management in buildings

Ref	Yr*	LD*	Grid	ES*	OSG*	EP*	PR*	Approach
[11]	2016		✔	✔	✔	✔	✔	Schedule the operation of a plug-in hybrid electric vehicle (PHEV) battery when connected as well as a diesel generator, using LP and GA. GA is used for determining which energy source will operate at what time interval of the day. LP decides the amount of power to be delivered to the load from each energy source. Forecasted PV and load are provided by ANN and uncertainties are addressed through Model Predictive Control (MPC). The objective function accounts for the operational cost of the diesel generator, PEV battery and electricity purchase from the grid.
[12]	2015		✔	✔		✔		Schedule the battery operation with LP and Markov Decision Process (MDP). The problem is initially modelled as LP and then it is reformed as a MDP problem to account for the load uncertainties. A constraint related to keep the load under the peak demand is integrated within the problem
[13]	2015		✔	✔	✔	✔		Schedule the battery operation with LP, based on the given PV generation and load demand. Load and PV uncertainties are addressed with the use of MPC. The objective function accounts for the grid purchase price and the battery wearing cost
[14]	2014		✔	✔	✔	✔		Schedule the battery of a PEV. The objective function considers the grid purchase and selling price as well as a subsidy for self-consuming the renewable energy. The limits of the charging/discharging rates are based on the travelling times and parking times of the PEV.
[15]	2010	✔	✔			✔	✔	Schedule the appliances with LP, based on price prediction. A weighted average price prediction filter is applied for providing the electricity price forecast. The objective function accounts for the grid purchase price and the associated cost of waiting of the appliances until they operate.
[16]	2017		✔	✔	✔	✔		Schedule the battery operation with LP, based on the daily energy cost. The optimization function also includes the battery operating cost.
[17]	2008	✔						Control the illuminance level output of luminaires of the room with LP, subject to user satisfaction. The occupants' preferences are assumed to be known in the model.

* Year (Yr), Load Dispatch (LP), Energy Storage(ES), On Site Generation (OSG), Energy Prices (ES), Prediction (PR)

Table 2: Studies related to daily MILP energy optimization in buildings

Ref.	Yr	LD	Grid	ES	OSG	EP	PR	Approach
[18]	2013	✓	✓	✓	✓	✓		Schedule the operation of appliances, storage on site generation with MILP. The objective function considers operational, maintenance, electricity purchasing costs as well as revenues from selling energy to grid. Peak demand charges are also integrated within the objective function.
[19]	2013	✓	✓	✓	✓	✓		Schedule appliance operation, storage charging/discharging and onsite generation with MILP. The objective function consists of the power consumption, renewable generation, power export, storage charge/discharge rates and thermal energy flows. Electricity buy/sell prices and storage maintenance costs are included in the objective function
[20]	2017		✓	✓	✓	✓		Schedule battery charging/discharging with MILP. The optimization function consists of the associated costs and revenues resulted from power imported from and exported to the grid, respectively and takes into account priorities related to the PV, battery discharge and EV discharge powers exported to the grid. The priorities are set manually using priority parameters for each power source. Uncertainty of the PV is characterized by the probability of a PV scenario to occur and is embedded in the objective function.
[21]	2016	✓	✓	✓		✓		Using MILP for scheduling electrical appliances scheduled taking into account electricity tariff and CO_2 footprint, which are integrated within the normalized objective function via weighted sums. The weight value could be chosen by the end-users, depending on their preferences. Uncertainty parameters, pre-estimated by empirical load models of the users were embedded in the objective function for handling user consumption variations.
[22]	2016	✓		✓	✓			Optimally schedule different load appliances, in a priority fashion, and the battery with MILP. Loads are prioritized based on user's needs.
[23]	2015	✓	✓	✓	✓	✓		Dispatch loads, battery, grid and on-site generation (diesel) with MILP. Two optimization problems with 1-hour and 5-mins intervals were sequentially solved. The dispatch from the first optimization problem is used by the second one, which is updated at every time-step, in a receding manner, and gives the final dispatch, based on the updated state of the system and the ahead schedule pre-calculated. operational costs, associated with the diesel generators and the battery were also included in the objective functions
[24]	2015	✓	✓	✓	✓	✓		Schedule the operation of battery and loads with MILP. Two objective functions are used; one for accounting for the total operational cost (electricity, gas, PV, wind-turbine) and the other for the user discomfort. The two objective functions are weighted and lumped in a single one. The weights' values are chosen a priori, from the end-users.
[25]	2015	✓	✓	✓	✓	✓		Schedule the operation of a plug-in-electric vehicle (PEV) battery, a combined heat and power (CHP) unit and loads with MILP. Electricity and gas energy tariffs are considered in the objective function.
[26]	2014	✓	✓	✓	✓	✓	✓	Schedule the operation of a battery, electrical and thermal loads as well as the operation of a CHP unit with MILP. The objective function considers the power supplied by the grid and the power provided by the CHP. Electricity and gas tariffs are also accounted in the objective function. Uncertainty in the load and PV generation are based on probabilities, which are embedded in the objective function. The forecasts for electrical and thermal loads as well as solar generation are provided by an ARMA model. A multi-stage

Ref.	Yr	LD	Grid	ES	OSG	EP	PR	Approach
								scenario-tree generation method is used for providing the load and generation uncertainties. The models are updated in a rolling schedule manner and steps forward one time-step once the updated information arrives.
[27]	2015	✓	✓	✓	✓	✓		Schedule the operation of battery and loads with MILP. The different objective functions associated with user discomfort, energy cost (electricity and gas), electricity consumption, carbon emissions and peak electricity power are normalized, weighted and lumped in a single objective function. Weights are assumed to be constant. Monte Carlo simulations are utilized for providing the uncertainties of different parameters (temperature, load RES generation, water usage and non-controllable loads), which are then provided to the optimization model and handled via MPC.
[28]	2015	✓	✓	✓	✓	✓		Schedule the battery of a PEV and load with MILP. The objective function considers the electricity cost, the electricity benefit from selling energy to the grid and the user discomfort.
[29]	2015	✓	✓	✓	✓	✓	✓	
[30]	2015	✓	✓			✓		A two stage MILP optimization is used. At the first stage the optimum hours of an appliance to be scheduled is determined. Based on the appliance scheduled predefined, the running of the appliances in the second stage is achieved through random behaviour models of the energy consumption generated by Monte Carlo Simulation.
[31]	2014	✓	✓		✓	✓		Schedule the operation of different power loads with MILP, based on given electricity prices, generation and load ahead profiles. The objective function integrates the benefits gained from each service appliance, electricity cost and a penalty cost related to peak power consumption and deviation from the optimum appliance operation
[32]	2014	✓	✓		✓	✓		Schedule the operation of the appliances based on PV generation, through MILP. The objective function accounts for electricity cost associated with the energy consumed by the dispatched appliances and the benefit gained from the utilization of the generated power from the PVs.
[33]	2012	✓	✓			✓		A multi-layer structure is used for providing the real-time appliance control with MILP, interfacing the system with grid information such as different electricity price schemes, informing the system for upcoming potential energy savings based on future electricity prices and energy consumption and optimally dispatching the different appliances over the optimization horizon. The objective function utilizes the electricity cost based on each appliance operation as well as start-up cost when an appliance starts operating. Recalculation of the dispatch is caused once a variation in energy consumption, grid prices and so on.
[34]	2012	✓	✓	✓		✓		Scenario-based stochastic and robust optimizations are used and compared for optimally dispatching the different appliances and the battery of a PEV, using MILP. In stochastic optimization, Monte-Carlo simulation is utilized for generating scenarios regarding potential future electricity prices. The objective function in the stochastic optimization accounts for the measured power of each appliance and electricity cost of the first time-step and the future scenarios for power consumption and electricity prices. In robust optimization, the objective function accounts for the measured power of each appliance and electricity cost of the first time-step and the future best case and worst-case scenarios (minimum and maximum values) in future electricity prices. Hence, Monte-Carlo simulation is not needed. A rolling window, stepping forward in time, is used in both approaches, which is updated with the current status of price and demand at every time-step and provides the optimum dispatch.

Ref.	Yr	LD	Grid	ES	OSG	EP	PR	Approach
[35]	2012		✓	✓	✓	✓		A battery and a CHP unit are dispatched with MILP, based on pre-defined energy prices (electricity and gas), PV generation and load demand.
[36]	2009	✓	✓	✓	✓	✓		Schedule the battery and different loads with MILP. The objective function included electricity buying/selling cost and an associated penalty cost related to the error of the forecasted and actual PV generation. Such difference is embedded as an absolute term within the objective function and linearization is achieved by substituting the absolute term with a constrained slack positive variable
[37]	2017	✓	✓	✓	✓	✓		Schedule different power loads and battery with MILP, based on perfect predictions for both PV generation and load demand. Different non-linear load models are linearized using state-space equations. The objective function considers only the maximum and minimum values, throughout the optimization horizon, of the net grid power (daily total import - export powers) and of the ratio between the purchasing and selling electricity prices (buy-back ratio), respectively.
[38]	2017	✓	✓			✓		Schedule the operation of different power loads with MILP, while preserving the user thermal comfort (predicted mean vote index - PMV) constraint within the desired levels. State-space modelling is utilized for the energy balance equation and different uncertainties in parameters such as indoor/outdoor temperatures, load consumption and so on are handled by an event triggered mechanism, which decides the recalculation of the whole dispatch in case an event occurs. The objective function accounts for the energy consumption of different loads and electricity cost. Recalculation of the dispatch occurs in a moving horizon manner
[39]	2016	✓						Adjust the temperature set-points and thus power demanded from HVAC systems with MILP. The maximum power demand of the HVACs for each time-step is provided to the model and the objective function accounts only for the time-step corresponding to the maximum HVAC power (peak hour), throughout the optimization horizon. Temperature limits set by the users are also embedded in the model.
[40]	2016		✓	✓	✓	✓		Dispatch the battery and a fuel cell operation with MILP, for covering electrical and thermal loads. Two objective functions are used. The one accounts for the annual electricity and gas costs as well as benefits from selling the surplus electrical energy to the grid. The other objective function accounts for the total annual CO_2 emissions resulted from the energy consumed from electrical and gas grids. The two optimization functions integrate a monthly fixed base rate, energy tariffs, the grid power demanded for covering the loads, the grid power demanded for charging the battery, the power output of the fuel cell for covering thermal loads and the heat recovered and generated for supplying thermal loads
[41]	2017		✓	✓	✓	✓		Schedule the charge/discharge of a battery and of a PEV battery with MILP. The objective function considers the grid import power, the power outputs of PV and micro-wind turbine, the discharging rates of the PEVs and the battery and the power exported to the grid. Operation and maintenance costs of the PV and micro-wind turbine systems, maintenance costs of the battery and PEVs as well as purchasing and selling electricity prices are also embedded in the objective function. Different scenarios regarding variations of the solar irradiance, consumption and number of EVs present are tested.
[42]	2016	✓	✓	✓	✓	✓		Dispatch the charge/discharge of a battery, the on/off operation of HVACs and the operation of a Distributed Generator (DG) with MILP. The objective function considers the operation costs of DG and battery and electricity purchasing costs. A battery constraint is developed for ensuring that there is enough battery SOC at the end of the day in order to compensate for any uncertainties in the

Ref.	Yr	LD	Grid	ES	OSG	EP	PR	Approach
								weather. The battery costs are related to the battery charging/discharging and cycling. MPC is utilized, in a rolling window scheme, for adapting the scheduled dispatch when variations occur.
[43]	2014		✓	✓	✓	✓		Schedule the charging/discharging of electrical and thermal storage systems as well as the operation of a Combined Cooling, Heating and Power (CCHP) generation unit with MILP. Two objective functions are used. The one considers the power imported from the grid, e fuel consumptions of the boiler and the CCHP, the discharging rate of the battery along with electricity time-of-use tariffs, natural gas prices and battery degradation cost related to discharge cycling. The second objective function considers the power imported from the grid and the fuel consumptions of both CCHP and boiler as well as the CO_2 emissions associated with electricity and fuel consumption. The two functions are lumped via a weighted sum approach.
[44]	2012	✓	✓	✓	✓	✓		Schedule the operation of HVAC, battery, internal combustion engine and CCHP with MILP. The objective function considers the import and export powers, the operation of the CCHP, the operation of the battery as well as investment costs of the battery, water tank and ice storage devices.
[45]	2011	✓	✓	✓	✓			Schedule the operation of different loads, distributed generators and a battery charging/discharging with MILP. The objective function takes into account the power generated from the distributed generators, the consumed power of the controllable loads, the power imported from the grid, the power exported to the grid, the charging and discharging rates of the batteries and the battery SOC. Uncertainties in the distributed generation and energy consumption are handled by a real-time controller, in a receding horizon fashion, which updates the dispatch. The objective function minimizes the cost by choosing the sum of the argmin values from the set of the dispatch decisions.
[46]	2009	✓	✓	✓	✓	✓		Schedule the operation of different loads and battery with a two-layer optimization, using MILP. The first layer is the one giving the initial dispatch, throughout the optimization horizon and its objective function accounts for electricity purchasing cost and earnings from the energy exported to the grid. In the second layer, the uncertainty in generation and demand is handled. A second objective function here is applied and triggered once a variation incident occurs and recalculates the dispatch for the remaining optimization horizon, with initial conditions obtained from the previous time step. A third and non-linear objective function is used in case no feasible solution is found to the second one, which allows the load to be shed, so as to match generation and demand. The absolute difference of the new dispatch and the initial dispatch is the main goal of this objective function. The non-linear term is linearized by introducing a slack variable constrained accordingly.
[47]	2011	✓	✓	✓	✓	✓		Two MILP optimization schemes are proposed, one for a single user and one for multi-users. Both schemes concentrate on optimally dispatching different loads and batteries. In the multi-user scheme the amount of energies purchased by and sold to the grid is aggregated in the objective function. Both optimization functions consider the energy bought and sold to the grid, while the amount of maximum energy that can be bought (i.e. peak demand) by the single or multi-user schemes is limited with the aid of an added constraint.
[48]	2016	✓	✓	✓	✓	✓		MILP, Piecewise MILP and epsilon Differential Evolution (eDE - metaheuristic) are individually used and compared for dispatching the operation of different power loads, generation units and storage. In the MILP and piecewise MILP schemes the non-linear loads and generation units characteristics are simply and piecewise linearized, respectively, where in eDE the full non-linear nature of the problem is utilized. The objective function aggregates the operational cost of the different loads and power

Ref.	Yr	LD	Grid	ES	OSG	EP	PR	Approach
								generation sources used. Energy prices for both electricity and gas are also integrated in the objective function. The three optimization methods are compared in terms of objective function value and time for convergence.
[49]	2012	✓	✓	✓	✓	✓		Schedule the operation of different loads and battery with MILP. The optimization horizon is divided in a number of adjacent intervals of equal length, where the non-controllable loads are considered. Those adjacent intervals are further divided in smaller intervals, in a similar manner, where the controllable loads are considered. The amount of power imported from the grid is also limited below a threshold with the aid of a constraint. The user comfort is also taken into account. Uncertainties are handled by generating different scenarios.

Table 3: Studies related to daily QP energy optimization in buildings

Ref.	Yr	LD	Grid	ES	OSG	EP	PR	Approach	Aim/Contribution
[50]	2015	✓	✓		✓	✓		Dispatch different loads with QP based on PV day ahead production. The objective function takes into account the total power demanded by each appliance and the power generated by the PV, as well as electricity time-of-use and feed-in tariffs. A robust technique is developed for tuning the degree of the schedule response, based on the uncertainty level of the PV generation. In other words, users can select how much the load scheduling responds to PV uncertainties, by tuning a single parameter. The uncertainty of the PV generation is described by the minimum and maximum generation levels. The forecasted PV generation is assumed to be known.	
[51]	2014	✓	✓	✓		✓		Dispatch a group of users' appliances and PEVs batteries with QP, based on game-theoretic energy purchase and sale. The objective function considers the electricity cost and benefit based on the amount of total power demanded from each appliance and the amount of total power sold to the grid by the PEVs, respectively. The decided dispatch – i.e., the energy imported for appliances and the energy sold to the grid from PEVs - is based on the Nash equilibrium, at which all users have benefit and in case any user decides to alter the proposed dispatch the cost will be higher and thus the benefit lower.	
[52]	2013			✓	✓			Dispatch the operation of a diesel generator and a battery with QP, based on load and PV generation. The objective function considers the quadratic cost function of the diesel generator.	

Ref.	Yr	LD	Grid	ES	OSG	EP	PR	Approach	Aim/Contribution
[53]	2017	✓	✓	✓	✓	✓	✓	Dispatch the operation of load, battery and PV with QP. The objective function takes into account the thermal discomfort, energy cost, carbon emissions associated with PV curtailment, user inconvenience based on appliance desired operation and battery degradation. The different objectives are aggregated in the objective function, via weighted sum and the weights are calculated based on a survey conducted related to multiple user preferences. Forecasting used only for load via a simple averaging method.	
[54]	2020		✓	✓	✓			Schedule the charging/discharging of PEV with QP. The optimization was set up and tested for individual and centralized PEV charging/discharging. The optimization horizon begins when PEVs arrive and when PEVs depart. Both quadradic optimization functions take into account, respectively, the individual (single-user) and centralized (multi-user) charging power of the PEV battery, the net load power (power demanded - solar power generated) and the mean net load during parking period. The arrival and departure EV profiles were based on a survey adopted and Monte-Carlo simulations were utilized for generating random demand profiles. Perfect forecasts for load and PV generation are considered	

Mixed Integer Linear Programming

Ha et al. [55] developed a MILP controlling different loads and storage using dynamic models for loads, user satisfaction, storage and power sources. Required forecasted data (solar radiation, energy consumption, etc.) were provided as inputs with all the non-linear dynamic models linearized. Objective functions for energy cost, user dissatisfaction, CO_2 rejection and autonomy are proposed and uncertainties in the different input data are also handled. Tsui and Chan [56] achieved a building load management by dispatching the operation of different appliances and storage, using MILP. A regularization method is proposed for transforming the binary decision variables to continuous real-valued variables, in order to maintain the convexity of the problem. Weight factors are used for each transformed decision variable, which are manually predefined, and electricity prices are also incorporated into the problem. The objective function takes into account electric cost and user discomfort resulting from the appliances' operation. A MILP approach was also proposed by Zong et al. [57] with two objective functions. The first one is activated in case the renewable generation is larger than the minimum renewable generation threshold, while the second one is activated when the renewable generation is lower than the minimum renewable threshold. The first objective function considers the associated electricity cost when the load consumes energy from local RES and from grid, while the second objective function considers the associated electricity cost when load consumes energy from the grid. Both objective functions aggregate electricity cost with the weighted absolute temperature difference between the actual indoor temperature and the desired indoor temperature (i.e., user comfort) and with the weight factor being manually selected. The objective functions are modelled using Model Predictive Control (MPC) for handling uncertainties. Ashouri et al. [58] developed a MILP model for selecting optimum design parameters of different electrical and thermal power generation sources, storage systems and loads and dispatching the different selected system components. The objective function accounts for the total investment cost, the running energy cost, the user discomfort in terms of building desired temperature and subsidies for each of the selected system component. The Net-Present Value (NPV) for the components' operation is used and the period of operation is extended up to 20 years. Constraints related to CO_2 emissions ($ton/m^2/yr$) and nZEB consumption ($kWh/m^2/yr$) are also used for maintaining the energy consumption and CO_2 emission levels below a desired threshold. Stadler et al. [59]

demonstrated a MILP dispatch problem for managing the operation of different loads and storage. The objective function aggregates, via a weighted sum approach, the normalized annual energy costs and CO_2 emissions. The weighting factor takes values from 0 to 1 and, depending on the desired scenario (minimization of cost or carbon emissions or a combination of both), this value is manually selected. A Zero Net Energy Building equality constraint is used for maintaining the annual sum of electricity imported, electricity exported and electricity generated on site, to zero. Sichilalu and Xia [60] presented an optimized battery dispatch scheme, using MILP, for scheduling the battery charge/discharge operation with the battery only allowed to charge from the grid, during time slots when electricity prices are cheap. The objective function considers the difference of electricity purchased from the grid and the electricity sold back to the grid with the two terms weighted. The weight values are manually selected, based on the desired scenario such as minimization of electricity purchase and/or maximization of electricity sale back to the grid. Meinrenken and Mehmani [61] proposed a MINLP scheme with two optimization schemes being concurrently solved. The one is used for obtaining the optimal battery capacity, based on historical weather and load data and the annual profit (difference of annual tariff charge reduction and the annual battery cost resulted from investment and financing). The other (real-time) one is used for adjusting the grid demand limits by scheduling the battery charging/discharging strategy. The day ahead battery operation is driven by the pre-generated day ahead load profiles and with the day-ahead load profiles generated from historical weather data. The uncertainties in load profiles are handled by using the Particle Swarm Optimization (PSO) method. Hassan et al. [62] developed a MILP method with the objective function considering the PV generation, PV power export and grid import power for covering the load by charging/discharging the battery. PV incentives for generating power and for exporting power to the grid as well as electricity tariffs are considered in the optimization problem. The objective function aggregates the costs and revenues, where costs are directly related with the grid imported power and benefits, which are related to the PV generation, PV export power and battery discharge power. The authors did not consider any uncertainties in either the load or the PV. Fratean and Dobra [63] proposed a MILP strategy for scheduling the battery charging/discharging. The objective function considers the powers supplied to the load from grid, PV and battery, the power supplied from PV to battery and the power

exported from PV to grid. Real-time prices, feed-in-tariffs, PV levelized cost of electricity as well as levelized cost of storage are also incorporated within the objective function. Wi et al. [64] presented a MILP method for scheduling the charging/discharging of an EV battery, based on the PV generation and electricity consumption profiles. An exponential smoothing model is used for pre-estimating the PV generation and electricity consumption. An adaptation model is used for adjusting the pre-estimated value. The objective function integrates the electrical energy profile and the energy prices. Agnetis et al. [65] developed a MILP approach for optimizing the appliance and battery operation, based on three objective functions representing the overall energy related rewards provided by the market aggregator, user preferred time slots for appliance operation and climatic comfort. The objective functions are lumped in a single one via weights. Weights are constant at all times and are manually preselected based on the desired operational mode. Wang et al. [66] proposed a MILP optimization scheme for scheduling the charging/discharging of an EV storage. The stochastic objective function consists of the day-ahead prices for buying/selling energy and the associated penalty costs related to the mismatch between the estimated and measured energy consumption. Further similar studies using MILP are shown in Table 2, in the same manner as Table 1.

Quadratic Programming

Ratnam et al. [67] proposed an approach for charging/discharging a battery with QP and Greedy search heuristic algorithm. The objective function accounts for the quadratic net power balance, which is defined as the difference between load, generation and battery. For maximizing customer benefits, the net power balance is multiplied by a weighting factor at each time-step. Each time-dependent weighting factor is optimally selected with the aid of a Greedy-search heuristic algorithm, based on time-of-use and feed-in tariffs and the amount of electricity purchased/sold from/to the grid. Dagdougui et al. [68] addressed the optimization of different RES (PVs, flat plate solar collectors, wind turbines and biomass) along with an electrical storage system, in a green building. The operation of a storage and on-site generation was driven by QP, for meeting electrical and thermal loads as well as domestic water needs. The objective function aggregates, through a weighted sum approach, the equivalent energy balances for meeting thermal, electrical and domestic water demands, the overall energy imported from grid and the battery storage level. MPC is mentioned for handling uncertainties, but its performance

or method of application is not demonstrated. Tazvinga et al. [69] proposed an optimum battery dispatch scheme for scheduling the operation of a battery and a diesel generator with QP to meet the load demand, based on the PV production. The optimization function aggregates, through a weighted sum approach, the power output of the diesel generator, the battery charging/discharging rate and the PV generation. Based on the battery operation and degradation characteristics, the wear cost is calculated. Fuel cost of the diesel generator and battery wear cost are also integrated in the objective function with the weights of the objective function being manually selected. Tazvinga et al. [70] further developed their initial model presented in [69] and added wind generation into their quadratic optimization problem. Nevertheless, neither study utilizes a forecasting tool. Similar to the previous optimization methods and in the same manner as Table 1, Table 3 shows other studies using QP for optimizing a building's energy consumption.

2.2 Convex Optimization versus other Energy Management methods

Convex optimization always guarantees global optimum solutions, if they exist. However, in many engineering optimization problems, especially in the building sector, complex and nonlinear dynamics are present, where not a single global optimum solution exists, and the problem is thus, non-convex. In that case, heuristic approaches are able to handle such problems. Examples of such heuristic approaches are GA, Simulated Annealing, Tabu Search Algorithms, PSO, Lyapunov Optimization Approach, Markov Decision Process, Imperialist Competitive Algorithm, Quantum behaved Particle Swarm Optimization, Ant Colony Optimization, Cuckoo Optimization Algorithm and others. Such methods may be used mainly for searching for a near optimum or approximate solution within the optimization space [12], [71]–[76].

On the other hand, conventional algorithms based on different scenarios may be used for BEM applications. Conventional algorithms (aka rule-based algorithms) rely on different possible scenarios, which, for instance, may represent: (i) The discharge of the storage system during the period where electricity price is high and the charge of the battery when electricity price is low; (ii) the charge of the battery when there is a surplus PV generation and the release of the stored energy when the load is greater than the PV generation [77].

Comparing the different optimization methods (convex and non-convex) together is difficult and can be done in a very general way, as each problem is modelled and defined differently. Therefore, neither the methods are application specific nor the problem can be solved with any available method. The selection of the right approach is strictly dependent on the initial problem definition. Yet, such an attempt is made in the sequel of this subsection by summarizing the different comparisons reported by some authors who tried to solve the same problem with different approaches. Nevertheless, this should not be taken as a rule-of-thumb, as each method has its own properties and effectiveness for each specific application. Nevertheless, in general, it is known that convex optimization, always guarantees global solutions and hence, if applicable, it is mostly preferred.

Chen et al. [8] reported a 41% expense reduction when deterministic LP – along with a stochastic appliance schedule – was applied, compared to a traditional rule-based scheduling scheme. Hanna et al. [7] also demonstrated that their LP model is superior

and has a better performance, compared to a traditional real-time on/off strategy of the battery for peak load reduction. The main reason was that the battery was utilized in a more optimized manner due to the forecasting of the demand and the forecasting error handling capability of the model. Nottrot et al. [6] compared the proposed LP routine with two traditional battery schedule algorithms. The two algorithms, named by the authors as OFFON and Real Time, were based on the same principle; to charge the battery during the off-peak hours and discharge it during the on-peak hours. The authors found that a 26% and a 45% cost reduction was possible, compared to the OFFON and Real Time strategies, respectively. Ha et al. [55] showed that the proposed advanced MILP management model compared to the Basic Management (e.g. turn the heater on when the temperature level is below the threshold) is superior, as it achieved ~22% reduction in the operational cost and ~65% reduction in CO_2. However, the dissatisfaction indices were slightly increased. Wi et el. [64] tested a MILP model for the optimal charging of EVs in a building and found that it can reduce operational costs by 6% when compared to the baseline scenario of charging the electric vehicles as soon as they park, and 15.2% compared to the baseline scenario of charging the available electric vehicles after lunchtime. Similar comparisons between CP and rule (or basic) based management techniques were also made in [23], [27], [28], [30], [37], [43], [53] indicating the superiority of mathematical optimization.

Paridari et al. [78] used MILP for optimizing the daily operation of smart appliances with storage, by both considering electricity bills and CO_2 reduction, in a building block. The authors also compared their proposed method with two other optimization methods known as Dynamic Programming (DP) and Minimum Cut Algorithm (MCA). They found that in terms of computational time, DP and MCA are better, where in terms of cost optimality MILP is more suitable. Zhou et al. [13] developed an LP model in combination with a MPC) an advanced control tool for handling variabilities/uncertainties of the input variables within an optimization problem, for optimally dispatching the battery of a building. The authors made comparisons of the net income earnings when MPC-LP (closed-loop control) and LP (open loop control) were applied and found that the MPC-LP model could increase the net income earnings by 31%, in the case when the actual demand is larger than the predicted one and by 27% in the case when the actual PV generation was larger than the predicted one. Pickering et al. [48] compared the case of reducing electrical and thermal energy needs, with the

aid of local PVs and electrical storage in a hotel, using three individual optimization approaches, namely single linear MILP, piecewise MILP (piecewise refers to a common method for linearizing non-linear functions) and epsilon Differential Evolution (a metaheuristic approach). They showed that for the case studied, piecewise MILP was the best option as it reduced the costs by 0.1% and 0.7% compared to the simple linear MILP and epsilon Differential Evolution, respectively. The times to find the optimum solution for simple linear MILP, piecewise MILP and epsilon Differential Evolution were 0.08s, 1.64s and 295s, respectively.

2.3 Discussion

As can be concluded from the previous sub-sections, three main algorithms are mostly used for globally optimizing the energy consumption of a building, with such methods being LP, MILP and QP. Other convex optimization methods exist in the literature (e.g. conic optimization, geometric optimization, or special cases of the ones addressed above), which are all more complex and more time-consuming to solve and are hence, very seldom used in building energy optimization problems. As this concept is not very mature, due to the ongoing research on BEM, the number of studies (n = 66) reviewed, to the author's understanding, constitutes a sufficiently large indicative sample.

It is clear from Tables 1−3 presented, that when there is a need for different loads (e.g. electrical appliances, HVAC) to be dispatched, MILP is preferred, due to the load's nature (on/off operation). Furthermore, RES along with electrical storage are found in nearly all studies, as this combination is promising and very effective for daily building energy optimization. Additionally, nearly all studies considered energy prices, which is found useful for shifting the renewable generation with the aid of storage from peak periods, where electricity prices may be higher, to non-peak periods. Nevertheless, driving the optimization problem with energy tariffs is highly sensitive to the applied energy policies and may not be efficient in potential policy amendments affecting energy tariffs.

In the context of daily BEM global optimization, the values of the uncontrolled variables must be known *a priori* and hence, some studies also use forecasting methods for predicting parameters such as weather, electricity prices, demand and RES ([11], [15], [26], [29], [53], [64]). Furthermore, stochasticity in such variables always exist and thus, the uncertainty of the forecasted parameters is also addressed in some studies,

even if a forecasting model was absent. Such uncertainties are commonly addressed by MPC optimization or by simply updating the predicted values with the measured ones and recalculating the dispatch in a receding horizon manner, or driving the dispatch problem using scenario-based approaches such as Monte Carlo simulation (e.g. [23], [42], [54]).

Another feature commonly found in global optimization schemes is the so-called weighted sum method – see also section I.2 in Appendix I. This approach integrates multiple objective functions in a single one and hence, allows multi-objective optimization with a low computational burden. For instance, in some studies the main aim/contribution was the simultaneous energy cost and consumer discomfort level minimization. For allowing a concurrent optimization of these objectives, the weighting sum approach may be utilized, which weighs each objective function accordingly and lumps them in one. Nevertheless, manual weight pre-selection is mostly preferred, since finding the optimum values of such weights requires advanced techniques (e.g. heuristic methods), as it was attempted by Ratnam et al. and Georgiou et al. [10], [67], [79].

Despite the use of weighted multi-objective optimization by the majority of the studies, each study – focusing in the sector of the daily BEM optimization – may be generalized and categorized based on their aim/contribution. The aim/contribution may be defined by the parameters included in the objective function proposed. For instance, an objective function integrating parameters for minimizing the daily energy cost and the daily operational cost may be included in two separate categories, such as (1) minimization of operational costs and (2) minimization of energy costs. In general, six different categories may be extracted from the presented literature, and are listed and summarized below.

- *Minimization of operational cost*: It includes the studies that integrate in the objective function operational costs of the different on-site generation sources. Therefore, fuel costs, levelized cost of electricity for RES and/or storage and battery wearing costs may be included. The dispatch of the different power generation sources is decided based on the lowest operational cost of the day

- *Minimization of energy cost*: It includes the studies that integrate in the objective function energy prices related to the energy purchase and sale from and to the grid. A variety of electricity tariffs may be present (e.g. dynamic prices, flat-rate

prices and so on), according to the policy applied. The dispatch (usually battery and/or load) is decided based on the lowest energy costs (billing costs) of the day

- *Maximization of economic benefits*: It includes studies that integrate in the objective function economic benefits gained from the RES self-consumed energy and any revenues gained from feed-in-tariffs or other incentives. The energy dispatch (usually battery) is decided based on the maximum economic benefit of the day

- *Minimization of load*: It includes studies that integrate in the objective function the power demanded from different loads or from the building itself. The dispatch (usually load and/or battery) is decided in order to minimize the daily peak load

- *Minimization of CO_2 emissions:* It includes studies that integrate in the objective function the associated CO_2 emissions. The dispatch of the day (usually non-RES power generation sources, battery and/or load) is driven by the amount of CO_2 emitted by non-RES (e.g. gas, diesel generators and so on)

- *Minimization of user discomfort:* It includes studies that integrate the level of user discomfort into their objective function. The dispatch (usually thermal load dispatch such as HVAC operation) is based on the requirement for maintaining the user discomfort (e.g. Predicted Mean Vote Index, indoor temperature and so on) to minimum levels
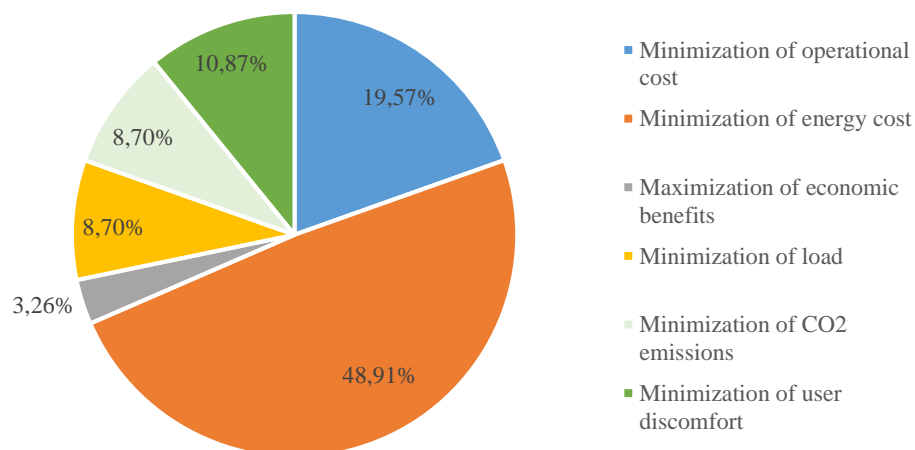
Figure 3: Aim/Contribution share of studies focusing on the daily BEM optimization

Figure 3 shows the percentage share among the six different categories mentioned above. It is clearly shown here that the majority of studies contribute in minimizing the daily energy cost of the building followed by the category related to the daily minimization of the operational costs, as both categories result to lower economic costs. Finally, minimization of user discomfort, CO_2 emissions, load and economic benefits are also beneficial for BEM daily optimization; though they are not very commonly found.

As it was shown, convex optimization is widely used in BEM optimization scenarios, as it guarantees global (best) solutions, regarding the reduced energy consumption of the building, while in operation. Moreover, different studies – presented in section I.1 of Appendix I – propose different nZEB design methods for lowering the primary energy consumption of a building and thus, are in line with the nZEB Directive. Recall that the EU nZEB Directive requires buildings to consume low (nearly zero) primary energy (i.e., grid energy) and utilize integrated RES as much as possible. Nevertheless, such studies lack in supporting the nZEB requirements on a daily basis, since the building consumes energy from the grids, while there is no REG and uncertainties in RES generation and load consumption in the long run exist.

On the other hand, as it was shown, studies related to the optimum daily BEM focus in themes outside the nZEB philosophy. Although some studies attempted to minimize CO_2 emissions and introduced nZEB constraints, they also integrate operational costs, energy costs and/or user dissatisfaction in the objective function, which are price sensitive and are clearly beyond the main requirement of the EU nZEB Directive. Hence, there is a lack of a method in supporting the conservation and possible further reduction of the building's low primary energy levels, on a daily basis, and be in line with the Directive.

Following the nZEB official definition, a method considering, on a daily basis, a nearly zero net-grid energy criterion and hence, maintaining a low primary energy consumption of the building throughout the year – despite the uncertainties of the RES and consumption profiles – is yet to be proposed. Within this context, the rest of the Chapters present, explain and demonstrate a novel holistic method that contributes toward a daily smooth and flat net grid energy of the building, which is closer to the

zero-energy requirement (i.e. nearly zero) and achieves a lower primary energy consumption of the building throughout the year.

3   Proposed Approach and Methodology

As mentioned in the Introduction, the proposed approach in this Thesis utilizes (i) LP for dispatching a battery in a daily global optimum manner, (ii) ANNs, which are necessary for providing the load consumption and PV generation forecast *a priori,* so as to achieve global optimality, (iii) GA, necessary for automatically determining the LP's weighting factors, based on the forecasted consumption and generation, so that the daily net-grid energy of the building is flattened, smoothed and brought closer to the desired zero level, and (iv) SAM for calculating a more realistic battery dispatch, based on that obtained from LP.
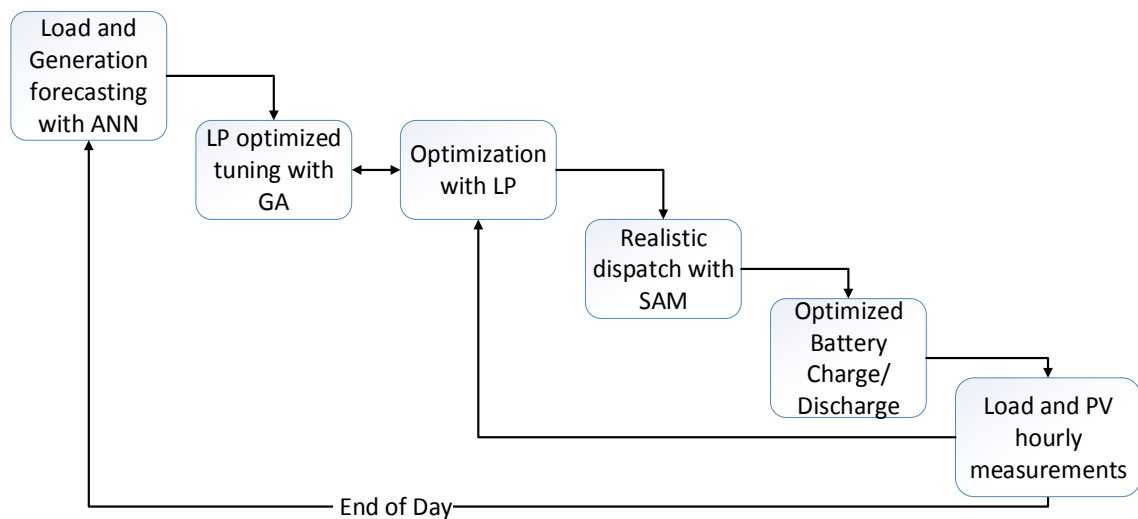
Figure 4: Proposed approach

The integrated approach is illustrated in Figure 4, where it is shown how the battery dispatch is calculated from the beginning and up to the end of the optimization horizon. In summary, at the beginning of each day the ANNs provide the forecast for load consumption and PV generation, which are taken as inputs by the LP algorithm. Once the ANNs provide the forecasts, the GA algorithm repeatedly runs LP until the optimum weight factors are found, based on the forecasted data, and as soon as the optimum weights are found, LP decides for the optimum battery dispatch of the whole day, based on the precalculated weights. The ideal battery dispatch from LP is then imported in SAM, as it is necessary to calculate the final battery dispatch, driven by the optimum LP

dispatch. Once the load consumption and PV measurements are available at every time-step, the battery dispatch is repeatedly updated for every time-step up to the last time-step of the optimization horizon (i.e., end of the day). Hence, daily global optimization is possible, since LP repeatedly considers historical, current and future values of PV and load. Finally, the algorithm returns to its initial point at the end of each optimization horizon.

The following sub-sections will present in detail each part of the algorithm – i.e., the mathematical model of LP, the mathematical model of GA and the ANN models, with some intermediate results, for demonstrating the individual behaviour and performance of LP, GA and ANN.

3.1   Linear Programming Model[2]

This sub-section presents the general formulation of a LP in MATLAB and the proposed LP model along with its outcomes when applied to a building case study. It is worth mentioning that, for simplicity, in this sub-section the predictions for PV and load are considered perfect. Nevertheless, the adaptiveness and ability of the proposed model to handle PV and load uncertainties is demonstrated later in section 3.4 through its holistic integration with a forecasting tool (ANN), a heuristic optimization method (GA) and a realistic dispatch software (SAM).

3.1.1   Linear Programming in MATLAB

This study uses MATLAB for solving the linear optimization problem through a LP algorithm. MATLAB requires the optimization functions, equality/inequality constraints and boundaries of the problem to be written in matrix form as shown below [80]. For further information regarding mathematical and convex optimization the reader may refer to section I.1 in Appendix I.

$$\text{Minimize } \mathbf{C}^{\text{T}}\mathbf{x} \text{ subject to } \begin{cases} \text{A}\mathbf{x} \leq \mathbf{b}, \\ \text{A}_{\text{eq}}\mathbf{x} = \mathbf{b_{eq}} \\ \mathbf{lb} \leq \mathbf{x} \leq \mathbf{ub} \end{cases} \tag{1}$$

where:

---

[2] Material from published paper [144]

44

- **C** is the real-valued the optimization function coefficients vector

- A and A_{eq} are the inequality and equality constraints coefficients matrices

- **b, beq, lb, ub** are the inequality and equality constraints constant vectors and the lower bound and the upper bound vectors, respectively

- **x** is the real-valued vector of optimization variables

Algorithms such as Dantzig's simplex method and interior point method may be used for solving LP problems of the form of equation (1). LP may be found in many applications, especially in engineering and is mostly preferred due to the existence of mature and efficient algorithms for solving such problems [81], [82].

3.1.2 Mathematical formulation of the LP model

The following non-linear optimization model was initially developed, integrating three optimization functions in a single objective function, using a weighted sum approach.

$$\text{Minimize } f(E_{\text{grid}}, E_{\text{bat}}, E_s) = \sum_{t=1}^{24} \left\{ w_1 \left| E_{\text{grid}}^*(t) \right| + w_2 \left| E_{\text{bat}}^*(t) \right| + w_3 E_s^*(t) \right\} \qquad (2)$$

subject to

$$E_{\text{grid}}(t) - E_{\text{bat}}(t) = E_{\text{load}}(t) - E_{\text{PV}}(t) \qquad (3)$$

$$-E_{\text{bat}}(t) + E_s(t) = E_s(t-1), \quad E_s(0) = \text{constant} \qquad (4)$$

$$E_{\text{grid}}(t) \leq E_{\text{load}}(t) \qquad (5)$$

$$E_{\text{bat}}(t) \leq E_{\text{load}}(t) \qquad (6)$$

$$-E_{\text{bat,max}} \leq E_{\text{bat}}(t) \leq E_{\text{bat,max}} \qquad (7)$$

$$E_{\text{s,min}} \leq E_s(t) \leq E_{\text{s,max}} \qquad (8)$$

where:

- f is the objective function to be minimized

- t is the time interval [h]

- w_1, w_2 and w_3 are weights for each optimization term, with $w_1 + w_2 + w_3 = 1$ and $w_1, w_2, w_3 \geq 0$

- E_{grid} is the electrical energy imported/exported from/to the grid – negative for exporting and positive for importing [kWh]

- E_{bat} is the energy supplied or received by the battery – negative for supplying energy and positive for receiving energy [kWh]

- E_s is the energy stored in the battery [kWh]

- E_{PV} is the electrical energy supplied by the PVs [kWh]

- E_{load} is the load consumption [kWh]

- $E_{bat,max}$ is the maximum energy that can be received by the battery [kWh] (meaning that $-E_{bat,max}$ is the maximum energy that can be supplied by the battery)

- $E_{s,min}$ and $E_{s,max}$ are the minimum and maximum allowable energy to be stored in the battery, respectively [kWh].

Note that the associated power of each energy source as well as the load can be calculated by dividing the energy with the time interval (step), which in this case is equal to 1.

The star symbol means that the optimization variable within *f* is "normalized" (i.e., non-dimensionalized). Normalization is achieved by dividing the optimization variable with the difference of its upper and lower bounds, as it will be shown later. The use of the "normalized" weighted sum method through w_1, w_2 and w_3, allows for the determination of each variable (function – i.e., E_{grid}, E_{bat} and E_s) importance within the objective function, depending on the scales and the nature of problem. Lumping these three variables together allows the management of both the building's import and export energies and the battery usage, simultaneously. In addition, according to the definition of LP shown by equation (1), the objective function ($\mathbf{C}^T\mathbf{x}$) is composed by the decision variables ($\mathbf{x}$) defined within the problem. Hence, the decision variables E_{grid}, E_{bat} and E_s are added within the objective function and are lumped using appropriate weights, due to the difference in their scale. Further to the mathematical definition of LP, lumping these variables within a single objective function allows for the individual control, via the weight values, of grid and battery.

Moreover, both E_{grid} and E_{bat} may be assigned with negative values when energy is exported and battery discharges, respectively. The negative values within the objective

function drive the algorithm toward a solution with the largest negative value possible. In practice, this means that the export energy (negative E_{grid}) as well as battery discharging (negative E_{bat}) would become as large as possible, which is not desired in a low energy building such as nZEB. To overcome this, the absolute terms in equation (2) were introduced. Consequently, it is of great importance to have the daily net grid energy as close to zero as possible, which is achieved by assigning the appropriate weight values.

Equation (**3**) refers to the energy balance between the different energy sources (PVs, battery and grid) and the load. It can be clearly seen by this equation that the difference between the PV generation and the load demand (i.e., a mismatch) is handled by the difference of import/export grid energy and the battery charging/discharging energy, depending on the combination decided by the LP model. The available dispatches through this equation are: i) when the PV generation is larger than (or equal to) the load consumption there is an option to charge the battery and/or export energy to the grid and ii) when the PV generation is lower than (or equal to) the load demand there is an option to discharge the battery and/or import energy from the grid. Whichever combination is decided by the LP, clearly depends on the PV and load profiles and weight values giving the minimum objective function.

The dispatch cases mentioned are subjected to the constraints given by equations (**3**)–(**8**). The minus sign appearing is necessary for distinguishing between the charging and discharging states of the battery. Equation (**4**) keeps a "record" of the energy left within the battery during interval t, based on the previous interval $t - 1$. It should be noted here that for the very first day of the optimization period the battery may have an initial storage, which may come directly from the manufacturer. Equation (**5**) ensures that the battery is never charged from the grid. A relaxation to the optimization problem may be allowed by removing this constraint; yet, ignoring such a constraint it is possible to induce peak loads (from the grid's perspective), battery degradation due to increased usage, voltage drop and frequency unbalance to the grid as the battery draws power from the grid. Constraint (**6**) ensures that the battery never exports energy to the grid. Similar to constraint (**5**), the optimization problem may be relaxed by eliminating this constraint. Nevertheless, ignoring this constraint may cause voltage rise and frequency unbalance to the network. Finally, the battery limits are presented by boundaries (**7**) and (**8**).

The model governed by equations (2)–(**8**) is not linear. This inconvenience can be overcome by transforming the model into an equivalent linear model – which can be easily and effectively solved – through expressing variables $E_{\text{grid}}(t)$ and $E_{\text{bat}}(t)$ as the difference of two slack non-negative variables [81], [83] (see section I.2, in Appendix I). Specifically, letting $E_{\text{grid}}(t) = E_{\text{grid,im}}(t) - E_{\text{grid,ex}}(t)$ and $E_{\text{bat}}(t) = E_{\text{bat,ch}}(t) - E_{\text{bat,dis}}(t)$, which represent the energies imported/exported (not occurring simultaneously) from/to the grid and the energy received/supplied (not occurring simultaneously) by/from the battery, respectively, yields the following equivalent linear problem, where all variables are positive and given in their opposite form as negative (see constraints (**12**)–(**15**) below).

$$\text{Minimize} f\left(E_{\text{grid,im}}, E_{\text{grid,ex}}, E_{\text{bat,ch}}, E_{\text{bat,dis}}, E_s\right)$$

$$= \sum_{t=1}^{24} \left\{ w_1 \left[E^*_{\text{grid,im}}(t) + E^*_{\text{grid,ex}}(t) \right] + w_2 \left[E^*_{\text{bat,ch}}(t) + E^*_{\text{bat,dis}}(t) \right] + w_3 E^*_s(t) \right\} \tag{9}$$

subject to:

$$E_{\text{grid,im}}(t) - E_{\text{grid,ex}}(t) - E_{\text{bat,ch}}(t) + E_{\text{bat,dis}}(t) = E_{\text{load}}(t) - E_{\text{PV}}(t) \tag{10}$$

$$-E_{\text{bat,ch}}(t) + E_{\text{bat,dis}}(t) + E_s(t) - E_s(t-1) = 0, \quad E_s(0) = \text{constant.} \tag{11}$$

$$-E_{\text{grid,im}}(t) \leq 0 \tag{12}$$

$$-E_{\text{grid,ex}}(t) \leq 0 \tag{13}$$

$$-E_{\text{bat,ch}}(t) \leq 0 \tag{14}$$

$$-E_{\text{bat,dis}}(t) \leq 0 \tag{15}$$

$$-E_{\text{bat,ch}}(t) + E_{\text{bat,dis}}(t) \leq E_{\text{load}}(t) \tag{16}$$

$$E_{\text{grid,im}}(t) - E_{\text{grid,ex}}(t) \leq E_{\text{load}}(t) \tag{17}$$

$$-E_{\text{bat,ch}}(t) + E_{\text{bat,dis}}(t) \leq E_{\text{bat,max}} \tag{18}$$

$$E_{\text{bat,ch}}(t) - E_{\text{bat,dis}}(t) \leq E_{\text{bat,max}} \tag{19}$$

$$E_{\text{s,min}} \leq E_s(t) \leq E_{\text{s,max}} \tag{20}$$

Note that the boundary condition (**7**) is replaced by inequality constraints (**18**) and (**19**) and that the conditions $\{E_{\text{grid,im}}(t) > 0 \cap E_{\text{grid,ex}}(t) = 0\} \cup \{E_{\text{grid,im}}(t) = 0 \cap E_{\text{grid,ex}}(t) > 0\}$ and $\{E_{\text{bat,ch}}(t) > 0 \cap E_{\text{bat,dis}}(t) = 0\} \cup \{E_{\text{bat,ch}}(t) = 0 \cap E_{\text{bat,dis}}(t) > 0\}$ are always true at

optimality. This means that, neither $E_{grid,im}$ nor $E_{grid,ex}$ can occur simultaneously, at any time-step. This condition also holds for $E_{bat,ch}$ and $E_{bat,dis}$, and may be clarified through the following reduced problem, which is of similar type to the one above.

$$\text{Minimize } f(E_{grid,im}, E_{grid,ex}) = w\left(E_{grid,im}^* + E_{grid,ex}^*\right) \tag{21}$$

subject to:

$$E_{grid,im} \geq 0 \tag{22}$$

$$E_{grid,ex} \geq 0 \tag{23}$$

$$w > 0 \tag{24}$$

If for some reason (due to other possible constraints) the optimum value of f is greater than 0, then obviously next optimum value of f is either $wE_{grid,im}^*$ or $wE_{grid,ex}^*$, showing that at optimality the condition $E_{grid,im} \times E_{grid,ex} = 0$ is always met, which is equivalent to the condition $\{E_{grid,im}(t) > 0 \cap E_{grid,ex}(t) = 0\} \cup \{E_{grid,im}(t) = 0 \cap E_{grid,ex}(t) > 0\}$; a condition that is also valid with variables $E_{bat,ch}(t)$ and $E_{bat,dis}(t)$. This key property allows the non-linear problem to be linearized without affecting optimization.

Equations (**9**)–(**20**) may now represent a linear (convex) optimization problem, which can be used for minimizing the net grid energy of a building having PVs and a battery system installed. Finally, due to linearity, equation (**9**) can be further relaxed to

$$\text{Minimize } f(E_{grid,im}, E_{grid,ex}, E_{bat,ch}, E_{bat,dis}, E_s)$$

$$= \sum_{t=1}^{24} \left\{ \begin{array}{c} w_{im}E_{grid,im}^*(t) + w_{ex}E_{grid,ex}^*(t) \\ + w_{bat,ch}E_{bat,ch}^*(t) \\ + w_{bat,dis}E_{bat,dis}^*(t) + w_s E_s^*(t) \end{array} \right\} \tag{25}$$

where:

- w_{im}, w_{ex}, $w_{bat,ch}$, $w_{bat,dis}$ and w_s, are the weights associated with import energy, export energy, battery charging, battery discharging and energy stored, respectively

As mentioned earlier, each decision variable within the objective function is of different scale and the normalization of the three different objective functions is necessary. Normalization here is achieved using the following mathematical formulation.

$$E_{\text{grid,im}}^* = E_{\text{grid,im}} / \left(E_{\text{load,max}} - E_{\text{load,min}} \right) \tag{26}$$

$$E_{\text{grid,ex}}^* = E_{\text{grid,ex}} / \left(E_{\text{PV,max}} - E_{\text{PV,min}} \right) \tag{27}$$

$$E_{\text{bat,ch}}^* = E_{\text{bat,ch}} / \left(E_{\text{bat,ch,max}} - E_{\text{bat,ch,min}} \right) \tag{28}$$

$$E_{\text{bat,dis}}^* = E_{\text{bat,dis}} / \left(E_{\text{bat,dis,max}} - E_{\text{bat,dis,min}} \right) \tag{29}$$

$$E_s^* = E_s / \left(E_{\text{s,max}} - E_{\text{s,min}} \right) \tag{30}$$

where:

- $E_{\text{load,max}}$ and $E_{\text{load,min}}$ are the maximum and minimum allowable demand, respectively, with $E_{\text{load,min}} = 0$ kWh

- $E_{\text{PV,max}}$ and $E_{\text{PV,min}}$ are the maximum and minimum PV generation, respectively, with $E_{\text{PV}}^{\min} = 0$ kWh

- $E_{\text{bat,ch,max}}$ and $E_{\text{bat,ch,min}}$ are the maximum and minimum energies that can be received by the battery, during charging, respectively, with $E_{\text{bat,ch,max}} = E_{\text{bat,max}}$ and $E_{\text{bat,ch,min}} = 0$ kWh

- $E_{\text{bat,dis,max}}$ and $E_{\text{bat,dis,min}}$ are the maximum and minimum energies that can be supplied by the battery, during discharging, respectively, with $E_{\text{bat,dis,max}} = E_{\text{bat,max}}$ and $E_{\text{bat,dis,min}} = 0$ kWh

With the proposed approach, each desired weight w may be assigned accordingly with a value from 0 to 1, in order to select which variables are of greatest importance and thus need to be minimized. For instance, in nZEBs, where the minimization of the net grid energy is of high priority, $w_{\text{im}} E_{\text{grid,im}}^*(t) + w_{\text{ex}} E_{\text{grid,ex}}^*(t)$ must be greater than $w_{\text{bat,ch}} E_{\text{bat,ch}}^*(t) + w_{\text{bat,dis}} E_{\text{bat,dis}}^*(t) + w_s E_s^*(t)$ and so on.

3.1.3 MATLAB formulation of the Proposed LP model

Based on equation (1), equations (**10**)–(**20**) and (**25**) should be written in matrix form so as the LP model can be developed in MATLAB. The mathematical algorithm is shown in the following equations.

$$\mathbf{C}^{\text{T}} = [\mathbf{C_i}] \in \mathbb{R}^{1 \times (nv \times h)} \quad (i = 1, ..., h) \tag{31}$$

$$\mathbf{x} = [\mathbf{x_i}] \in \mathbb{R}^{(nv \times h) \times 1} \quad (i = 1, ..., h) \tag{32}$$

$$A_{eq} = \left[A_{eq}^{i}\right] \in \mathbb{R}^{(ne)(h) \times (nv)(h)} \quad (i = 1, ..., ne) \tag{33}$$

$$\mathbf{b_{eq}} = \left[\mathbf{b_{eq}^{i}}\right] \in \mathbb{R}^{(ne)(h) \times 1} \quad (i = 1, ..., ne) \tag{34}$$

$$A = [A_i] \in \mathbb{R}^{(ni)(h) \times (nv)(h)} \quad (i = 1, ..., ni) \tag{35}$$

$$\mathbf{b} = [\mathbf{b_i}] \in \mathbb{R}^{(ni)(h) \times 1} \quad (i = 1, ..., ni) \tag{36}$$

$$\mathbf{lb} = [\mathbf{lb_1} \quad ... \quad \mathbf{lb_1}] \in \mathbb{R}^{(nv)(h) \times 1} \tag{37}$$

$$\mathbf{ub} = [\mathbf{ub_1} \quad ... \quad \mathbf{ub_1}] \in \mathbb{R}^{(nv)(h) \times 1} \tag{38}$$

where:

- nv represents the number of optimization variables, here equal to 5

- ne represents the number of equality constraints, here equal to 2

- ni represents the number of inequality constraints, here equal to 8

- h represents the optimization horizon, here equal to 24.

Expanding equations (31)–(38) the complete problem formulation is as follows.

$$\mathbf{C_i} = [w_{im}(t) \quad w_{ex}(t) \quad w_{bat,ch}(t) \quad w_{bat,dis}(t) \quad w_s(t)] \in \mathbb{R}^{1 \times nv}, \quad (t = 1, ..., h) \tag{39}$$

$$\mathbf{x_i} = [E_{grid,im}(t) \quad E_{grid,ex}(t) \quad E_{bat,ch}(t) \quad E_{bat,dis}(t) \quad E_s(t)]^T \in \mathbb{R}^{nv \times 1}, \quad (t = 1, ..., h) \tag{40}$$

$$A_{eq}^{1} = \text{diag}\left\{A_{eq}^{11} \quad ... \quad A_{eq}^{11}\right\} \in \mathbb{R}^{h \times (nv)(h)} \tag{41}$$

$$A_{eq}^{11} = [1 \quad -1 \quad -1 \quad 1 \quad 0] \in \mathbb{R}^{1 \times nv} \tag{42}$$

$$A_{eq}^{2} = \left[\text{diag}\left\{A_{eq}^{22} \quad ... \quad A_{eq}^{22}\right\} + Y\right] \in \mathbb{R}^{h \times (nv)(h)} \tag{43}$$

$$A_{eq}^{22} = [0 \quad 0 \quad -1 \quad 1 \quad 1] \in \mathbb{R}^{1 \times nv} \tag{44}$$

$$Y = [Y_1 \quad Y_2] \in \mathbb{R}^{h \times (nv)(h)} \tag{45}$$

$$Y_1 = \begin{bmatrix} Y_{11} \\ Y_{12} \end{bmatrix} \in \mathbb{R}^{h \times (h-1)(nv)} \tag{46}$$

$$Y_2 = 0 \in \mathbb{R}^{h \times nv} \tag{47}$$

$$Y_{11} = 0 \in \mathbb{R}^{1 \times (h-1)(nv)} \tag{48}$$

$$Y_{12} = \text{diag}\{Y_{12}^1 \quad ... \quad Y_{12}^1\} \in \mathbb{R}^{(h-1) \times (h-1)(nv)} \tag{49}$$

$$Y_{12}^1 = [0 \quad 0 \quad 0 \quad 0 \quad -1] \in \mathbb{R}^{1 \times nv} \tag{50}$$

$$\mathbf{b}_{\text{eq}}^1 = [E_{\text{load}}(t_1) - E_{\text{PV}}(t_1) \quad ... \quad E_{\text{load}}(t_h) - E_{\text{PV}}(t_h)]^T \in \mathbb{R}^{h \times 1} \tag{51}$$

$$\mathbf{b}_{\text{eq}}^2 = [E_s(0) \quad 0 \quad ... \quad 0]^T \in \mathbb{R}^{h \times 1} \tag{52}$$

$$A_i = \text{diag}\{A_{ii} \quad ... \quad A_{ii}\} \in \mathbb{R}^{nv \times (nv)(h)} \quad (i = 1, ..., ni) \tag{53}$$

$$A_{11} = [-1 \quad 0 \quad 0 \quad 0 \quad 0] \in \mathbb{R}^{1 \times nv} \tag{54}$$

$$A_{22} = [0 \quad -1 \quad 0 \quad 0 \quad 0] \in \mathbb{R}^{1 \times nv} \tag{55}$$

$$A_{33} = [0 \quad 0 \quad -1 \quad 0 \quad 0] \in \mathbb{R}^{1 \times nv} \tag{56}$$

$$A_{44} = [0 \quad 0 \quad 0 \quad -1 \quad 0] \in \mathbb{R}^{1 \times nv} \tag{57}$$

$$A_{55} = [0 \quad 0 \quad -1 \quad 1 \quad 0] \in \mathbb{R}^{1 \times nv} \tag{58}$$

$$A_{66} = [1 \quad -1 \quad 0 \quad 0 \quad 0] \in \mathbb{R}^{1 \times nv} \tag{59}$$

$$A_{77} = [0 \quad 0 \quad -1 \quad 1 \quad 0] \in \mathbb{R}^{1 \times nv} \tag{60}$$

$$A_{88} = [0 \quad 0 \quad 1 \quad -1 \quad 0] \in \mathbb{R}^{1 \times nv} \tag{61}$$

$$\mathbf{b}_1 = \mathbf{0} \in \mathbb{R}^{h \times 1} \tag{62}$$

$$\mathbf{b}_2 = \mathbf{0} \in \mathbb{R}^{h \times 1} \tag{63}$$

$$\mathbf{b}_3 = \mathbf{0} \in \mathbb{R}^{h \times 1} \tag{64}$$

$$\mathbf{b}_4 = \mathbf{0} \in \mathbb{R}^{h \times 1} \tag{65}$$

$$\mathbf{b}_5 = [E_{\text{load}}(t_1) \quad ... \quad E_{\text{load}}(t_h)]^T \in \mathbb{R}^{h \times 1} \tag{66}$$

$$\mathbf{b}_6 = [E_{\text{load}}(t_1) \quad ... \quad E_{\text{load}}(t_h)]^T \in \mathbb{R}^{h \times 1} \tag{67}$$

$$\mathbf{b}_7 = [E_{\text{bat,max}} \quad ... \quad E_{\text{bat,max}}]^T \in \mathbb{R}^{h \times 1} \tag{68}$$

$$\mathbf{b}_8 = [E_{\text{bat,max}} \quad ... \quad E_{\text{bat,max}}]^T \in \mathbb{R}^{h \times 1} \tag{69}$$

$$\mathbf{lb}_1 = [-\infty \quad -\infty \quad -\infty \quad -\infty \quad E_{s,\text{min}}]^T \in \mathbb{R}^{nv \times 1} \tag{70}$$

$$\mathbf{ub}_1 = [+\infty \quad +\infty \quad +\infty \quad +\infty \quad E_{s,\text{max}}]^T \in \mathbb{R}^{nv \times 1} \tag{71}$$

Equations (31)–(38) show the mathematical algorithm of the problem and the size of each vector and matrix used. Equations (39)–(71) show the linear matrix equations built

in MATLAB, which correspond to the objective function and the constraint functions. The integer values appearing in the matrices above, indicate the status of the corresponding decision variables (i.e., active or non-active) within the objective function and the constraints and may also take non-integer values, depending on the problem's formulation. Equations (45)–(50) were developed, as it is necessary to account for the current status of stored energy, which is related to the previous period. Concerning the upper and lower bounds (**ub** and **lb**), the infinity symbol is necessary for those variables that are not bounded, despite if they are present in other constraint functions. The minus sign indicates that these variables can be assigned with any negative value, while the positive sign indicates that these variables can be assigned with any positive value.

3.1.4   Assessing a building base study with LP

For the reader to understand the behaviour and performance of the LP model, some intermediate results are presented here, which determine how the LP model behaves under different scenarios and why ANN and GA models were necessary to be developed and utilized. It should be noted that, due to the need of utilizing ANN, the data here differs from the one used for examining the behaviour, performance and validity of the holistic-integrated model (ANN-GA-LP-SAM), which will be demonstrated in Chapter 4.

Real measurements corresponding to PV generation and load consumption data, from a dwelling located in Nicosia, Cyprus, were used in this case. The reader may refer to section I.3, in Appendix I, for further reading on the simulation data and methodology used for this base study.

For comparison reasons, two cases with and without battery were tested, in order to examine the benefits of utilizing storage in a building having integrated PV. In the scenario without battery $w_{bat,ch}$, $w_{bat,dis}$, w_s, E_{bat}, $E_{bat,max}$, E_s, $E_{s,min}$ and $E_{s,max}$ are forced to zero, with the problem formulation presented in section 3.1.2 remaining unchanged. The battery parameters used are shown in Table 4.

Table 4: Battery Parameters

Parameter description	Value [kWh]
Minimum Capacity $E_{s,min}$	0
Maximum Capacity $E_{s,max}$	13.5
Max./Min. Energy during charging/discharging $E_{bat,max}$	5
Initial stored energy $E_s(0)$	0

For the sake of simplicity, the values for $E_{s,min}$ and $E_s(0)$ were set to 0 kWh, which in practice may not be valid, since batteries have integrated mechanisms protecting them from deep discharges. Nevertheless, realistic battery parameters and power conversion losses are considered in a later section with the aid of SAM.

Effect of weight variation

As it is necessary to examine the effect of the weights on the LP behaviour, Table 5 presents the three weight cases attempted. Case 1 refers to the scenario where w_{im} is maximum and w_{ex} is minimum. Case 2 refers to the scenario when w_{im} and w_{ex} are equal and Case 3 refers to the scenario where w_{im} is minimum and w_{ex} is maximum. By studying these three cases, the daily utilization of battery can be examined when: i) only the import energy is "penalized" – Case 1, ii) export energy as well as import grid energy are "penalized" with the same amount – Case 2 and iii) only the export energy is "penalized" – Case 3. The idea behind this, is to examine the model's performance in terms of the amount of import and export energies, with different weight values. Finally, for the sake of these results, the weights $w_{bat,ch}$, $w_{bat,dis}$ and w_s are assigned with the value of zero. Yet, as it will be demonstrated in a later section, these weights are considered when GA is applied. Figures 5(a)–(c), 6(a)–(c) and 07(a)–(c) show the load balance, the energy stored profile as well as the load dispatch for the different desired weights mentioned, respectively.

Table 5: Experimental desired weight values

Case	w_{im}	w_{ex}	$w_{im} - w_{ex}$	$w_{bat,ch}$	$w_{bat,dis}$	w_s
1	1	0	1	0	0	0
2	0.5	0.5	0	0	0	0
3	0	1	−1	0	0	0
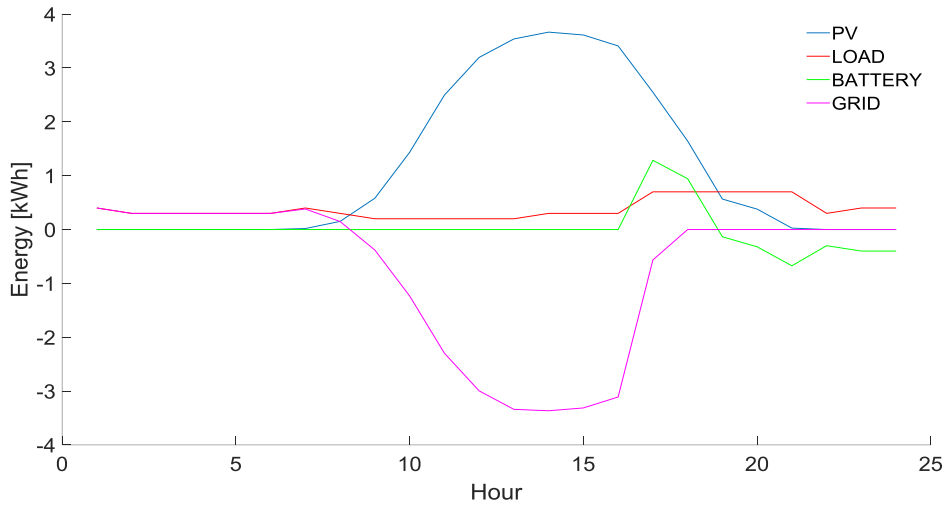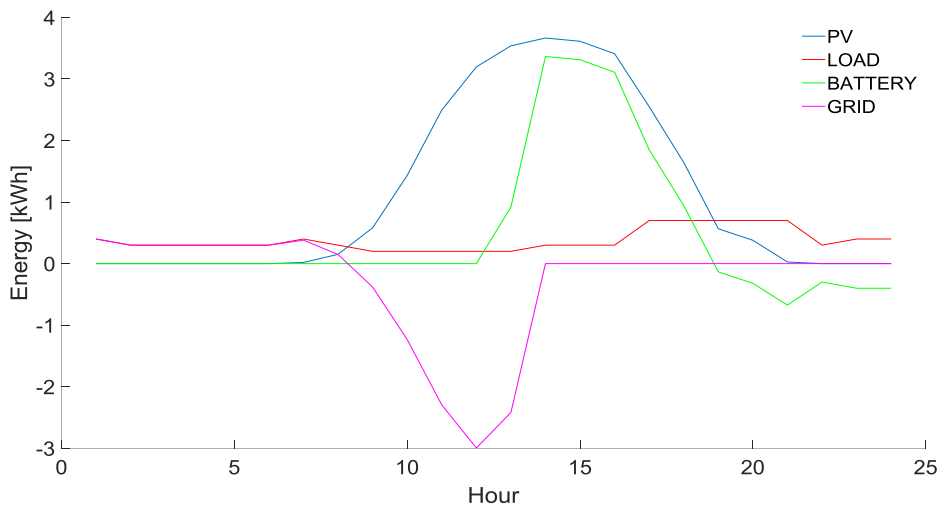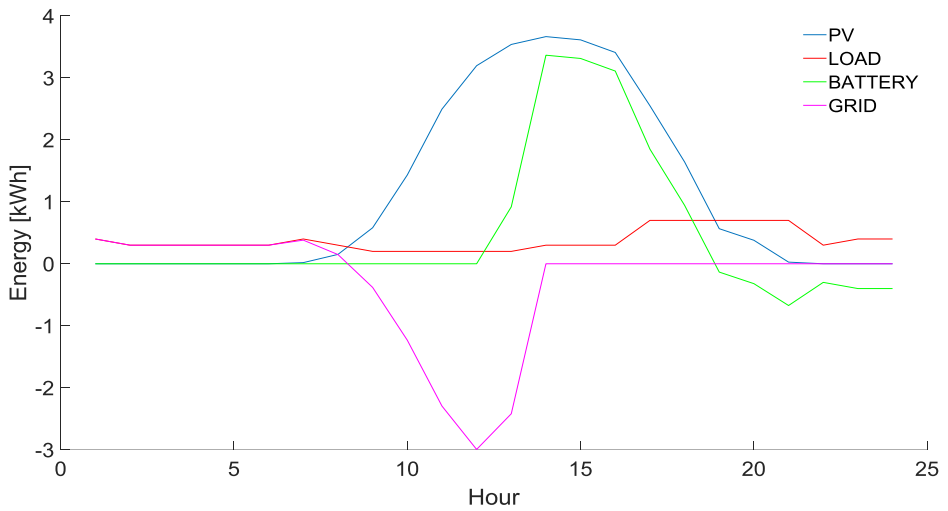
Figure 5: (a) Load balance for $w_{im} = 1$ and $w_{ex} = 0$ ($w_{im} - w_{ex} = 1$); (b) Load balance for $w_{im} = w_{ex} = 0.5$ ($w_{im} - w_{ex} = 0$); (c) Load balance for $w_{im} = 0$ and $w_{ex} = 1$ ($w_{im} - w_{ex} = -1$)
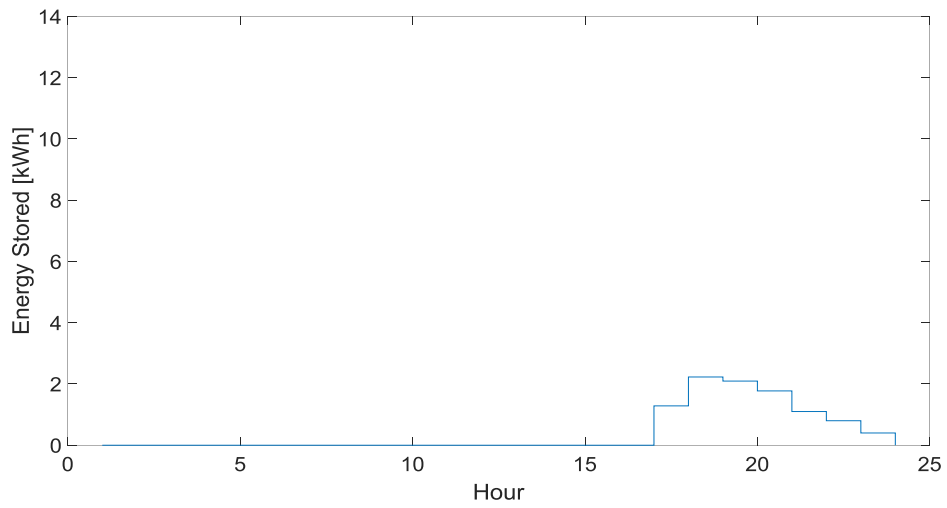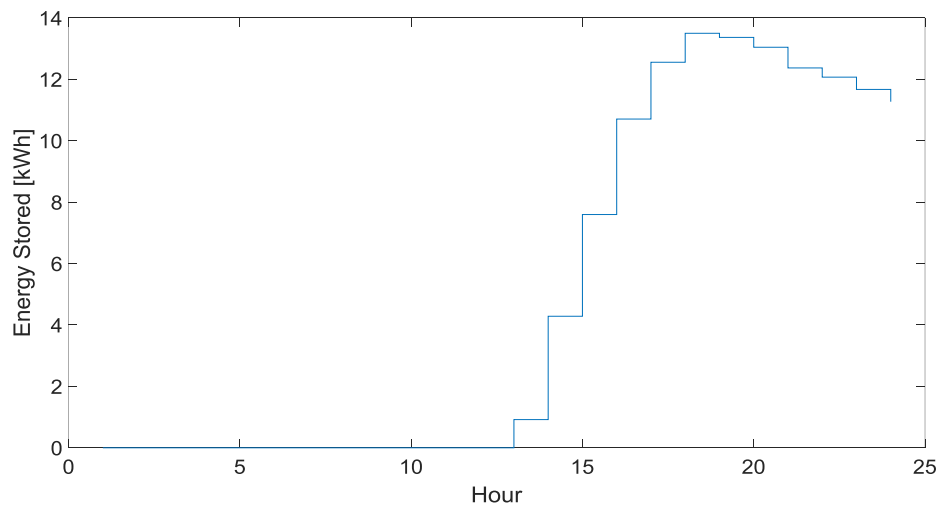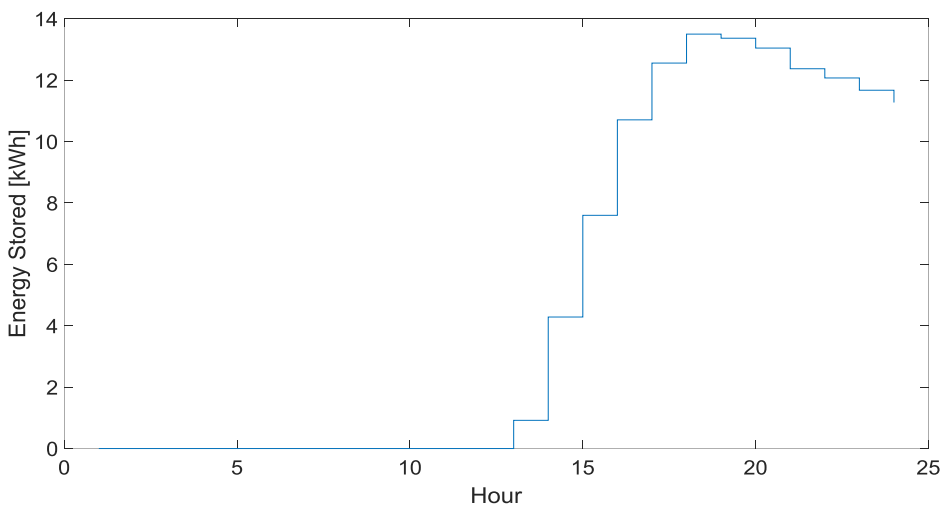
Figure 6: (a) E_s profile for $w_{im} = 1$ and $w_{ex} = 0$ ($w_{im} - w_{ex} = 1$); (b) E_s profile for $w_{im} = 0.5$ and $w_{ex} = 0.5$ ($w_{im} - w_{ex} = 0$); (c) E_s profile for $w_{im} = 0$ and $w_{ex} = 1$ ($w_{im} - w_{ex} = -1$).
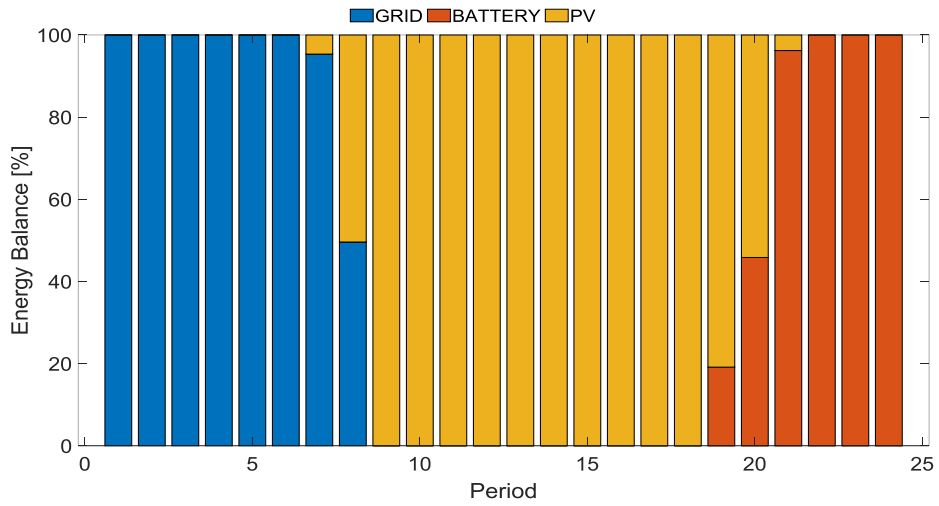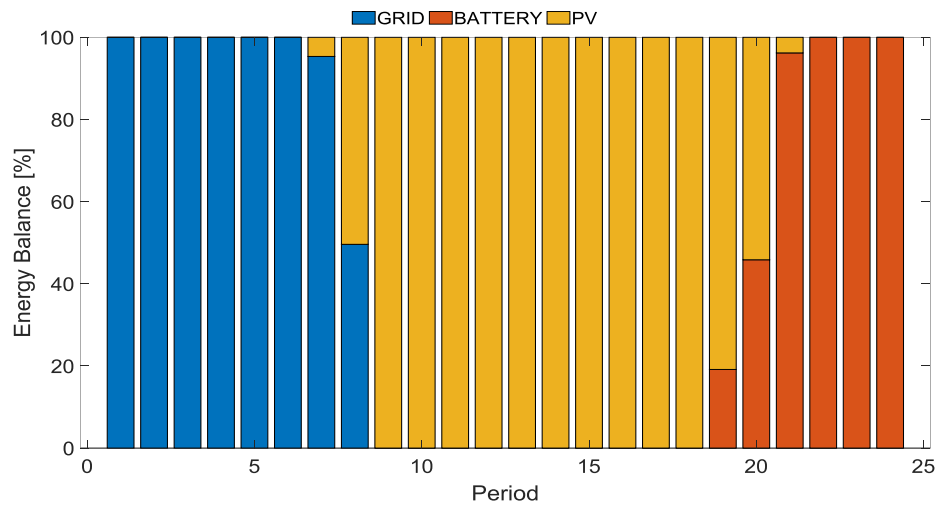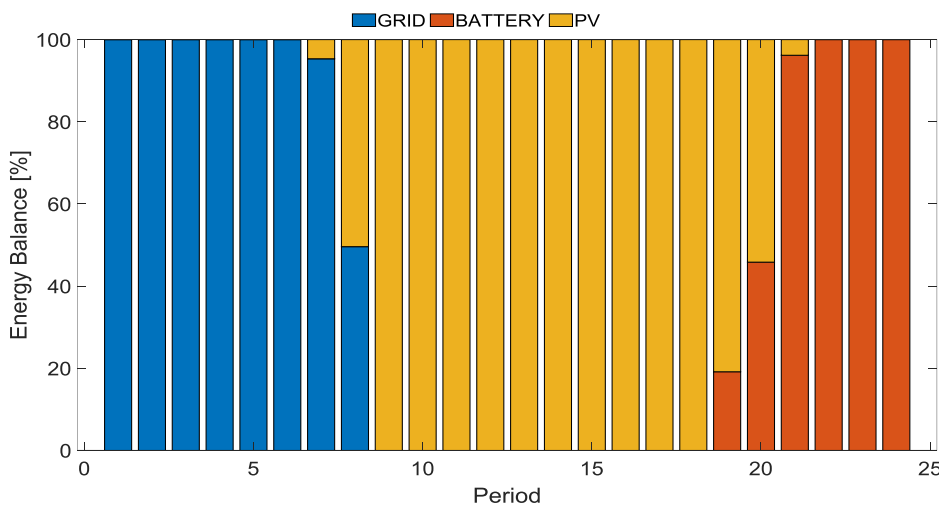
Figure 7: (a) Load optimum dispatch for $w_{im} = 1$ and $w_{ex} = 0$ ($w_{im} - w_{ex} = 1$); (b) Load optimum dispatch for $w_{im} = 0.5$, $w_{ex} = 0.5$ ($w_{im} - w_{ex} = 0$); (c) Load optimum dispatch for $w_{im} = 0$, $w_{ex} = 1$ ($w_{im} - w_{ex} = -1$).

In the case when $w_{im} = 1$ and $w_{ex} = 0$, Figures 05(a) and 06(a) show that the export energy is maximized and the battery is charged only with the amount of energy necessary to supply the load during the late hours when the PV generation is insufficient or zero. Such a scheme may increase the battery life, as the battery experiences low cycling during the day. However, the grid suffers from high energy exports, a phenomenon non-abiding with the concept of nZEB. On the other hand, the cases when $w_{im} = w_{ex} = 0.5$ and $w_{im} = 0$ and $w_{ex} = 1$, behave in a similar between them manner and opposite to the case when $w_{im} = 1$ and $w_{ex} = 0$, as shown in Figures 05(b)–(c) and Figures 06(b)–(c). In cases 2 and 3 there is a penalty associated with the export energy and consequently the minimum value of f is achieved when the export energy is minimum. As a result, the battery is charged to maximum to store the surplus PV energy and releases energy during the late hours to supply the demand. Obviously, without the battery, all the surplus PV energy would be injected to the grid, resulting to a high imbalance of the net grid energy. Despite the optimum usage of battery, there is still some energy export to the grid as shown in Figures 05(b) and 05(c), which may lead to grid imbalance issues. This is due to the high mismatch between the PV generation and the load demand, in this case, which may be solved by the proper sizing of the PV and battery. However, this is an issue beyond the scope of this study.

As shown by Figure 7, in all three cases the energy sharing of the load is identical, regardless of the different desired weight values. Particularly, the load during the early hours is supplied by the grid, as there is no initial stored energy ($E_s(0) = 0$), later by the PV when there is enough generation and then by the battery, during the late hours, when there is insufficient or no PV generation. A possible question that may arise, when $w_{ex} = 1$ and $w_{im} = w_{bat,ch} = w_{bat,dis} = w_s = 0$, is why the battery discharges during the late hours, instead of having imported energy from the grid. The answer may be that due to the fact that the problem presented in equation (**9**) is convex and, by definition, only one global solution exists, any other dispatch scheme will result to a higher amount of export energy and thus to a higher value of f.

Finding the Optimum Values for Weights w_{im} and w_{ex}

As it was observed E_s is affected, based on the weight values and hence, the optimization scheme. Particularly, in cases when $w_{ex} \geq 0$ the daily E_s is either low with the battery being partially charged and fully discharged or high with the battery being fully charged and partially discharged. This implies that when $w_{ex} > 0$, $E_s(t = 0)$ is larger

than 0 and therefore, the battery is able to supply the load during the early hours of the next day. However, the amount of $E_s(t = 0)$ depends on both the PV generation and the load profiles for $t = 0, 1, 2, \ldots, 23$ and therefore, the value of the objective function f changes, based on the amount of import and export energy. Consequently, finding the optimum combination of w_{im} and w_{ex}, which gives the lowest value of f, is necessary. The mathematical algorithm for finding the optimum weights is shown below. It is worth mentioning that the non-convexity nature and the high number of combinations for finding the optimum values for battery related weights (w_{ch}, w_{dis} and w_s), in addition to those for w_{im} and w_{ex}, require the use of a heuristic approach, as it is later demonstrated in section 3.2.

Equations (72)–(83) show the mathematical algorithm developed for finding the optimum values for w_{im} and w_{ex}.

$$\mathbf{EL(0)} = [0^{(1\times11)} \quad 0.1^{(1\times11)} \quad \ldots \quad 1^{(1\times11)}] \in \mathbb{R}^{1 \times 121} \tag{72}$$

$$E_s(0) = E_s^{max} \mathbf{EL(0)}^{(i)} \in \mathbb{R}, \, i = \{1, 2, \ldots, 121\} \tag{73}$$

$$\mathbf{WIM} = [\mathbf{W}^i_{g,im}] \in \mathbb{R}^{1 \times 121}, \, i = \{1, 2, \ldots, 11\} \tag{74}$$

$$\mathbf{W}^i_{g,im} = [1 \quad 0.9 \quad \ldots \quad 0] \in \mathbb{R}^{1 \times 11} \tag{75}$$

$$\mathbf{WEX} = [\mathbf{W}^i_{g,ex}] \in \mathbb{R}^{1 \times 121}, \, i = \{1, 2, \ldots, 11\} \tag{76}$$

$$\mathbf{W}^i_{g,ex} = [0 \quad 0.1 \quad \ldots \quad 1] \in \mathbb{R}^{1 \times 11} \tag{77}$$

$$\mathbf{f_{val,tot}} = [g_i] \in \mathbb{R}^{121 \times 1}, \, i = \{1, 2, \ldots, 121\} \tag{78}$$

$$\mathbf{ex_{tot}} = [h_i] \in \mathbb{R}^{121 \times 1}, \, i = \{1, 2, \ldots, 121\} \tag{79}$$

$$\mathbf{im_{tot}} = [k_i] \in \mathbb{R}^{121 \times 1}, \, i = \{1, 2, \ldots, 121\} \tag{80}$$

$$g_i = \sum_{d=1}^{D} f_d\big(\mathbf{WIM}^{(i)}, \mathbf{WEX}^{(i)}, \mathbf{EL(0)}^{(i)}\big) \in \mathbb{R} \tag{81}$$

$$h_i = \sum_{d=1}^{D} \sum_{t=1}^{T} ex_{d,t}\big(\mathbf{WIM}^{(i)}, \mathbf{WEX}^{(i)}, \mathbf{EL(0)}^{(i)}\big) \in \mathbb{R} \tag{82}$$

$$k_i = \sum_{d=1}^{D} \sum_{t=1}^{T} im_{d,t}\big(\mathbf{WIM}^{(i)}, \mathbf{WEX}^{(i)}, \mathbf{EL(0)}^{(i)}\big) \in \mathbb{R} \tag{83}$$

where:

- **EL(0)** is the vector containing all the battery energy level "multipliers" giving all the possible $E_s(0)$ values at the beginning of the day and vary from 0 up to 1 in increments of 0.1

- **WIM** and **WEX** are the vectors containing all the possible desired weight values and vary from 1 to 0 and 0 to 1, in increments of 0.1, respectively

- **f$_{val,tot}$** is the vector containing all the objective functions for all days simulated

- g_i is the sum of all the objective functions for each current day of optimization, based on the pregiven values of $w_{im} \in$ **WIM**, $w_{ex} \in$ **WEX** and $EL(0)^{(i)} \in$ **EL(0)**

- d is the current day of simulation and f_d is the corresponding value of the objective function

- D is the total number of days simulated (here simulation is carried for a whole year – i.e., $D = 365$)

- **ex$_{tot}$** is the vector containing the export energies for each day simulated

- h_i is the sum of export energies $ex_{d,t}$ for all time steps of the current day and for all days simulated

- **im$_{tot}$** is the vector containing the import energies for each day simulated

- k_i is the sum of import energies $im_{d,t}$ for all time steps of the current day and for all days simulated

- t is the time step and T is the optimization period – here $t = 1$ and $T = 24$

Note that the import and export energies (im$_{d,t}$ and ex$_{d,t}$), for each current day of optimization, are based on the pregiven values of w_{im}, w_{ex} and $EL(0)^{(i)}$.
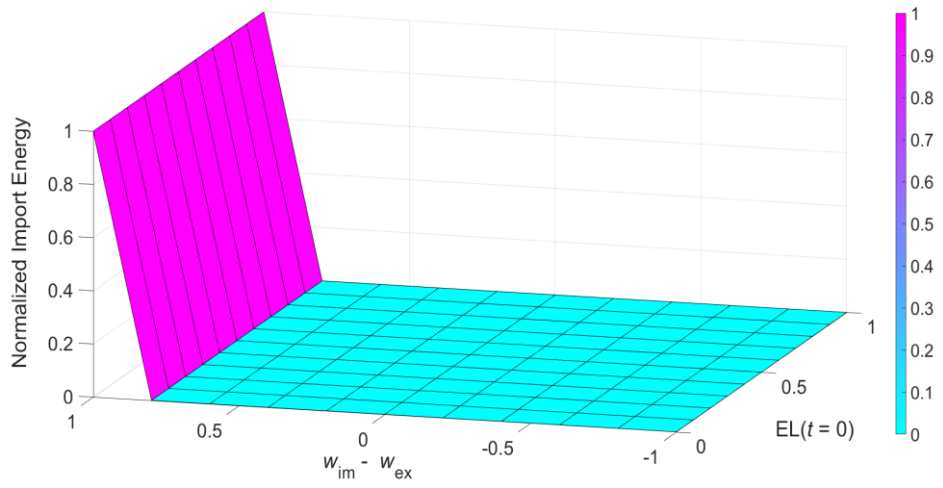
(a)
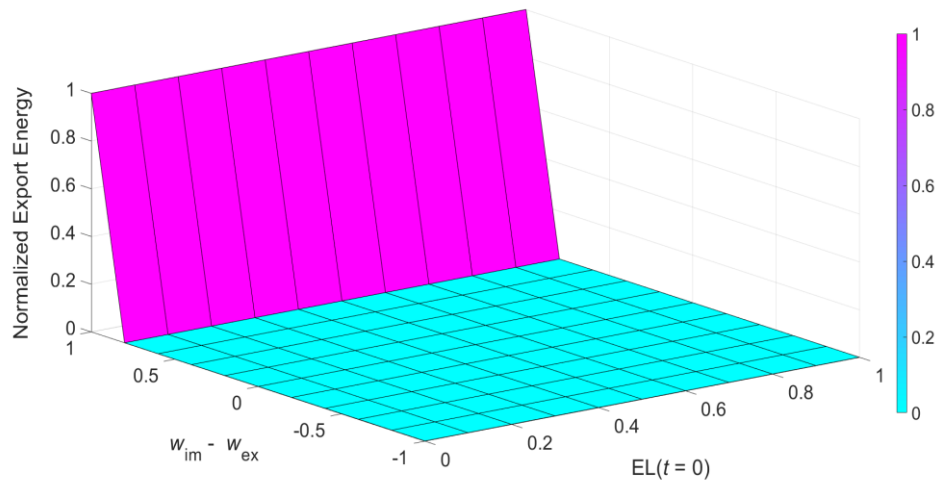
(b)
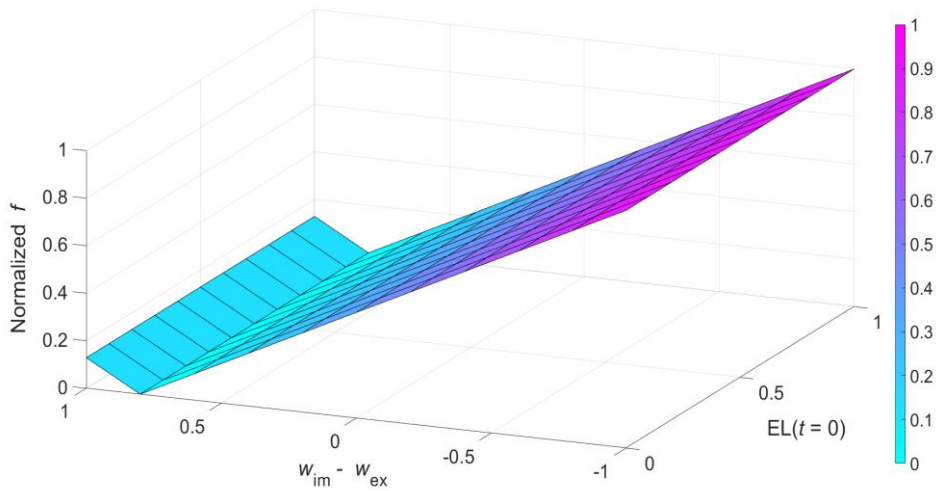
(c)

Figure 8: (a) Effect of $\mathrm{EL}(0)^{(i)}$ and $w_{\mathrm{im}} - w_{\mathrm{ex}}$ on import energy; (b) Effect of $\mathrm{EL}(0)^{(i)}$ and $w_{\mathrm{im}} - w_{\mathrm{ex}}$ on export energy; (c) Effect of $\mathrm{EL}(0)^{(i)}$ and $w_{\mathrm{im}} - w_{\mathrm{ex}}$ on objective function f.

Figure 8 shows, for a whole year, how the normalized import and export energies as well as the normalized value of the objective f are affected with respect to w_{im}, w_{ex} and $EL(0)^{(i)}$. By examining these figures, it is easy to obtain the boundaries for the terms w_{im}, w_{ex} and $EL(0)^{(i)}$, for achieving the minimum export and import energy. Thus, in order to satisfy the requirements of a low energy building – i.e., have the minimum import and export energies as well as the minimum value of f – the following boundaries apply.

- Figure 8(a) (import energy): $-1 \leq w_{im} - w_{ex} \leq 0.8$ and $0 \leq EL(0)^{(i)} \leq 1$

- Figure 8(b) (export energy): $-1 \leq w_{im} - w_{ex} \leq 0.8$ and $0 \leq EL(0)^{(i)} \leq 1$

- Figure 8(c) (value of f): $w_{im} - w_{ex} = 0.8$ and $0 \leq EL(0)^{(i)} \leq 1$

Based on the above boundaries, $EL(0)^{(i)}$ can vary from 0 to 1 with $w_{im} - w_{ex}$ equal to 0.8 (i.e., $w_{im} = 0.9$ and $w_{ex} = 0.1$). This gives the minimum import and export energies as well as the minimum value for f. The above procedure could be repeated for each optimization horizon (i.e., every 24 hours), since the shape of the 3D plots change, depending on the upcoming load and PV generation profiles. For the sake of simplicity, the algorithm shown in equations (72)–(83) is applied on a yearly basis using data from the preceding year.

Finally, a comparison is made in order to evaluate the use of storage in BEM. The simulation period considered here is for the whole year (i.e., $D = 365$) with the optimum values for w_{im} and w_{ex} being 0.9 and 0.1, respectively. The results shown in Table 6 indicate the dramatic decrease in import and export energies as well as the value of the objective function f when the battery is used.

Table 6: Comparison of import energy, export energy and value of f with and without a battery

Case Description	Import Energy (kWh)	Export Energy (kWh)	f
With Battery	352.11	3799.4	137.77
Without Battery	2312.7	5764.7	1136.6

Cross-checking with SAM software

In order to test the validity of the proposed model, a trusted software, known as SAM and developed by NREL, was used. This software is used by both academics and professionals mainly for designing and simulating PV systems with the option of storage. The validity of SAM as well as its battery models and dispatch algorithms can be found in [84]–[89].

Here, the simulations and the results obtained from MATLAB (LP proposed model) were crossed-checked with SAM. The battery type used was a SAM's default model, which refers to a default model for Li-on NMC with a storage capacity of 10 kWh-ac, a charging/discharging rate of 5 kW-ac and a maximum and minimum State of Charge (SoC) of 15% and 95%, respectively. For comparison reasons, these parameter values were also adopted in the proposed LP model. Moreover, SAM's default value of 96% for both ac/dc and dc/ac power conversion efficiencies was also considered in the annual simulation.

To check the validity of the proposed model, the results obtained from both SAM and the proposed LP model, under different case scenarios, were compared. The variables compared are the battery annual dispatch and the annual net grid energy. SAM has the option of running a load dispatch based on a user pre-imported battery dispatch, ensuring that the battery operates within its physical limits. For this reason, the resulting battery dispatch of the LP model was used as the pre-imported battery dispatch for SAM. Then the SAM's resulting battery dispatch was compared to the one of the LP model.

On the other hand, SAM has the additional option to run a dispatch based on a conventional dispatch algorithm, known as automated target controller, which aims to maintain the net grid energy below or close to a user predefined level, at every time-step during the simulation [86]. Hence, a level of 0 kWh was set for every time-step during the annual simulation. For such a scenario, SAM's automated target controller discharges the battery once the load is larger than the PV production, charges the battery once the PV production is larger than load, or keeps the battery in idle when the PV production is equal to the load [86]. In addition to the above-mentioned comparison of the battery annual dispatch, the total net grid energy given by SAM was then compared to the one computed by the LP model.
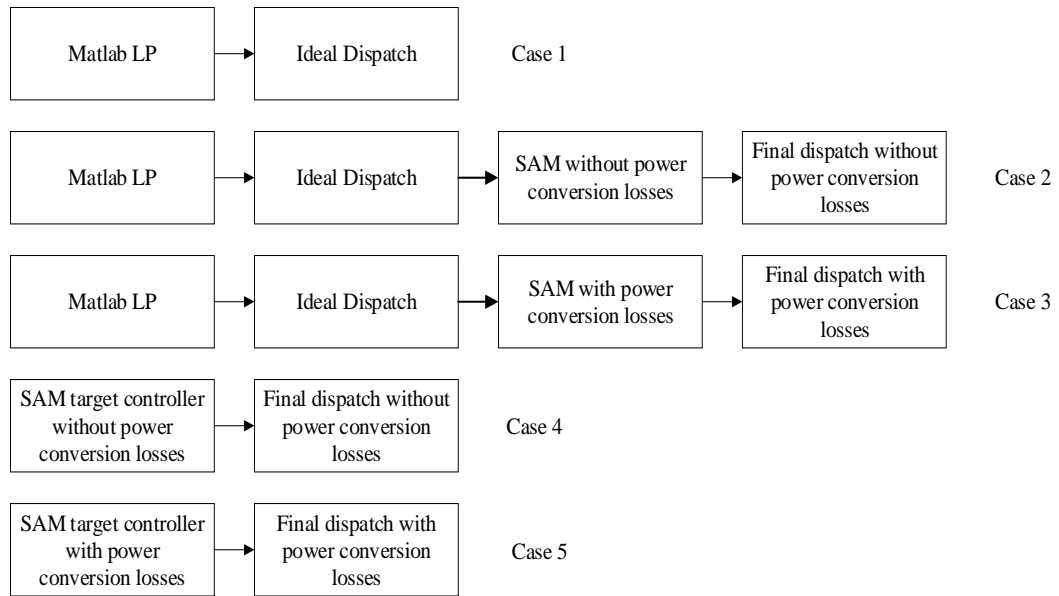
Figure 9: Different cases studied with the LP model and SAM. Power conversion losses mean the losses from dc to ac power conversion and vice versa

Five different case scenarios were studied (Figure 9), referring to two main different dispatches: the proposed LP model and the SAM's automated target controller. In summary, Case 1 refers to the resulting dispatch obtained from the proposed LP model, while Cases 2 and 3 refer to the combined LP-SAM resulted dispatch without and with the power conversion losses, respectively. Finally, Cases 4 and 5 refer to the dispatch obtained from SAM's automated target controller, without and with the power conversion losses, respectively.

Figure 10 shows the 24-hour average annual resulted dispatch of the battery given by the LP model and the combined LP-SAM model (i.e., Cases 1, 2 and 3 of Figure 9). It can clearly be seen that the profile of the LP model case is in a very good agreement with the two globally accepted as realistic cases of SAM, indicating a very good precision for a valid LP model. When comparing Case 1 with Case 3 (no losses) the normalized Root Mean Squared Error (nRMSE) is 1.88%, probably owing to the SAM's non-linear battery model [87]. Particularly, during the running of SAM it was observed that, in SAM the battery requires longer time to fully charge than in the LP model. When comparing Case 1 with Case 2 (losses) the nRMSE is 2.10%, with the dispatch slightly reduced (shifted downward), as expected, due to energy lost inside the power

converters. The result of this comparison suggests that the combined LP-SAM model yields a probably even more accurate model for implementation.
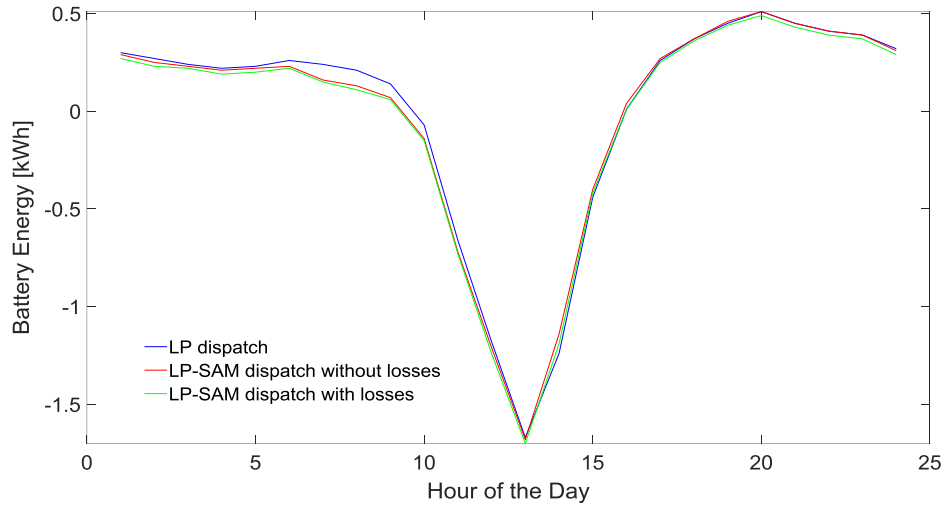
Figure 10: Annual 24-h average battery dispatch. Positive and negative power means discharging and charging, respectively. The resulting dispatch from the LP model (blue line) is also imported in SAM and SAM gives the final dispatch, with the red line corresponding to the combined LP-SAM final dispatch without power conversion losses, and the green line corresponding to the combined LP-SAM final dispatch with power conversion losses

Finally, Figure 11 presents the annual net grid energy resulting from the dispatch models of Case 2 vs Case 4 and Case 3 vs. Case 5 of Figure 9. It is observed that either without or with the power conversion losses considered, the two resulting annual net grid energies are close to each other, with the proposed combined LP-SAM model giving a lower value for both scenarios than SAM's automated target controller model.

The corresponding Absolute Percentage Errors are 1.7% without losses and 2.0% with losses. The outcome of Figure 11 further enhances the trust for the validity of the proposed LP dispatch model, presented in section 3.1.2. Compared to SAM's Target Controller, one has to mention that SAM (i) does not know the upcoming demand and generation and (ii) does not use a global optimization scheme. Since, the proposed LP paradigm can satisfy points (i) and (ii), a further reduction in Annual Net Grid Energy may be observed.

In the upcoming sections, the consideration of the automatic optimum determination of the appropriate desired weight values for enhancing the nearly zero energy target levels, the daily forecasting of both PV generation and load consumption and the effect of the forecasting error caused by the stochastic behaviour of PV generation and consumption are addressed.
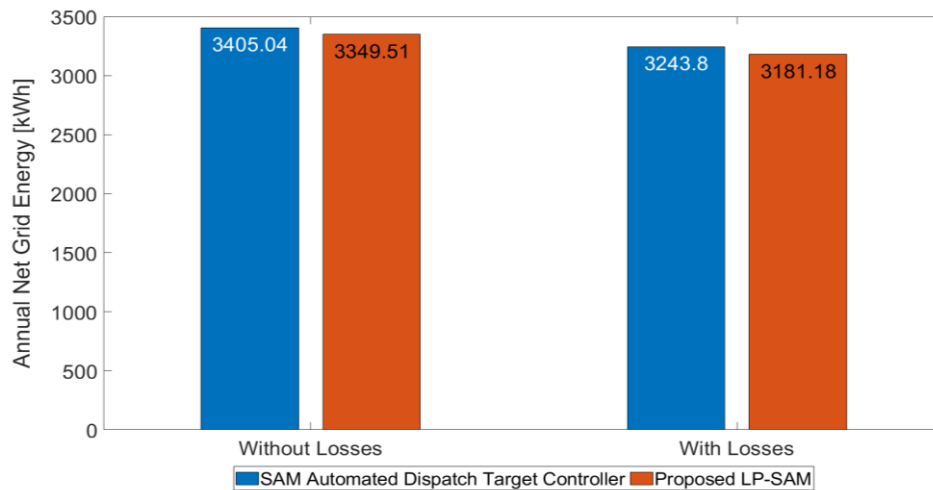
Figure 11: Annual net grid energy comparison between Case 2 and Case 4 (Figure 9) without power conversion losses, and between Case 3 and Case 5 (Figure 9) with power conversion losses. The blue bar refers to the resultant annual net grid energy with the SAM's automated target controller dispatch. The orange bar refers to the resultant annual net grid energy with the combined LP-SAM model dispatch.

3.2   Genetic Algorithm Model[3]

As already mentioned, finding the optimum weight values is strongly related to the PV generation and load consumption profiles. Due to the stochasticity involved, the problem becomes a NP-hard optimization (non-convex) problem and thus, for addressing this issue, a heuristic optimization method, namely GA, is used in parallel with LP for finding the optimum weight values, based on the forecasted PV generation and load consumption provided by ANN (presented in section 3.3). Other heuristic optimization approaches may be applied of course; however, GA was chosen due to its

---

[3] Material from published paper [10]

general superiority when compared with other MATLAB available heuristic optimization methods [90].

GA is a branch of AI and constitutes a method for solving constrained, NP-hard optimization problems relying on natural selection processes that imitates biological evolution [91]. In contrast to classical algorithms, which generate a single point at each iteration, GA produces a population of points and recommends the best point as an optimal solution to the next iteration [92]. Using random number generators (rather than deterministic computation), GA repeatedly modifies a population of solutions to progressively lead to an optimal solution. Hence, it constitutes a heuristic technique for optimization capable of minimizing the burden of computational time as well as the number of function evaluations needed [93].

The main steps comprising the optimization process include the initial population generation, its evaluation, selection of the best candidate, crossover and mutation. This procedure is repeated until convergence. The general criterion for convergence is 'a no change in the solution for n generations' [92]. Thus, the exploitation of best solutions via the exploration of new regions guarantees a large search space, which heuristically provides a high-quality solution.

The developed GA mathematical formulation, which searches for the optimum weight values based on the feedback from the proposed LP model, is shown below.

$$\text{Min.} f_{\text{GA}} = \sum_{t}^{T} \left| E_{\text{im,LP}}(t) - E_{\text{ex,LP}}(t) \right| \tag{84}$$

subject to

$$w_{\text{im}} + w_{\text{ex}} + w_{\text{ch}} + w_{\text{dis}} + w_s = 1 \tag{85}$$

$$w_{\text{im}}, w_{\text{ex}}, w_{\text{ch}}, w_{\text{dis}} \ \& \ w_s > 0 \tag{86}$$

$$w_{\text{im}} + w_{\text{ex}} \geq w_{\text{ch}} + w_{\text{dis}} + w_s \tag{87}$$

where f_{GA} corresponds to the GA objective function; $E_{\text{im,LP}}$ and $E_{\text{ex,LP}}$ correspond to the import and export energies, respectively, obtained from the LP.

The objective function in Equation (84), the nearly zero net-grid energy criterion as may be called, is necessary for flattening (or nearly zeroing) the daily net grid electrical

energy. Specifically, the absolute term is necessary for maintaining the positive difference between the import and export energies and thus, preventing the maximization of the export energy. In other words, the net sum of both energies shall ideally be 0 kWh or practically, as close to 0 kWh as possible.

Due to the normalization of Equation (**25**), the sum of weights must equal to unity – see Equation (85) – and with constraint (86) none of the weights is assigned with the value of zero. To account for all optimization variables, this is also necessary for Equation (**25**). Finally, as mentioned in sub-section 3.1.2, for nZEBs the minimization of the net grid energy is of high priority and hence, the term $w_{im}E^*_{grid,im}(t) + w_{ex}E^*_{grid,ex}(t)$ must be greater than $w_{bat,ch}E^*_{bat,ch}(t) + w_{bat,dis}E^*_{bat,dis}(t) + w_sE^*_s(t)$. This is ensured with the aid of constraint (87) and in this regard, the feasible exploration space is further decreased, mitigating the consequent computational burden. The mathematical model shown above constitutes an amelioration of a previously applied model presented in [10] and assists LP for minimizing the grid energy usage.

Georgiou et al. [10] showed that the weights can adapt to the PV generation and load consumption of the day. For instance, with the aid of cross-correlation and Principal Component Analysis the authors presented that GA tunes each individual weight in a way that when the import energy is "penalized" with a low weight value, the battery discharging is penalized with a low weight value too, in order to increase its supply to the load. Similarly, when there is a need to charge the battery more, the weight associated with the energy storage is relaxed, in order to allow the battery to store more energy. This way, the export and import energies are minimized in an optimum manner, as it will also be demonstrated in Chapter 4.

Figure 12 shows the different values assigned to the five different weights of the LP objective function by GA, for a complete annual simulation period. It can be clearly seen that w_{im} and w_{ex} mostly share values closer to 1 and with the battery related weights (w_{ch}, w_{dis} and w_s) mostly sharing values closer to 0. With this figure it is clearly shown that GA mostly penalizes import and export energies with higher values, in order to allow the battery to harvest the PV energy as much as possible and thus minimize the energy exchange between the building and the grid.
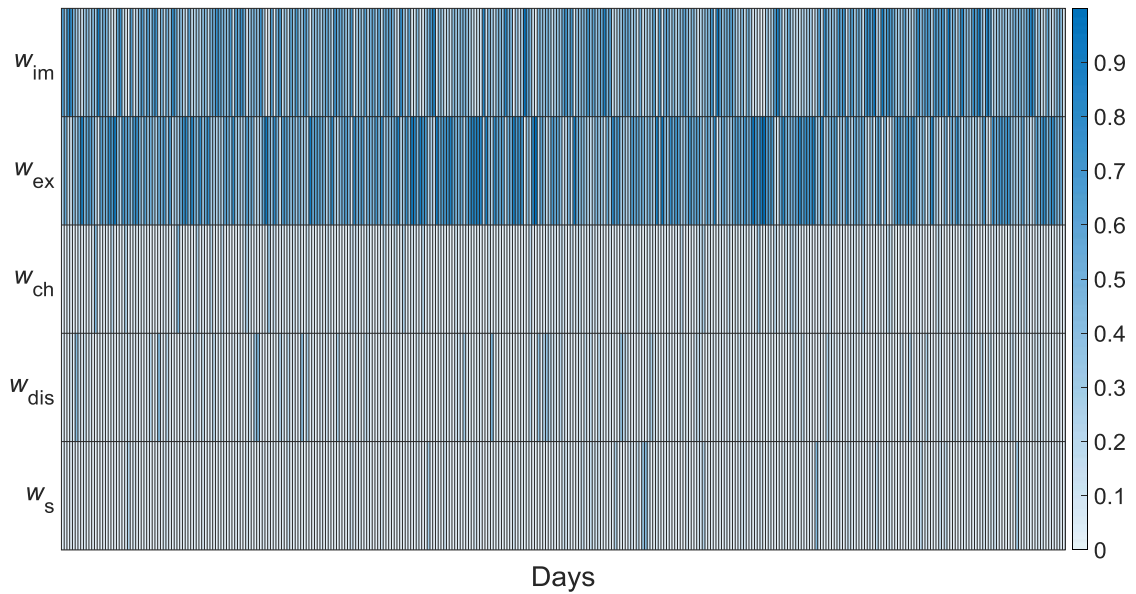
Figure 12: Weights heat map

3.3 Artificial Neural Network Model[4]

As already mentioned, for achieving daily global optimization, forecasting is necessary and for this purpose, two ANNs are utilized. The reader may refer to section I.4, in Appendix I, for more information regarding the relevant background theory, history and applications of ANN, as well as how a preliminary ANN design contributed toward the final ANN design presented here.

The two ANN models here are used for forecasting the next day PV generation and load consumption, which are used as inputs by the LP-GA model. In this application two feedforward ANNs are used for forecasting the next day's PV generation and load consumption, with their architectures shown in Figure 13. The ANN used for the 24-hour PV forecasting (Figure 13(a)) utilizes as inputs the hourly PV ac generation of the previous day, from a dwelling located in the town of Nicosia in Cyprus, and the next day's hourly forecast of the Global Horizontal Irradiance (GHI), for the same location. GHI is given from the Department of Meteorology of Cyprus, which uses a Numerical Weather Prediction (NWP) model for forecasting different meteorological parameters at 20 different locations in Cyprus, as shown in Figure 14.

---

[4] Material from paper [79]
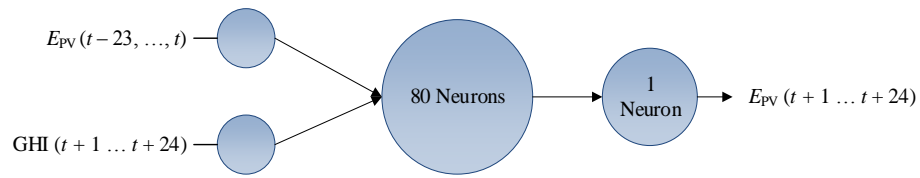
(a)
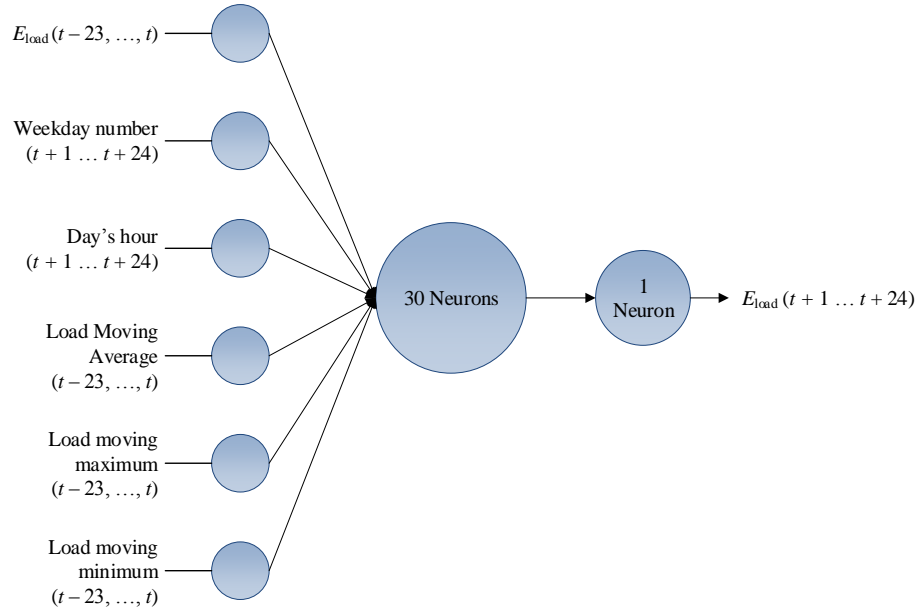
(b)

Figure 13: (a) Proposed Feedforward ANN for PV Generation and (b) Proposed Feedforward ANN for load consumption forecasting

Figure 14: Weather forecasting from Cyprus Department of Meteorology at 20 different locations (NWP model)

Further to the correlation results presented in section I.4.3.2.1, in Appendix I, using the generation of the previous day as one of the two inputs, allows exogenous factors affecting production, which are not measured or quantified in this case, to be captured and considered by the ANN. Such parameters may reflect to partial loss of production due to module, string and/or inverter failures, atmospheric pressure, PV panel soiling and so on. On the other hand, as it is known that, (i) the PV generation is highly correlated with Sun's radiation, (ii) irradiance forecasts from Meteorological Departments are commonly given for horizontal surfaces and (iii) converting GHI to the actual irradiance hitting the PV modules (PoA Irradiance) is complex and not straight forward, GHI is chosen as the second input. With the aid of a trial and error approach, using nRMSE as the performance metric, 80 neurons in the hidden layer are used having sigmoid as their activation function and 1 output neuron in the output layer having a linear activation function for giving the next day's PV generation forecast. With this configuration, a nRMSE of 11% was obtained for the studied year.

Regarding the ANN used for the load consumption forecasting (Figure 13(b)), a similar to the PV forecast procedure explained above is followed. The load consumption of the previous day is used in this case, as it is necessary to capture exogenous factors not measured or quantified in this case, such as ambient temperature, CO_2 concentration, natural illuminance (ambient lighting) and so on. Moreover, the weekday number along with the hour of the day for the forecasted period are used, as the load pattern is strongly correlated with the day of the week and the hour of the day. For instance, the load behaves differently in Sundays compared to Mondays and the peak load occurs, generally, in the afternoon. Lastly, for improving the learning of the load profile, inputs such as load's moving average, moving minimum and moving maximum of the previous day are also utilized. With 30 neurons in the hidden layer having sigmoid as their activation function and 1 neuron in the output layer that possesses a linear activation function, a nRMSE of 6% is obtained for the studied year. In both networks, the training process is performed using the backpropagation learning algorithm and an annual training dataset obtained from a dwelling, located at Lat/Lon: 35.101765, 33.348838, for 2017.
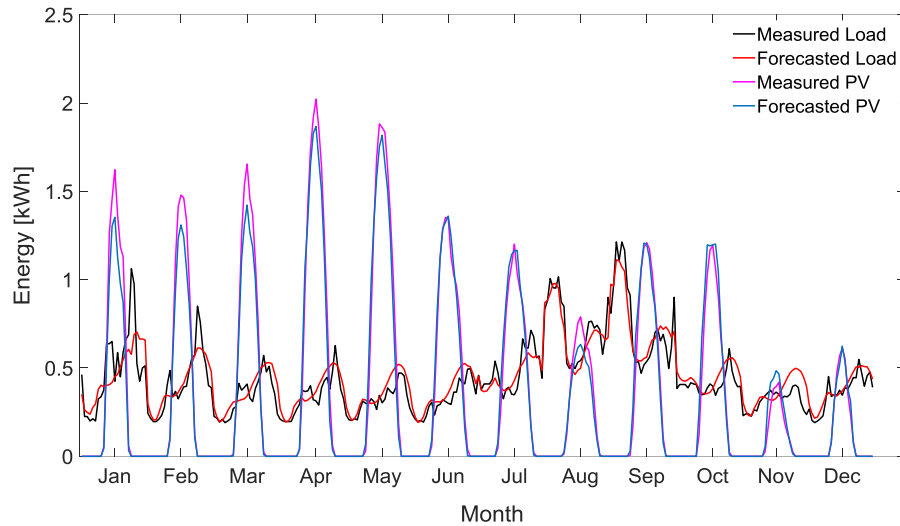
Figure 15: Monthly per daily-hour average of Forecasted and Measured PV and Load

Finally, the ANN forecasts versus the measured values, on a monthly per daily-hour average, are shown in Figure 15, indicating the accuracy of the proposed ANN models and their ability to assist GA for searching the optimum weights and LP for minimizing the grid energy usage. Although the ANN models showed a good accuracy, it is known that the final solution of the dispatch becomes closer to the "real" optimum when the error between the predictions and the real values becomes lower. The study of such phenomenon requires a further considerable effort and consists a subject field of future work.

3.4 Integrating ANN, GA, LP and SAM[5]

So far, the proposed LP model was tested and validated with the aid of SAM using real – but at the same time historical – PV and load data without any consideration of the PV's and load's stochasticity. In other words, the proposed model, presented in section 3.1, assumes perfect predictions and is not updated at every time-step when variations in the given (forecasted) PV and load may occur. Thus, it was impossible so far, to update LP with the SAM's recalculated values (e.g. SoC) for every time-step and hence, achieve a more realistic global optimum dispatch. Moreover, due to the daily change in PV generation and load consumption, the optimum exploration of the daily optimum weights constitutes a NP-hard (i.e., non-convex) optimization problem and requires the

---

[5] Material from paper [79]

use of a heuristic approach. For addressing such issues above, the development, utilization and integration of both GA and ANN were necessary.

This section demonstrates the holistic integration of ANN, GA, LP and SAM. With ANN forecasting the next 24-hour PV generation and load consumption, once per day, and GA giving the optimum weight values, based on the given forecasted data, the battery is dispatched in an adaptive and global optimum manner. This allows a battery dispatch to be globally optimized, daily, since historical, current and future values for both PV and load are recurrently considered, during the optimization horizon. Therefore, based on the input information mixture of the measured and forecasted values, the dispatch is rescheduled in a repetitive – but not receding – manner, for every timestep (one hour) of the optimization horizon (24 hours). As mentioned earlier in the Introduction and showed in section 3.1.4, for addressing the non-linear and complex nature of the battery and model its performance in a more realistic fashion, SAM is embedded in the proposed algorithm.

At the end of each simulation day, the two ANNs forecast the next day's PV generation and load consumption, while GA – based on the forecasts – repeatedly runs the LP algorithm until the next day's optimum weights are found. With the resulting optimum weights, a forecasted dispatch for the next 24 hours is attained through LP and the final dispatch is then obtained with the aid of SAM. During the updating phase, at each time step, the matrices containing the PV and load forecasts are substituted by their corresponding measured values, the LP reruns relying on the new-updated data and SAM recalculates the final dispatch, based on the updated ideal battery dispatch from LP. Finally, at the end of the day, the resulting State of Charge (SoC) of the battery calculated by SAM is used as the initial SoC of the next day. This procedure is repeated for each day of the simulation period – i.e., for one year in this case.

In Figures 16 and 17 the aforementioned procedure is graphically demonstrated with the aid of a block diagram and a flowchart. As mentioned earlier in this section, the information mixture of historical, current and future PV and load values leads to the daily global optimization scheme. This may be verified through Figure 16, as the input matrix to LP (PV and load) continually consists of previous (e.g., $t - 1$), current (e.g., $t = 0$) and upcoming (e.g., $t = 1 \ldots 23$) PV and load values, for each time-step of the optimization horizon, and with the 24-hour dispatch repeatedly rescheduled for every time-step. Hence, based on the LP equations presented in section 3.1.2 and by the

definition of LP shown in section I.2 of Appendix I, a daily global optimization is always achieved. Finally, as of the algorithm's flowchart shown in Figure 17, the parameters displayed on the right of each block, correspond to the output parameters of the current algorithm's state, which are used as inputs by the algorithm's next state. For instance, the state "*GA weights optimization and LP*", the state at which both the optimum weights and the forecasted dispatch are obtained, provides the next state's inputs such as the optimum battery charging and discharging energies along with the day's initial storage level.

Figure 18 shows an example of the proposed ANN-GA-LP-SAM model's outcome, regarding the forecasted and updated dispatches and the battery's SoC, for a three-day simulation period. A snapshot of the simulation, representing the forecasted dispatch for the 24th of January 2018 and the status of the updated dispatch for the same day at 15:00, is shown in Figures 18(a) and 18(b).

The top diagrams show the expected dispatch and the battery's SoC of the day, whereas the bottom diagrams show how both the dispatch and the battery's SoC evolve during the day when changes in PV and load occur. Similarly, Figures 18(c) and 18(d) show the overall forecasted (or expected) dispatch and the battery's SoC along with their evolution, during the day, for the complete three-day simulation period.

A visual comparison of the forecasted and measured values, for both PV and load, shows that a noticeable difference exists, resulting to a different from the expected dispatch. Despite the forecasting errors, it is clearly shown that the proposed model is able to adapt to any uncertain changes, in every timestep, and maintain the energy balance as well as the battery operation within its SoC limits.
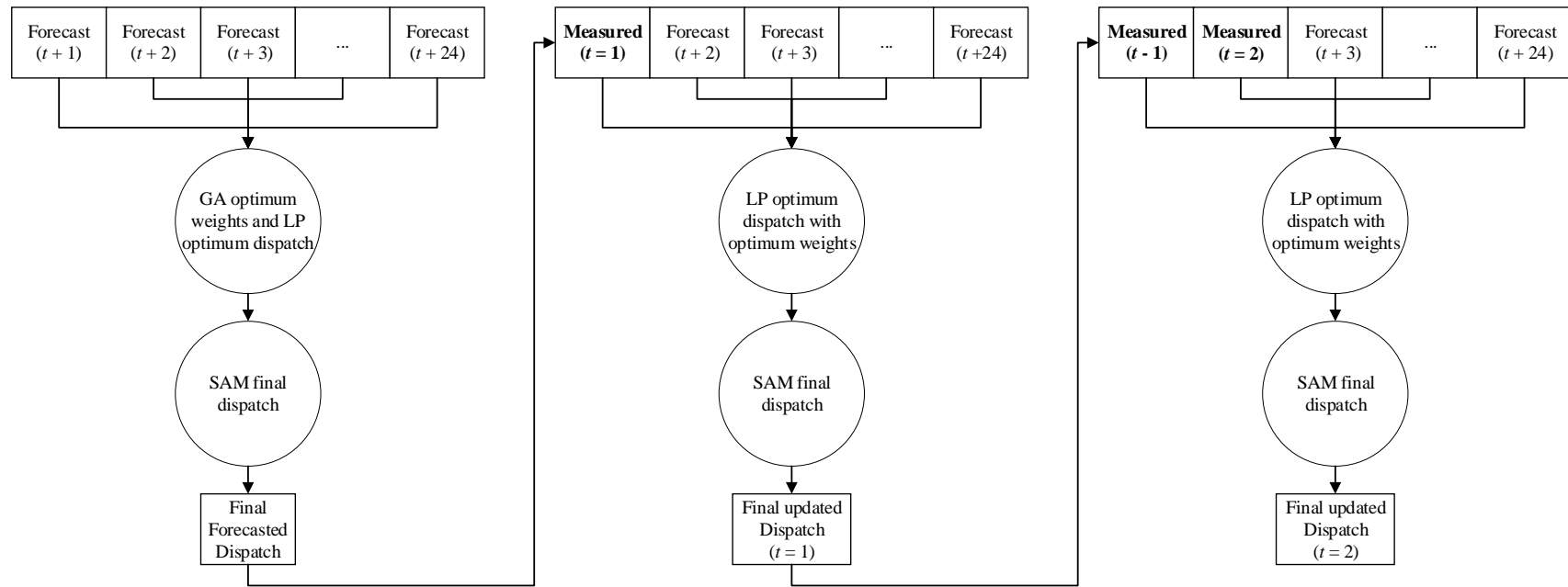
Figure 16: Procedure of the forecasted and updated optimum dispatches, for a single day
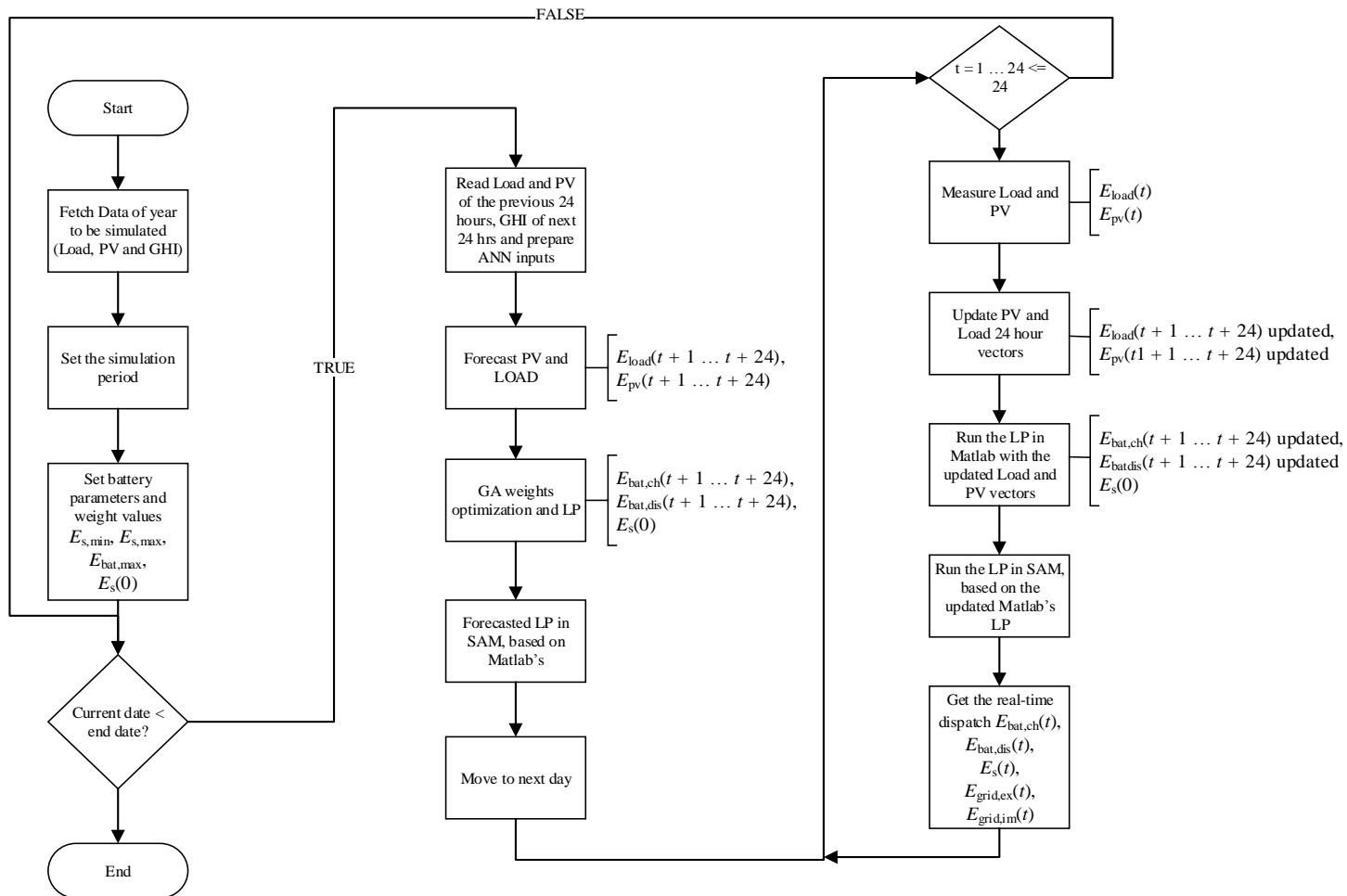
Figure 17: Simulation algorithm flowchart
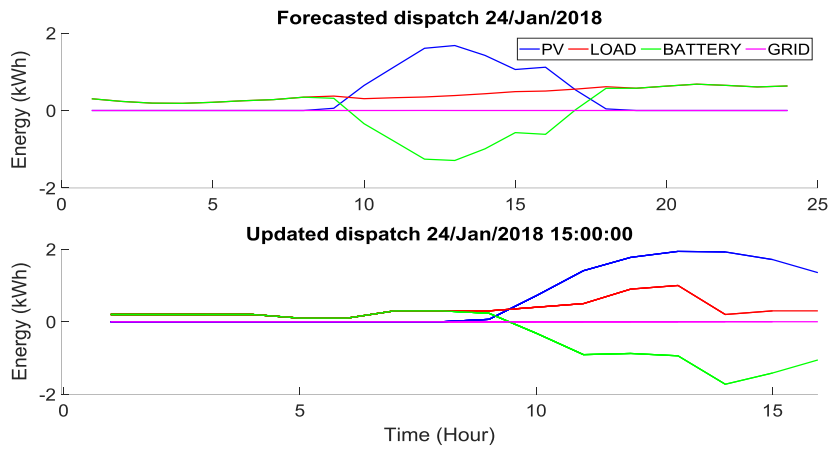
(a)
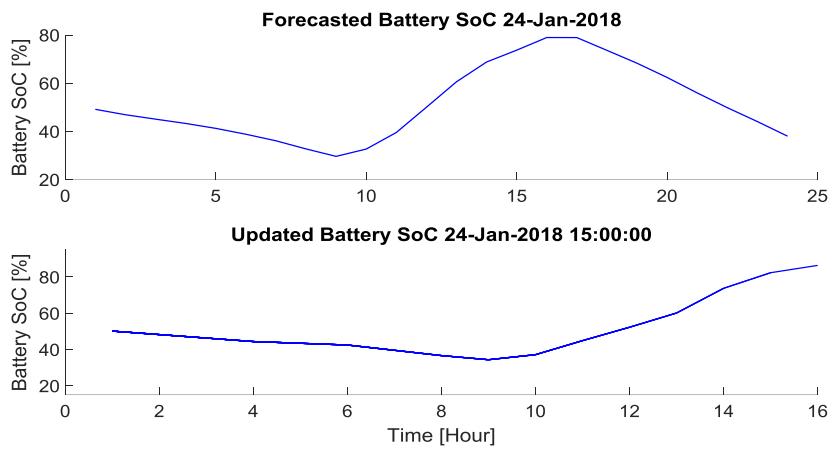
(b)
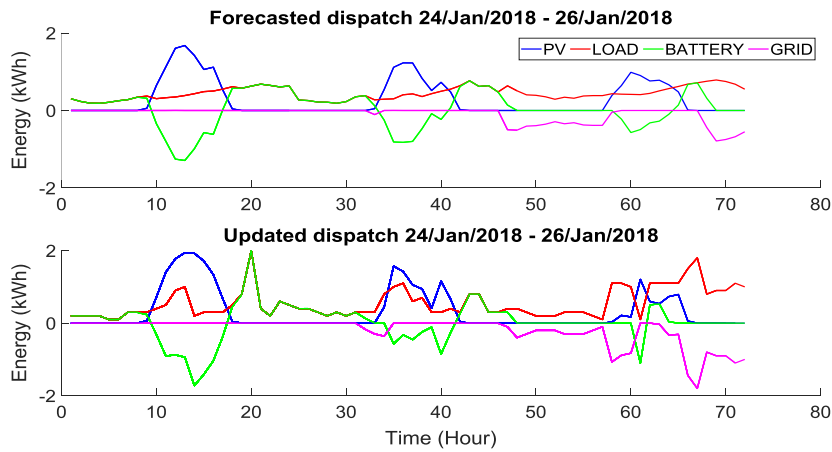
(c)
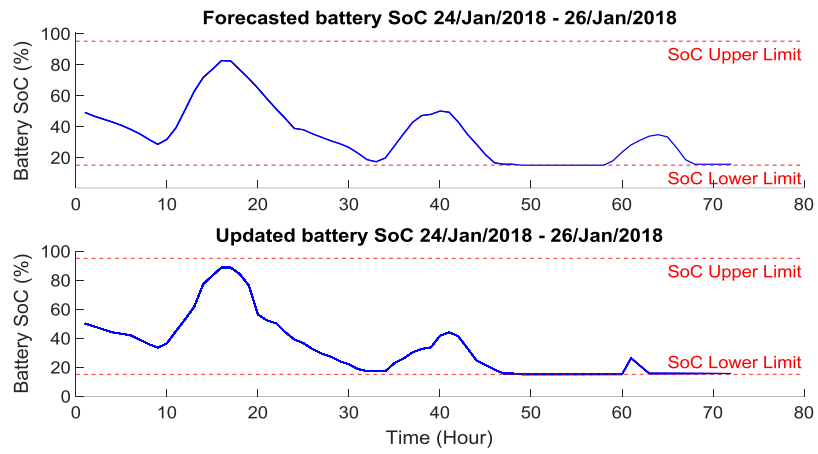
(d)

Figure 18: (a) Forecasted Dispatch for 24/01/2018 and updated Dispatch for 24/01/2018 (up to 15:00); (b) Forecasted battery SoC for 24/01/2018 and updated battery SoC for 24/01/2018 (up to 15:00); (c) Forecasted vs. updated Dispatch for 24–26/01/2018 and (d) Forecasted vs. updated SoC for 24–26/01/2018. Storage Capacity = 9.3 kWh

4 Enhancing nZEBs based on Battery Performance, AI, Heuristic and Convex Optimization. A Base Study Results [6]

Chapter 3 demonstrated (i) the validity and the ability of the proposed LP model to reduce the daily import and export energies in a global optimum manner, (ii) the exploration of the optimum weight values utilizing a heuristic approach (GA) based on the forecasted data, (iii) the forecast of the next 24-hour PV generation and load consumption utilizing AI (ANN) and (iv) the integration of the LP along with ANN, GA and SAM for assisting the dispatch. Through the above, it was shown that the holistic proposed model is able to maximize the battery's utilization throughout the day, based on the PV generation and load consumption and without worrying about users' satisfaction, since the dispatch adapts to any uncertainties present in both the load consumption and PV generation.

This Chapter presents the application of the proposed hybrid optimization model in a building case and demonstrates the outperformance of the proposed paradigm compared to the case when there is no storage and to an alternative dispatch case with storage. In particular, (i) the simulation data used is summarized and presented, (ii) a second cross-validation (with the final simulation data) of the ideal dispatch obtained from the LP is attained with the aid of SAM, and (iii) a demonstration of the different annual results is made.

4.1 Simulation Data

As a base study, real PV and load measurements from a building, in Nicosia Cyprus, were collected and used for the period between 23 January 2018 and 22 January 2019. Recall that this this data is different from the one presented in section 3.1, since now an ANN is utilized using GHI forecasts for a different location given by the Cyprus Meteorological Department (Lat/Lon: 35.101765, 33.348838).

With the PV and load data lying in the range of 15-min and hourly resolutions, respectively, the PV is converted to an hourly resolution data, by simply aggregating the 15-min energy delivered in each hour. For instance, the hourly energy delivered at

---

[6] Material from paper [79]

08:00 am is the sum of the energy delivered at 07:15, 07:30, 07:45, and 08:00, and so on.

For having a clearer understanding of the weather, at the location under study, Figure 19 shows different weather-related parameters for one representative month per season in 2018. The representative months selected are January for winter, April for spring, July for summer and October for autumn. By closely examining these parameters, one may conclude that in Cyprus the climate is significantly warm with high humidity levels. Despite the high temperature and humidity, which may affect the generation of the PV system, high irradiance levels are observed, leading to significant PV energy generation. On the other hand, the presence of high humidity and high temperatures lead to the intense use of cooling systems in summer, thus increasing the energy needs of a building.
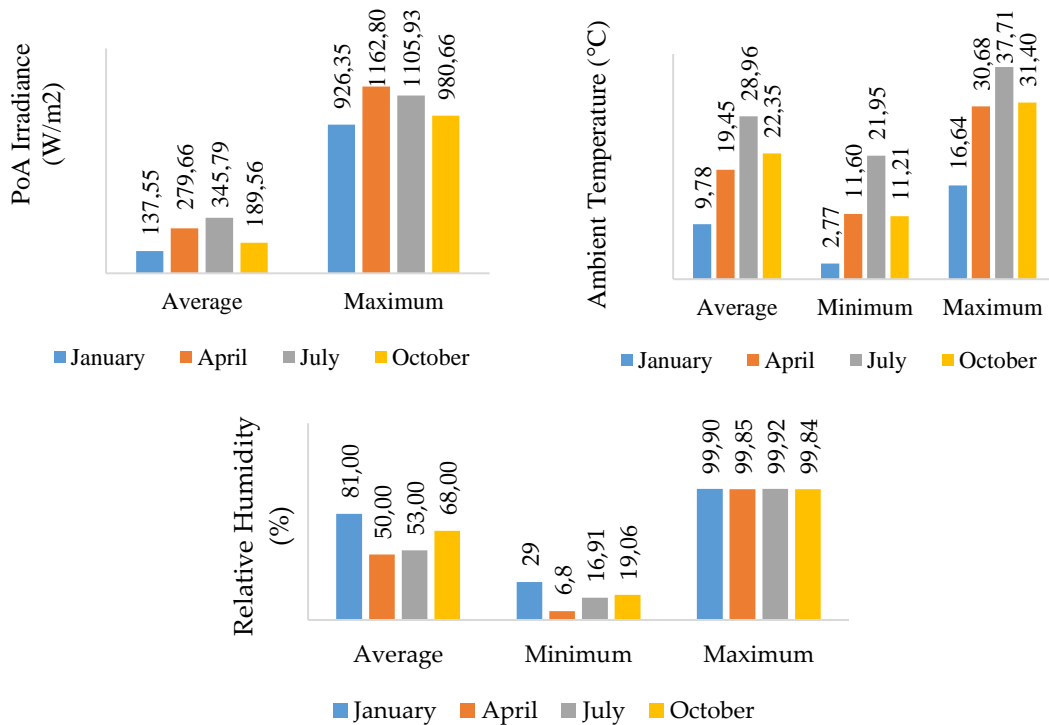
Figure 19: Maximum, Minimum and Average PV Generation, PoA Irradiance (including night-times), Ambient Temperature and Relative Humidity at the location under study

Figures 20 and 21 present the total PV energy generated and load consumption and their daily average profiles, for the studied year, respectively. As can be observed, the highest

PV energy levels are gained in the 2nd quarter of the year (April – June), due to the high irradiance and relatively low temperatures, while the last quarter owns the lowest production, due to the increased number of cloudy days. With an average of a 12-hour daily generation (07:00–19:00), the concept of harvesting PV energy via storage in buildings, constitutes a key solution toward nZEBs.
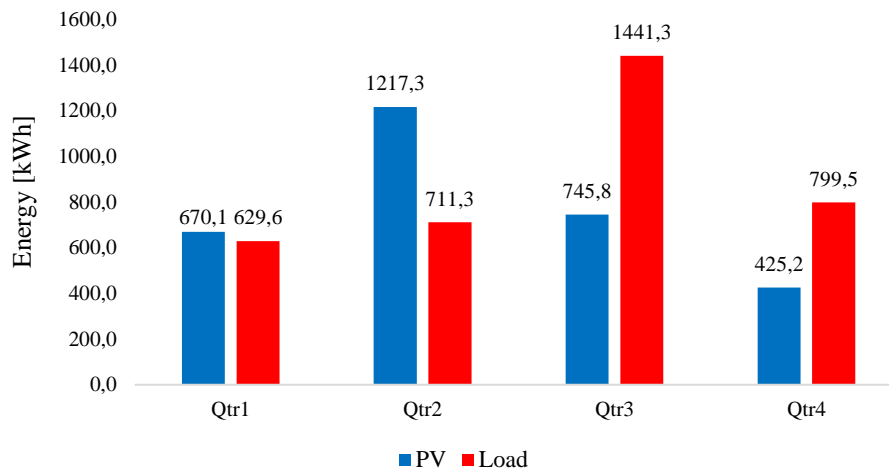
Figure 20: Total PV Generation and Load consumption by quarter in 2018
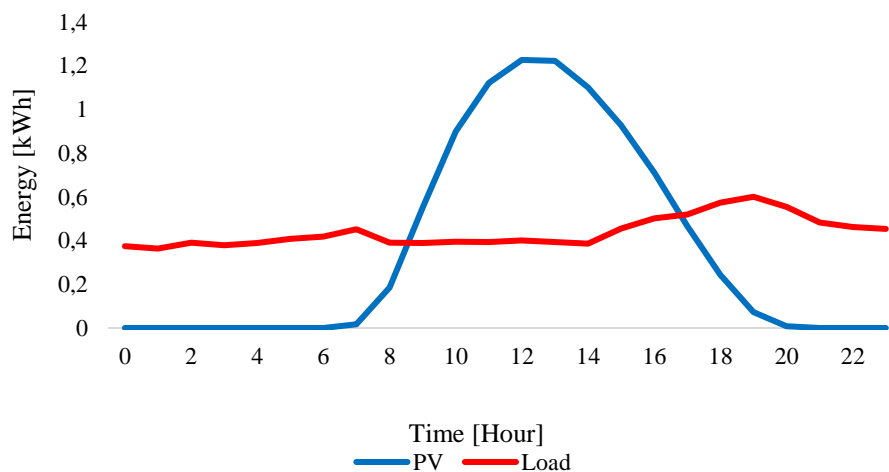
Figure 21: Average 24-hour PV generation and Load consumption for 2018

Compared to the PV generation, Figures 20 and 21 show that the total building's energy needs, behave in a relatively opposite manner. Particularly, during quarters 2, 3 and 4 either the load is greater or lower than the PV, with the only exception occurring in quarter 1, where generation is close to consumption. Moreover, the annual peak

consumption occurs in the 3rd quarter due to the increased cooling needs, the lowest consumption occurs in the 1st quarter due to the reduced cooling and heating needs and finally the daily peak load occurs roughly at 20:00. With the high imbalance between generation and consumption, which is a common phenomenon with existing building PV installations, the need of handling the daily and thus quarterly and annual mismatches is of great importance. As it was already shown, storage can enhance the daily self-consumption, by significantly reducing both the grid import energy (primary energy needs) and the grid export energy, contributing toward the nZEB attainment. This is also verified in the sequel of this Chapter.

4.2 Cross-validating the proposed hybrid optimization model with SAM

As showed in section 3.1.4, due to the non-linear and complex behaviour of batteries, SAM has been employed in this study for giving a more realistic and the final battery dispatch. According to the proposed mechanism, the final dispatch is driven by LP and obtained by SAM with the ideal battery dispatch imported in SAM, where the battery internal losses, dc and ac power conversion efficiencies and other complex calculations (e.g., SoC estimation, battery roundtrip efficiency and so on) are applied.

As a case for the cross-validation analysis, PV and load data presented in sub-section 4.1 along with a SAM model for Li-on NMC batteries were used. The main parameters of the battery used are mentioned in Table 7.

Table 7: Battery Specifications

Battery Parameter	Value
Storage Capacity	9.3 kWh
Charging/Discharging Rate	5 kW
Minimum SoC level	15%
Maximum SoC level	95%
dc-dc conversion efficiency	98%
ac-dc charging efficiency	96%
dc-ac discharging efficiency	96%

Further to the validation of the LP model shown by Figure 10, Figure 22 shows – for a ten-day simulation period – the resulting hourly dispatch of the battery given by the LP model and the final dispatch given by SAM. As can be seen, due to the various non-linear and complex battery parameters, such as power losses and non-linear SoC estimation, the resulting final dispatch is slightly different from the one provided by LP. Specifically, the battery charging and discharging energies, initially dispatched by the LP model, are slightly lower and higher, respectively, due to the power losses of both the battery and the inverters.
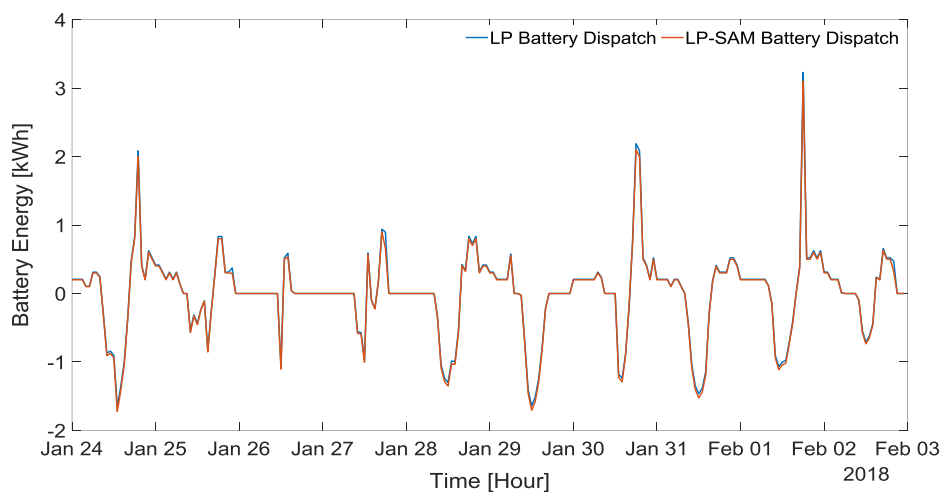
Figure 22: Battery Energy Dispatch of LP and LP–SAM for a 10-day simulation period with 9.3 kWh Storage Capacity. Positive energy means discharging and negative energy means charging
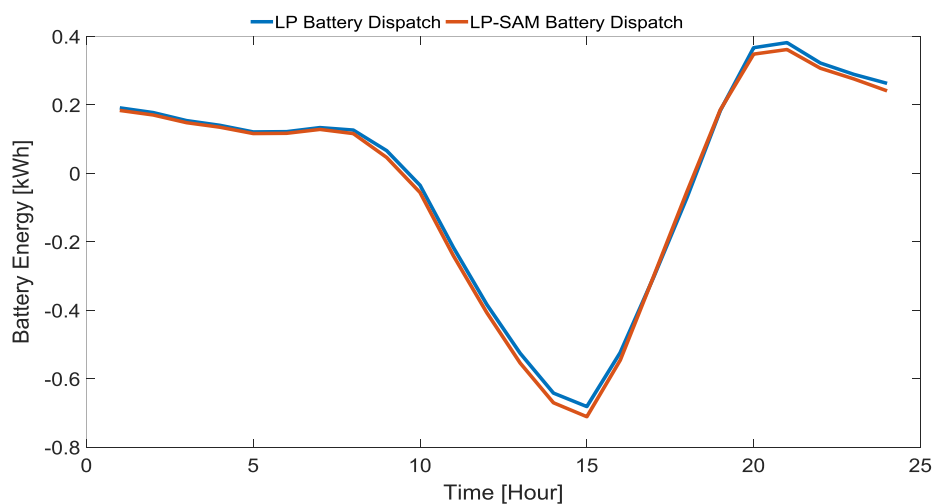
Figure 23: Annual 24-hour average dispatch between the LP model and the combined LP-SAM model with a 9.3 kWh Storage Capacity

83

The existence of such phenomenon may also be verified with the aid of Figure 23, where the annual daily average of the battery's ideal profile is slightly higher than the more realistic dispatch. Nevertheless, it can clearly be observed that the profile of the LP model case is again in a very good agreement with the globally accepted as realistic case of SAM, indicating a very good precision for a valid model. The result of this comparison suggests that the combined LP-SAM model yields a probably even more accurate model for implementation (an important novel feature of the proposed method).

4.3 Annual Net-grid Energy, Self-Consumption and Primary Energy Consumption

Maintaining low primary energy needs in buildings and simultaneously maximizing the consumption from buildings' RES is vital and a key requirement toward nZEBs. In this regard and from the electrical point of view, the concept of balancing (or equating) the annual load consumption with the annual PV generation by merely sizing the system, either with or without storage, does not necessarily achieve the best solution for maintaining the import energy at low levels, without making use of a global optimization dispatch scheme. Even if a building is energy efficient and the annual aggregated PV generation is very close to the annual aggregated load consumption – a common design approach for nZEBs – a noticeable daily imbalance may exist, as shown with the grey line in Figure 24.
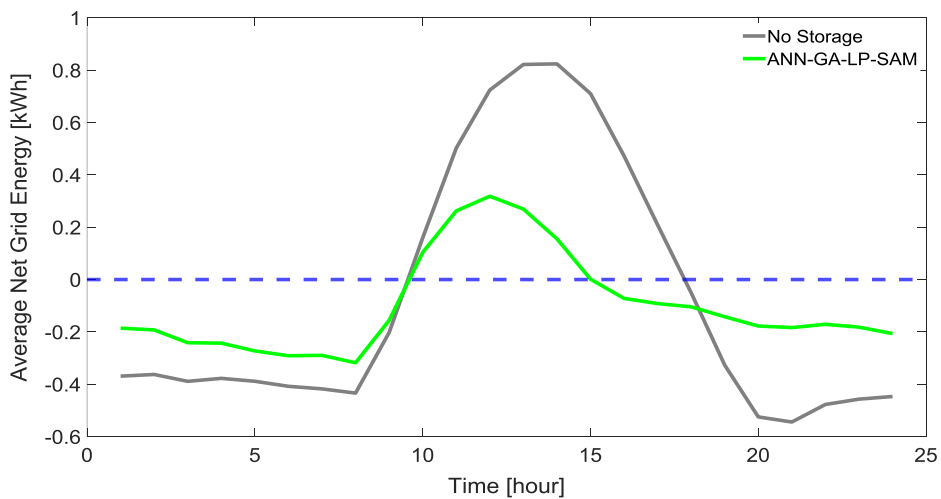
Figure 24: Annual per daily-hour average profile of net grid energy with 9.3 kWh storage capacity

Therein, the annual per daily-hour average profiles of the net grid energy are presented for two different cases: (i) when no storage is used, and (ii) when daily global optimization dispatch, with storage, is utilized. When no storage is used, the REG is self-consumed only when there is PV generation and hence, with the surplus energy exported to the grid, whereas in the second case, the nZEB requirement is further achieved with the initial curve flattened, smoothed and maintained closer to the reference line of 0 kWh. This indicates that the proposed method for managing the nearly zero net-grid energy consumption, daily, may be in line with 2010/31/EU Directive requirement.

To further highlight the need of a daily global optimization scheme, the proposed model is compared with a conventional default controller of SAM, known as Target Controller [86]. As already mentioned in section 3.1.4, this controller aims to maintain the grid energy at a predefined by the user level and thus, it is possible to preserve the net-grid energy to low levels by simply defining a level of 0 kWh for each timestep of the simulation period.
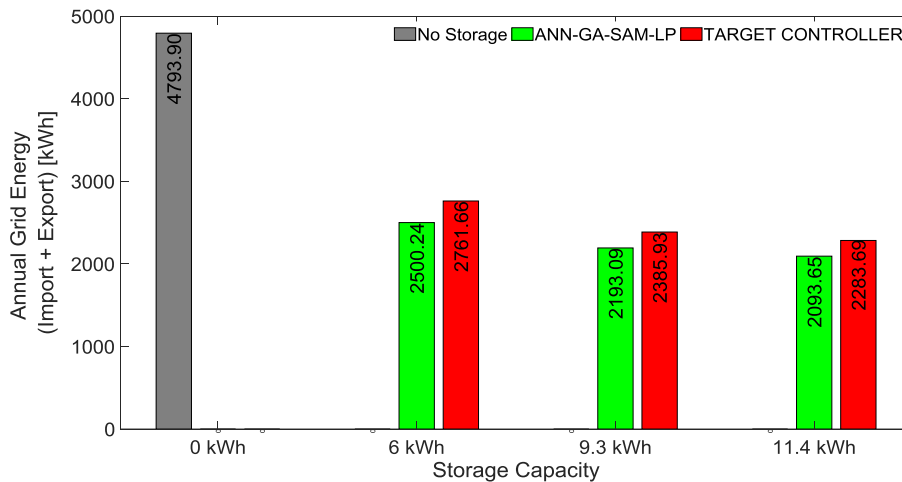
Figure 25: Comparison of the annual Total Grid Energy (Import + Export) for cases without storage, with Target Controller and with the proposed model, for storage capacity cases of 6 kWh, 9.3 kWh and 11.4 kWh

For comparison purposes, a parametric study is also conducted in order to observe the effect of three different storage sizes of 6 kWh, 9.3 kWh and 11.4 kWh – found from residential batteries available in the market – leaving all parameters (see Table 7) other

than the storage capacity unaltered. As a first outcome of the parametric study, Figure 25 illustrates the annual aggregated usage of the grid, described by the sum of the annual import and export energies. In this analysis, the three cases studied correspond to a scenario when (i) no storage is used, (ii) when storage is used and dispatched by a conventional controller (Target Controller) and (iii) when storage is used and dispatched by the proposed global optimization scheme (ANN-GA-LP-SAM).

As can be observed, and as expected, without storage the annual aggregated usage of grid is much higher, compared to the cases when storage is used. The case with Target Controller returns an average (considering all battery sizes) reduction of ~48%. Finally, the case making use of the proposed global optimization scheme exhibits a further average reduction of 5% (total average: ~53%), thus indicating the dominance of a daily global optimization dispatch. Regardless of the further reduction in the aggregated usage of the grid as the battery sizes increases, as shown in Figure 25, it is found that with a battery size of 11.4 kWh a minimum usage of ~2090 kWh is achieved. However, it was found that the use of larger batteries does not imply further improvements, due to the nature of the studied PV and load.
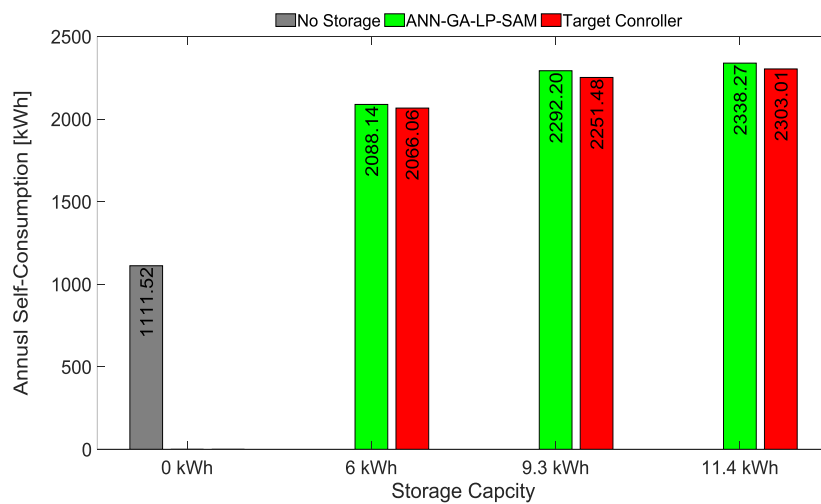
Figure 26: Self consumption for cases without storage, with Target Controller and with the proposed model, for storage capacity cases of 6 kWh, 9.3 kWh and 11.4 kWh

Lastly, the outcome presented in Figures 24 and 25 is reflected in Figure 26, where the annual self-consumption seems to be enhanced by application of the proposed model. Compared to the case without storage, self-consumption is almost double on average

when storage is dispatched with Target Controller, and a further average increase of 3% is achieved when storage is dispatched by the proposed paradigm.
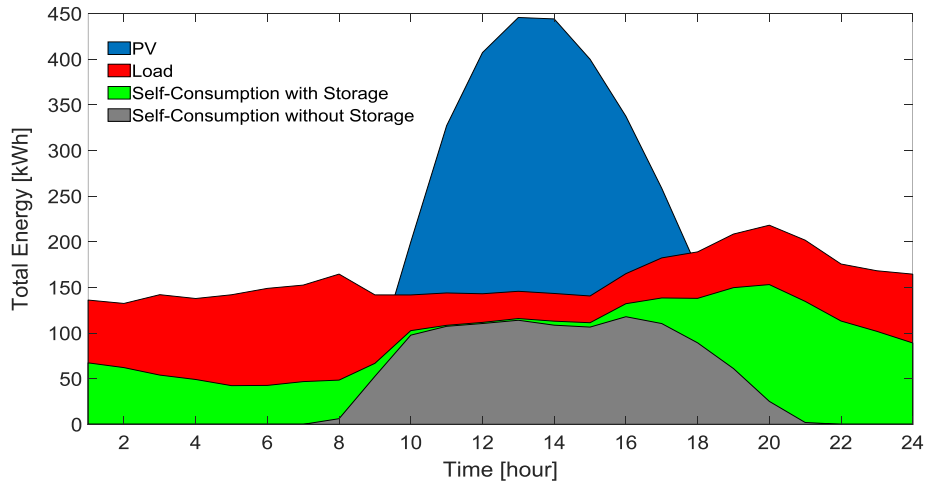
Figure 27: Annual per daily-hour Self-Consumption without storage and with a 9.3kWh storage, shown with PV generation and building load
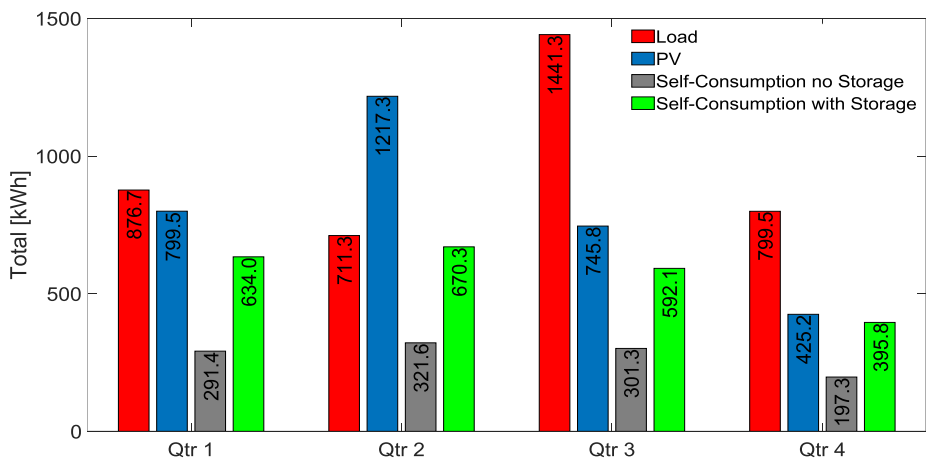
Figure 28: Self-Consumption by Quarter, for the year studied, without storage and with a storage of 9.3 kWh capacity, shown with PV generation and building load

Furthermore, taking the high mismatch between the PV generation and load consumption into consideration (presented in Figures 20 and 21 and further verified in Figure 24), the significant enhancement – by the use of storage – of self-consumption in each hour and seasons, throughout the year, are demonstrated respectively in Figures 27

and 28. It is clearly shown here that without storage there is a strong daily mismatch between PV and load (Figure 27) and thus a higher import energy.

On the other hand, self-consumption is increased, as shown in Figure 28, when storage and daily global optimization dispatch are considered, with the storage bringing self-consumption closer to either the load consumption or the PV generation, in each of the annual quarters. Finally, the extended self-consumption throughout the day, due to the battery behaviour driven by the proposed model, may be observed in Figure 27. It is clearly observed here that the battery stores the PV surplus energy and supplies the load when there is not enough PV generation. Owing to this dispatch scheme and as one may conclude through Figure 28, 60% of the annual consumption is covered by the PV.

Finally, for proving the enhancement of the nZEB levels of a building with the aid of the proposed approach, the primary energy consumption of the building throughout the annual simulation period is calculated and compared. According to a primary energy example calculation presented in the "Technical Guidance for nZEBs", published by the Cyprus Ministry of Energy, a similar calculation may be attempted for verifying the outperformance of the proposed methodology in maintaining and enhancing the nZEB levels of a building. According to the example, the primary energy consumption of a building may be calculated by the difference of the grid energy needs and the energy self-consumed via the integrated RES such as PVs. Finally, by multiplying the resultant final energy with the final to primary energy conversion factor, the primary energy consumption of the building, in $kWh/m^2/year$, may be obtained.

Table 8 shows the primary energy consumption results for a 1-bedroom apartment case of $50m^2$, located in Limassol, Cyprus and built in 2008, before the current legislation for nZEBs in Cyprus. The measured data corresponds to the period of 23/01/2019 – 22/01/2020 and as it was found the apartment consumed 60 kg of Liquefied Petroleum Gas (LPG) for heating, during a 4-month winter period (December – April). Moreover, the rest of the energy needs – i.e. cooling, lighting, cooking, domestic hot water and appliances – are supplied by electricity and it was measured that those needs correspond to a final electrical energy of 2299.76 kWh. By taking into account that a 1 kg of LPG contains 14.019 kWh of primary energy [94] and the final to primary energy conversion factor for electricity in Cyprus is 2.7 [95], the primary energy consumption of the apartment, during the measured period, can be calculated when: i) no PV is used; ii) a PV is used; iii) PV along with a battery is used and the proposed method is applied; iv)

PV along with a battery is used and the Target Controller of SAM is applied. The table shows that the proposed model outperforms a rule-based algorithm as the Target Controller, with the outcomes of both methods in a good agreement; hence, indicating once again the validity of the proposed model.

Table 8: Primary Energy consumption calculation of a 50 m^2 1-bedroom apartment for the period 23/01/2019 – 22/01/2020

	no PV	PV	PV+BESS (TARGET CONTROLLER)	PV+ BESS (ANN-GA-LP-SAM)
LPG - Heating Primary Energy consumption (kWh)	841.14	841.14	841.14	841.14
All other energy needs from electricity (kWh)	2299.76	1774.50	708.08	705.87
Final to Primary Energy conversion factor (electricity)	2.70	2.70	2.70	2.70
Building Area	50.00	50.00	50.00	50.00
Primary Energy Consumption (kWh/year)	7050.49	5632.30	2752.96	2746.99
Primary Energy Consumption (kWh/m^2/year)	**141.01**	**112.65**	**55.06**	**54.94**

Notes:

i)   The PV system is 1.5 kWp and generates ~2277 kWh/year

ii)   For the sake of simplicity, the battery size was kept to 9.3 kWh

iii) The scenario with the PV only is based on a simple if-else rule. If (Load – PV > 0) then (import energy = load – PV) else (import energy = 0). If (Load – PV < 0) then (export energy = $\lvert$ load - PV $\rvert$) else (export energy = 0)

Particularly, the 1-bedroom apartment has a primary energy consumption of 141.01 kWh/m^2/year and 112.65 kWh/m^2/year without and with PV, respectively and according to the Cyprus 121/2020 Decree for the nZEBs consumption, new buildings from 2020 onwards shall have a primary energy consumption of 100 kWh/m^2/year. Although the apartment was built in 2008 – before the 2020 nZEB legislation – it is possible to further reduce its primary energy consumption and maintain it below the current thresholds, simply using a Battery Energy Storage System (BESS) along with a PV and the proposed method. Of course, passive measures – such as thermal insulation and so on – may also be applied for reducing the energy needs and allowing smaller PV and battery sizes.

4.4   Potential application of the proposed method

For enabling the enhancement of a nZEB's energy autonomy, a potential application of the proposed method may be achieved through a step-by-step procedure. Firstly, historical data of GHI, PV production and load consumption profiles, at the location of interest and for a sufficient period of time (e.g. one year), are essential for properly training the proposed ANN models. Measurements regarding GHI may be provided either by local Meteorology Authorities or downloaded from an online solar radiation platform, such as PVGIS, which is the EU's official solar radiation database enabling access to hourly radiation profiles and other weather-related data at any location across Europe. Load consumption measurements may become available using either existing infrastructure of the building's installation such as Smart Meters or digital energy meters, such as efergy®, installed after the main circuit breaker of the installation. Finally, PV measurements could be either accessed through the embedded software of the PV system's inverter, or accurately estimated through a professional PV system design tool such as SAM. Nevertheless, it is recommended for the PV generation data to be obtained directly from the inverter, for a more accurate PV profile. Once a proper ANN training and validation is achieved and GHI forecasts are available through local Meteorology Authorities or Meteorology Companies (e.g. SOLARGIS), then the ANNs are ready to be embedded in the main algorithm.

For enabling the battery dispatch to be derived for the next day, different parameterizations and set ups are needed within the ANN algorithm. Specifically, with the aid of existing programming interfaces (e.g. APIs), an extension of the main algorithm may be developed for enabling the automatic download of the next day's GHI forecast (e.g. from PVGIS platform) and the previous day's PV generation and load consumption profiles (e.g. from inverter and efergy® meter). The ANN forecasting algorithm can then be set up to download the aforementioned data and forecast the next day's PV generation and load consumption profiles automatically, at the end of each current day (e.g. at 23:00).

Once the forecasts of the PV and load profiles have been provided by the ANN algorithm, the GA-LP-SAM algorithm may now calculate the battery's next 24-hour dispatch, as presented in Chapter 3. Moreover, once the measurements of the PV and the load are available at each current timestep (e.g. hour), the GA-LA-SAM algorithm is

ready to update and recalculate the 24-hour dispatch. Then, the fraction of the algorithm developed to communicate with the battery can send the command to the battery's controller requesting the desired energy from the battery for the current timestep – i.e., charge, discharge or remain idle. Finally, this procedure is repeated for each timestep of the algorithm (e.g. every hour, every 30 minutes, and so on), with the algorithm returning to its initial state (forecasting) at the final timestep of the current day – i.e., 23:00, 23:30 and so on.

5 Conclusions

In general, the plethora of proposals for moving towards nZEBs address the determination of the building parameter during the design and construction phase of such buildings, and different approaches focusing on the daily BEM optimization mostly concentrate in themes related to financial costs minimization. Hence, a model integrating the nZEB concept during the daily operation of the building was yet to be proposed.

Based on this fact, this Thesis proposed an approach, which mainly utilizes Convex Optimization for an nZEB's daily energy optimization, via storage and integrated PVs. For being in line with the EU nZEB related Directive, a nearly zero net-grid energy criterion is integrated within the optimization problem, in order to achieve the flattering (nearly zeroing) of the grid energy usage of a building, in a daily, optimum and adaptive manner. Furthermore, having in mind the rising trend of electrification in buildings, the inspiration of this work also rises from the fact that, a simple, yet very efficient optimization dispatch model in line with storage, can highly assist the design measures already taken and thus, further contribute toward the implementation of nZEBs.

To this extent, this work has aimed at covering the need for a new model able to manage an electrical storage system with an integrated PV system, on a daily basis. Such management allows the minimization of the primary energy consumption, from the electrical point of view, through a daily global optimization method within a building. This has been achieved through a novel approach holistically integrating ANNs' forecasts with a hybrid and adaptive GA-LP optimization approach and a battery realistic dispatch software (SAM). The current study showed the significant reduction of a building's aggregated grid usage, throughout the year, in relation to the sum of import and export energies. Owing to this minimization, the primary energy consumption of the building is further reduced, allowing the nZEB levels to be maintained, while the building is in operation.

It must be stressed that the model proposed in this Thesis has mainly focused on zeroing the daily net electrical energy, as it is expected for nZEBs. In the context of nZEB definitions, electricity prices, investment costs, operation and maintenance costs and so on, do not necessarily act as a low energy target and remain beyond the scope of this study. To use such factors/parameters in a problem, as the one presented here, would

limit its possible findings as the solutions to a specific and not a global problem, since these factors strongly rely on subsidies, loans, surplus energy sell price, electricity buying price, PV and battery prices, and so forth. Some of these – e.g., subsidies – may not even be available in many countries and, more importantly, they may change in an unpredictable way, based on a country's amendment on energy policies and/or energy economics. Hence, an optimized solution based on today's situation may not be suitable for future times. On the other hand, addressing the sheer energy size and not its cost toward achieving low energy targets is a common and global problem that can be adopted irrespective of costs and prices. Besides, it was shown by many authors that electrical storage and RES prices are continually falling, leading to the increased adoption and utilization of such technologies.

Returning to this study's findings, with the battery essentially acting as an "extension" of the PV generation throughout the day, a parametric study conducted using three different storage sizes has shown that – within the framework of the base study – the average self-consumption can increase by a factor of two, the annual aggregated grid usage (import + export energies) can be reduced by 53% on average, the annual load can be mostly supplied by the PV at a rate of 60% and the building's annual primary energy consumption can be significantly reduced, as compared to the no-storage scenario. Finally, by accurately forecasting the PV generation and the load consumption (RMSE of 11% for PV and RMSE of 6% for load) and optimally driving the coupled LP-SAM model through GA, an adaptiveness of the model in every timestep is observed, leading to better outcomes compared to a conventional, rule-based, dispatch model.

Based on the findings of this research, the usefulness of a practical application of the proposed approach in each individual building consists in contributing toward an energy efficient system. Particularly, aiming the enhancement of an nZEB's energy autonomy and its daily zeroing of the net grid energy, it is possible in a district to simultaneously achieve a higher penetration of Distributed Energy Resources (DER) and a lower energy exchange between the buildings and the grids. This will also allow existing grids to adapt to these challenges, without the need of introducing expensive and complex mechanisms from the Grid Operators. Yet, this remains a challenge, as current policies within the EU need to be altered in order to for support and enable such schemes. In this regard, researchers and professionals may be influenced toward the development of new

controllers, in order to meet the desired energy levels of an nZEB, on a daily basis and hence, throughout the year.

6 Future Work

Further to the step-by-step procedure described in section 4.4 and the study of the effect of prediction error on optimality, the model presented in this Thesis may be used as a basis for a potential future application. Nevertheless, for a complete and integrated real application, fields such as battery aging and degradation along with the integration of the proposed approach on existing technologies (e.g. Field Programmable Gate Arrays – FPGA) are essential.

With these kind of approaches existing PV systems may become, from passive generation systems, active generation systems, by adapting to users' energy needs. Thus, any need of users to have expert knowledge in fields such as Artificial Intelligence and Convex Optimization will not be required.
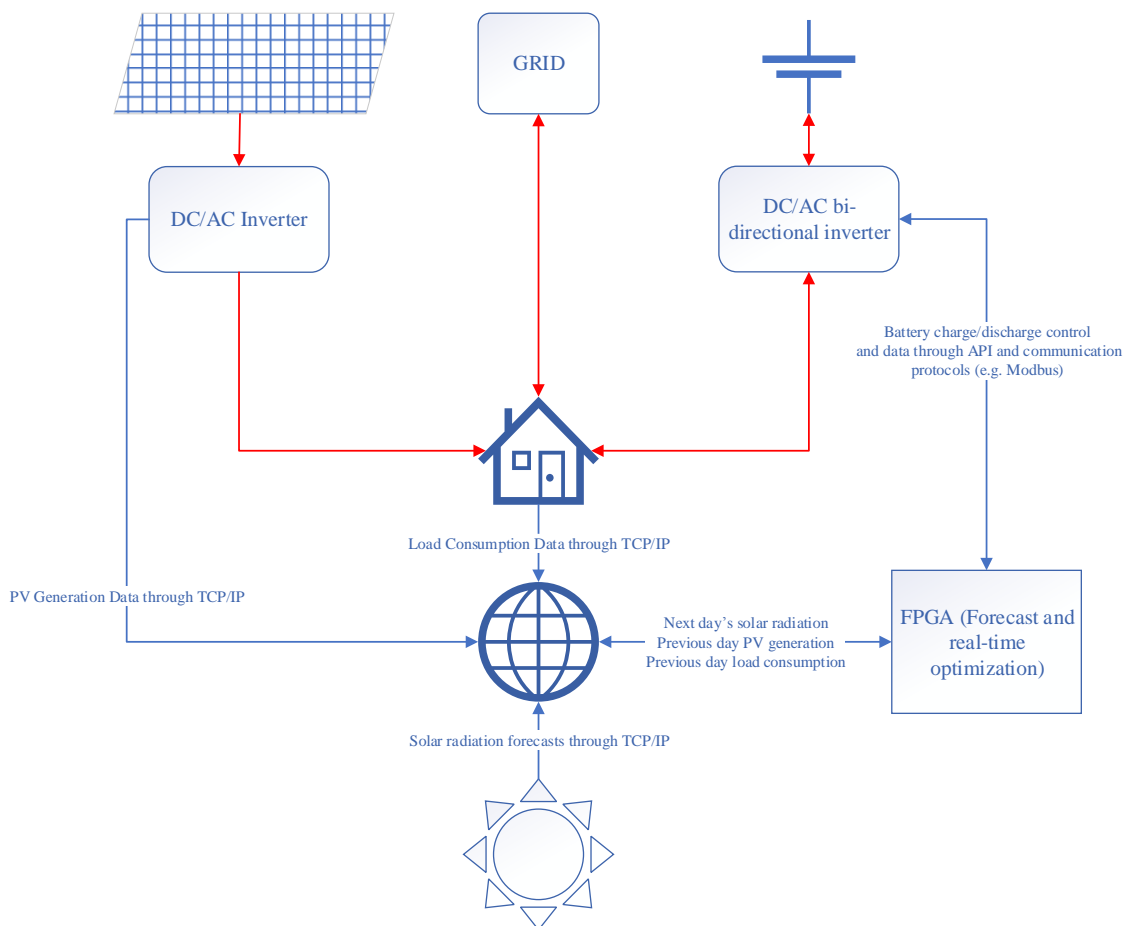
Figure 29: Proposed future work

Figure 29 proposes a potential real-life application of the hybrid optimization model presented in this Thesis. In this figure, power flow (red lines) along with data flow (blue lines) are shown. Within this context, energy may be exchanged between the grid, battery, load and PV and different data such as current and historical PV generation and load consumption along with solar radiation forecasts may be available through the web. Additionally, a FPGA or similar device may be used to collect the web-based data and decide the updated battery charge or discharge, based on the data aforementioned as well as data related to battery health, such as energy throughput, remaining capacity, remaining charge, charging/discharging cycles and so on. Data collection and command signalling may be used via standard programming interfaces (e.g. API) and communication protocols (TCP/IP, Modbus and so on). Nevertheless, such an application requires a more considerable effort and analysis and constitutes a naturally consequent study for the future.

REFERENCES

[1]   European Commission, "Proposal for a DIRECTIVE OF THE EUROPEAN PARLIAMENT AND OF THE COUNCIL," 2016.

[2]   IEA, "IEA World Energy Balances 2019," 2019. https://www.iea.org/subscribe-to-data-services/world-energy-balances-and-statistics (accessed May 23, 2020).

[3]   Y. Lu, S. Wang, and K. Shan, "Design optimization and optimal control of grid-connected and standalone nearly/net zero energy buildings," *Appl. Energy*, vol. 155, pp. 463–477, 2015, doi: 10.1016/j.apenergy.2015.06.007.

[4]   Ipsos Belgium and Navigant, "Comprehensive study of building energy renovation activities and the uptake of nearly zero-energy buildings in the EU Final report," 2019. [Online]. Available: https://ec.europa.eu/energy/sites/ener/files/documents/1.final_report.pdf.

[5]   J. Figueiredo and J. Martins, "Energy Production System Management - Renewable energy power supply integration with Building Automation System," *Energy Convers. Manag.*, vol. 51, no. 6, pp. 1120–1126, 2010, doi: 10.1016/j.enconman.2009.12.020.

[6]   A. Nottrott, J. Kleissl, and B. Washom, "Energy dispatch schedule optimization and cost benefit analysis for grid-connected, photovoltaic-battery storage systems," *Renew. Energy*, vol. 55, pp. 230–240, 2013, doi: 10.1016/j.renene.2012.12.036.

[7]   R. Hanna, J. Kleissl, A. Nottrott, and M. Ferry, "Energy dispatch schedule optimization for demand charge reduction using a photovoltaic-battery storage system with solar forecasting," *Sol. Energy*, vol. 103, pp. 269–287, 2014, doi: 10.1016/j.solener.2014.02.020.

[8]   X. Chen, T. Wei, and S. Hu, "Uncertainty-aware household appliance scheduling considering dynamic electricity pricing in smart home," *IEEE Trans. Smart Grid*, vol. 4, no. 2, pp. 932–941, 2013, doi: 10.1109/TSG.2012.2226065.

[9]   L. T. Youn and S. Cho, "Optimal Operation of Energy Storage Using Linear Programming Technique," in *World Congress on Engineering and Computer Science*, 2009, vol. I.

97

[10] G. S. Georgiou, P. Christodoulides, P. Nikolaidis, L. Lazari, and P. Christodoulides, "A Genetic Algorithm Driven Linear Programming for Battery Optimal Scheduling in nearly Zero Energy Buildings," in *Proceedings - 2019 54th International Universities Power Engineering Conference, UPEC 2019*, Sep. 2019, pp. 1–6, doi: 10.1109/UPEC.2019.8893514.

[11] M. Rahmani-Andebili and H. Shen, "Energy scheduling for a smart home applying stochastic model predictive control," in *2016 25th International Conference on Computer Communications and Networks, ICCCN 2016*, 2016, pp. 3–8, doi: 10.1109/ICCCN.2016.7568516.

[12] E. Oh, S.-Y. Son, H. Hwang, J.-B. Park, and K. Y. Lee, "Impact of Demand and Price Uncertainties on Customer-side Energy Storage System Operation with Peak Load Limitation," *Electr. Power Components Syst.*, vol. 43, no. 16, pp. 1872–1881, 2015, doi: 10.1080/15325008.2015.1057883.

[13] Z. Wu, H. Tazvinga, and X. Xia, "Demand side management of photovoltaic-battery hybrid system," *Appl. Energy*, vol. 148, pp. 294–304, 2015, doi: 10.1016/j.apenergy.2015.03.109.

[14] A. Dargahi, S. Ploix, A. Soroudi, and F. Wurtz, "Optimal household energy management using V2H flexibilities," *COMPEL - Int. J. Comput. Math. Electr. Electron. Eng.*, vol. 33, no. 3, pp. 777–792, 2014, doi: 10.1108/COMPEL-10-2012-0223.

[15] A. Leon-garcia and A.-H. Mohsenian-Rad, "Optimal Residential Load Control With Price Prediction in Real-Time Electricity Pricing Environments," *IEEE Trans. Smart Grid*, vol. 1, no. 2, pp. 120–133, 2010.

[16] X. Wu, X. Hu, Y. Teng, S. Qian, and R. Cheng, "Optimal integration of a hybrid solar-battery power source into smart home nanogrid with plug-in electric vehicle," *J. Power Sources*, vol. 363, pp. 277–283, 2017, doi: 10.1016/j.jpowsour.2017.07.086.

[17] Y. J. Wen and A. M. Agogino, "Wireless networked lighting systems for optimizing energy savings and user satisfaction," in *IEEE wireless hive networks conference*, 2008, pp. 1–6, [Online]. Available: http://ieeexplore.ieee.org/xpls/abs_all.jsp?arnumber=4629493.

[18]   D. Zhang, N. Shah, and L. G. Papageorgiou, "Efficient energy consumption and operation management in a smart building with microgrid," *Energy Convers. Manag.*, vol. 74, pp. 209–222, 2013, doi: 10.1016/j.enconman.2013.04.038.

[19]   F. De Angelis, M. Boaro, D. Fuselli, S. Squartini, F. Piazza, and Q. Wei, "Optimal home energy management under dynamic electrical and thermal constraints," *IEEE Trans. Ind. Informatics*, vol. 9, no. 3, pp. 1518–1527, 2013, doi: 10.1109/TII.2012.2230637.

[20]   D. Thomas, O. Deblecker, and C. S. Ioakimidis, "Optimal operation of an energy management system for a grid-connected smart building considering photovoltaics' uncertainty and stochastic electric vehicles' driving schedule," *Appl. Energy*, pp. 1–19, 2017, doi: 10.1016/j.apenergy.2017.07.035.

[21]   K. Paridari, A. Parisio, H. Sandberg, and K. H. Johansson, "Robust Scheduling of Smart Appliances in Active Apartments With User Behavior Uncertainty," *IEEE Trans. Autom. Sci. Eng.*, vol. 13, no. 1, pp. 247–259, 2016, doi: 10.1109/TASE.2015.2497300.

[22]   A. S. O. Ogunjuyigbe, T. R. Ayodele, and O. E. Oladimeji, "Management of loads in residential buildings installed with PV system under intermittent solar irradiation using mixed integer linear programming," *Energy Build.*, vol. 130, pp. 253–271, 2016, doi: 10.1016/j.enbuild.2016.08.042.

[23]   J. K. Gruber, F. Huerta, P. Matatagui, and M. Prodanović, "Advanced building energy management based on a two-stage receding horizon optimization," *Appl. Energy*, vol. 160, pp. 194–205, 2015, doi: 10.1016/j.apenergy.2015.09.049.

[24]   A. Anvari-Moghaddam, H. Monsef, and A. Rahimi-Kian, "Cost-effective and comfort-aware residential energy management under different pricing schemes and weather conditions," *Energy Build.*, vol. 86, pp. 782–793, 2015, doi: 10.1016/j.enbuild.2014.10.017.

[25]   M. Rastegar, M. Fotuhi-Firuzabad, and M. Lehtonen, "Home load management in a residential energy hub," *Electr. Power Syst. Res.*, vol. 119, pp. 322–328, 2015, doi: 10.1016/j.epsr.2014.10.011.

[26]   P. Liu, Y. Fu, and A. Kargarian Marvasti, "Multi-stage stochastic optimal operation of energy-efficient building with combined heat and power system,"

Electr. Power Components Syst., vol. 42, no. 3–4, pp. 327–338, 2014, doi: 10.1080/15325008.2013.862324.

[27] H. Wu, A. Pratt, and S. Chakraborty, "Stochastic optimal scheduling of residential appliances with renewable energy sources," in *Power & Energy Society General Meeting*, 2015, pp. 1–5, doi: 10.1109/PESGM.2015.7286584.

[28] A. Al Hasib, N. Nikitin, and L. Natvig, "Cost-comfort balancing in a smart residential building with bidirectional energy trading," in *Sustainable Internet and ICT for Sustainability, SustainIT 2015*, 2015, pp. 1–6, doi: 10.1109/SustainIT.2015.7101366.

[29] C. Rottondi, M. Duchon, D. Koss, G. Verticale, and B. Sch, "An Energy Management System for a Smart Office Environment," in *Networked Systems (NetSys), 2015 International Conference and Workshops*, 2015, pp. 11667–11684, doi: 10.3390/en81011667.

[30] M. H. Amini, J. Frye, M. D. Ilic, and O. Karabasoglu, "Smart residential energy scheduling utilizing two stage Mixed Integer Linear Programming," *2015 North Am. Power Symp. NAPS 2015*, pp. 1–6, 2015, doi: 10.1109/NAPS.2015.7335100.

[31] M. Beaudin, H. Zareipour, A. Kiani Bejestani, and A. Schellenberg, "Residential energy management using a two-horizon algorithm," *IEEE Trans. Smart Grid*, vol. 5, no. 4, pp. 1712–1723, 2014, doi: 10.1109/TSG.2014.2310395.

[32] D. Brunelli and L. Tamburini, "Residential load scheduling for energy cost minimization," in *ENERGYCON 2014 - IEEE International Energy Conference*, 2014, pp. 675–682, doi: 10.1109/ENERGYCON.2014.6850499.

[33] G. T. Costanzo, G. Zhu, M. F. Anjos, and G. Savard, "A system architecture for autonomous demand side load management in smart buildings," *IEEE Trans. Smart Grid*, vol. 3, no. 4, pp. 2157–2165, 2012, doi: 10.1109/TSG.2012.2217358.

[34] Z. Chen, L. Wu, and Y. Fu, "Real-time price-based demand response management for residential appliances via stochastic optimization and robust optimization," *IEEE Trans. Smart Grid*, vol. 3, no. 4, pp. 1822–1831, 2012, doi: 10.1109/TSG.2012.2212729.

[35] M. Tasdighi, P. Jambor Salamati, A. Rahimikian, and H. Ghasemi, "Energy

management in a smart residential building," in *Environment and Electrical Engineering EEEIC 2012 11th International Conference on*, 2012, pp. 128–133, doi: 10.1109/eeeic.2012.6221559.

[36] C. Clastres, T. T. Ha Pham, F. Wurtz, and S. Bacha, "Ancillary services and optimal household energy management with photovoltaic production," *Energy*, vol. 35, no. 1, pp. 55–64, 2010, doi: 10.1016/j.energy.2009.08.025.

[37] E. Georges, J. E. Braun, and V. Lemort, "A general methodology for optimal load management with distributed renewable energy generation and storage in residential housing," *J. Build. Perform. Simul.*, vol. 10, no. 2, pp. 224–241, 2017, doi: 10.1080/19401493.2016.1211738.

[38] Z. Xu, G. Hu, C. J. Spanos, and S. Schiavon, "PMV-based event-triggered mechanism for building energy management under uncertainties," *Energy Build.*, vol. 152, pp. 73–85, 2017, doi: 10.1016/j.enbuild.2017.07.008.

[39] B. Chai, W. Tushar, N. U. Hassan, C. Yuen, and Z. Yang, "Managing energy consumption in buildings through offline and online control of HVAC systems," in *IEEE Region 10 Annual International Conference, Proceedings/TENCON*, 2016, pp. 3368–3373, doi: 10.1109/TENCON.2016.7848677.

[40] H. Ren, Q. Wu, W. Gao, and W. Zhou, "Optimal operation of a grid-connected hybrid PV/fuel cell/battery energy system for residential applications," *Energy*, vol. 113, pp. 702–712, 2016, doi: 10.1016/j.energy.2016.07.091.

[41] F. Y. Melhem, O. Grunder, Z. Hammoudan, and N. Moubayed, "Optimization and Energy Management in Smart Home Considering Photovoltaic, Wind, and Battery Storage System With Integration of Electric Vehicles," *Can. J. Electr. Comput. Eng.*, vol. 40, no. 2, pp. 128–138, 2017, doi: 10.1109/CJECE.2017.2716780.

[42] I. Sharma *et al.*, "A modeling framework for optimal energy management of a residential building," *Energy Build.*, vol. 130, pp. 55–63, 2016, doi: 10.1016/j.enbuild.2016.08.009.

[43] F. Brahman and S. Jadid, "Optimal energy management of hybrid CCHP and PV in a residential building," in *2014 19th Conference on Electrical Power Distribution Networks (EPDC)*, 2014, pp. 19–24, doi:

10.1109/EPDC.2014.6867492.

[44]   Z. Xu, Q. Jia, X. Guan, J. Wu, D. Wang, and S. Chen, "Optimal Scheduling of Storage Devices for Building Energy Saving," in *Intelligent Control and Automation (WCICA), 2012 10th World Congress on*, 2012, pp. 2393–2398, doi: 10.1109/WCICA.2012.6358273.

[45]   M. B. Tellez Molina, T. Gafurov, and M. Prodanovic, "Proactive control for energy systems in Smart Buildings," in *Innovative Smart Grid Technologies (ISGT Europe), 2011 2nd IEEE PES International Conference and Exhibition on*, 2011, pp. 1–8.

[46]   T. T. Ha Pham, F. Wurtz, and S. Bacha, "Optimal operation of a PV based multi-source system and energy management for household application," 2009, doi: 10.1109/ICIT.2009.4939701.

[47]   A. Barbato *et al.*, "House Energy Demand Optimization in Single and Multi-User Scenarios," in *2011 IEEE International Conference on Smart Grid Communications (SmartGridComm)*, 2011, pp. 345–350.

[48]   B. Pickering, S. Ikeda, R. Choudhary, and R. Ooka, "Comparison of Metaheuristic and Linear Programming Models for the Purpose of Optimising Building Energy Supply Operation Schedule," in *proceedings of the 12th REHVA World*, 2016, vol. 6, [Online]. Available: http://vbn.aau.dk/files/233775414/paper_529.pdf.

[49]   T. Hubert and S. Grijalva, "Modeling for residential electricity optimization in dynamic pricing environments," *IEEE Trans. Smart Grid*, vol. 3, no. 4, pp. 2224–2231, 2012, doi: 10.1109/TSG.2012.2220385.

[50]   C. Wang, Y. Zhou, B. Jiao, Y. Wang, W. Liu, and D. Wang, "Robust optimization for load scheduling of a smart home with photovoltaic system," *Energy Convers. Manag.*, vol. 102, pp. 247–257, 2015, doi: 10.1016/j.enconman.2015.01.053.

[51]   B. Gao, W. Zhang, Y. Tang, M. Hu, M. Zhu, and H. Zhan, "Game-theoretic energy management for residential users with dischargeable plug-in electric vehicles," *Energies*, vol. 7, no. 11, pp. 7499–7518, 2014, doi: 10.3390/en7117499.

[52] H. Tazvinga, X. Xia, and J. Zhang, "Minimum cost solution of photovoltaic-diesel-battery hybrid power systems for remote consumers," *Sol. Energy*, vol. 96, pp. 292–299, 2013, doi: 10.1016/j.solener.2013.07.030.

[53] X. Jin, K. Baker, D. Christensen, and S. Isley, "Foresee: A user-centric home energy management system for energy efficiency and demand response," *Appl. Energy*, vol. 205, pp. 1583–1595, 2017, doi: 10.1016/j.apenergy.2017.08.166.

[54] R. Fachrizal and J. Munkhammar, "Improved Photovoltaic Self-Consumption in Residential Buildings with Distributed and Centralized Smart Charging of Electric Vehicles," *Energies*, vol. 13, no. 5, 2020, doi: 10.3390/en13051153.

[55] D. L. Ha, H. Joumaa, S. Ploix, and M. Jacomino, "An optimal approach for electrical management problem in dwellings," *Energy Build.*, vol. 45, pp. 1–14, 2012, doi: 10.1016/j.enbuild.2011.11.027.

[56] K. M. Tsui and S. C. Chan, "Demand Response Optimization for Smart Home Scheduling Under Real-Time Pricing," *IEEE Trans. Smart Grid*, vol. 3, no. 4, pp. 1812–1821, 2012.

[57] Y. Zong, L. Mihet-Popa, D. Kullmann, A. Thavlov, O. Gehrke, and H. W. Bindner, "Model predictive controller for active demand side management with PV self-consumption in an intelligent building," in *IEEE PES Innovative Smart Grid Technologies Conference Europe*, 2012, pp. 1–8, doi: 10.1109/ISGTEurope.2012.6465618.

[58] A. Ashouri, S. S. Fux, M. J. Benz, and L. Guzzella, "Optimal design and operation of building services using mixed-integer linear programming techniques," *Energy*, vol. 59, pp. 365–376, 2013, doi: 10.1016/j.energy.2013.06.053.

[59] M. Stadler, A. Siddiqui, C. Marnay, H. Aki, and J. Lai, "Control of greenhouse gas emissions by optimal DER technology investment and energy management in zero-net-energy buildings," *Eur. Trans. Electr. Power*, vol. 21, no. 2, pp. 1291–1309, 2011, doi: 10.1002/etep.418.

[60] S. M. Sichilalu and X. Xia, "Optimal power dispatch of a grid tied-battery-photovoltaic system supplying heat pump water heaters," *Energy Convers. Manag.*, vol. 102, pp. 81–91, 2015, doi: 10.1016/j.enconman.2015.03.087.

[61] C. J. Meinrenken and A. Mehmani, "Concurrent optimization of thermal and electric storage in commercial buildings to reduce operating cost and demand peaks under time-of-use tariffs," *Appl. Energy*, vol. 254, no. July, p. 113630, 2019, doi: 10.1016/j.apenergy.2019.113630.

[62] A. Sani Hassan, L. Cipcigan, and N. Jenkins, "Optimal battery storage operation for PV systems with tariff incentives," *Appl. Energy*, vol. 203, pp. 422–441, 2017, doi: 10.1016/j.apenergy.2017.06.043.

[63] A. Fratean and P. Dobra, "Control strategies for decreasing energy costs and increasing self-consumption in nearly zero-energy buildings," *Sustain. Cities Soc.*, vol. 39, pp. 459–475, 2018, doi: 10.1016/j.scs.2018.03.019.

[64] Y. M. Wi, J. U. Lee, and S. K. Joo, "Electric vehicle charging method for smart homes/buildings with a photovoltaic system," *IEEE Trans. Consum. Electron.*, vol. 59, no. 2, pp. 323–328, 2013, doi: 10.1109/TCE.2013.6531113.

[65] A. Agnetis, G. Dellino, P. Detti, G. Innocenti, G. De Pascale, and A. Vicino, "Appliance operation scheduling for electricity consumption optimization," *Proc. IEEE Conf. Decis. Control*, pp. 5899–5904, 2011, doi: 10.1109/CDC.2011.6160450.

[66] Y. Wang, B. Wang, C. Chu, H. Pota, and R. Gadh, "Energy management for a commercial building microgrid with stationary and mobile battery storage," *Energy Build.*, vol. 116, pp. 141–150, 2016, doi: 10.1016/j.enbuild.2015.12.055.

[67] E. L. Ratnam, S. R. Weller, and C. M. Kellett, "An optimization-based approach to scheduling residential battery storage with solar PV: Assessing customer benefit," *Renew. Energy*, vol. 75, pp. 123–134, 2015, doi: 10.1016/j.renene.2014.09.008.

[68] H. Dagdougui, R. Minciardi, A. Ouammi, M. Robba, and R. Sacile, "Modeling and optimization of a hybrid system for the energy supply of a 'Green' building," *Energy Convers. Manag.*, vol. 64, pp. 351–363, 2012, doi: 10.1016/j.enconman.2012.05.017.

[69] H. Tazvinga, B. Zhu, and X. Xia, "Optimal power flow management for distributed energy resources with batteries," *Energy Convers. Manag.*, vol. 102, pp. 104–110, 2015, doi: 10.1016/j.enconman.2015.01.015.

[70] H. Tazvinga, B. Zhu, and X. Xia, "Energy dispatch strategy for a photovoltaic-wind-diesel-battery hybrid power system," *Sol. Energy*, vol. 108, pp. 412–420, 2014, doi: 10.1016/j.solener.2014.07.025.

[71] A. Arabali, M. Ghofrani, M. Etezadi-Amoli, M. S. Fadali, and Y. Baghzouz, "Genetic-algorithm-based optimization approach for energy management," *IEEE Trans. Power Deliv.*, vol. 28, no. 1, pp. 162–170, 2013, doi: 10.1109/TPWRD.2012.2219598.

[72] R. A. Gallego, A. Monticelli, and R. Romero, "Transmission Network Expansion Planning," *Network*, vol. 13, no. 3, pp. 822–828, 1998.

[73] L. D. Ha, S. Ploix, E. Zamai, and M. Jacomino, "Tabu search for the optimization of household energy consumption," *Proc. 2006 IEEE Int. Conf. Inf. Reuse Integr. IRI-2006*, pp. 86–92, 2006, doi: 10.1109/IRI.2006.252393.

[74] Y. Guo, M. Pan, and Y. Fang, "Optimal power management of residential customers in the smart grid," *IEEE Trans. Parallel Distrib. Syst.*, vol. 23, no. 9, pp. 1593–1606, 2012, doi: 10.1109/TPDS.2012.25.

[75] J. Li, Y. Wang, T. Cui, S. Nazarian, and M. Pedram, "Negotiation-Based Task Scheduling to Minimize User ' s Electricity Bills under Dynamic Energy Prices," pp. 1–6, 2015.

[76] N. Bigdeli, "Optimal management of hybrid PV/fuel cell/battery power system: A comparison of optimal hybrid approaches," *Renew. Sustain. Energy Rev.*, vol. 42, pp. 377–393, 2015, doi: 10.1016/j.rser.2014.10.032.

[77] H. A. Özkan, "A new real time home power management system," *Energy Build.*, vol. 97, pp. 56–64, 2015, doi: 10.1016/j.enbuild.2015.03.038.

[78] K. Paridari, A. Parisio, H. Sandberg, and K. H. Johansson, "Energy and COinf2/inf efficient scheduling of smart appliances in active houses equipped with batteries," in *IEEE International Conference on Automation Science and Engineering*, 2014, pp. 632–639, doi: 10.1109/CoASE.2014.6899394.

[79] G. S. Georgiou, P. Nikolaidis, S. A. Kalogirou, and P. Christodoulides, "A hybrid optimization approach for autonomy enhancement of nearly Zero Energy Buildings based on battery performance and Artificial Neural Networks," *Energies*, vol. in press, 2020.

[80] I. The MathWorks, "Solve linear programming problems - MATLAB linprog."
      2016, [Online]. Available:
      https://www.mathworks.com/help/optim/ug/linprog.html.

[81] S. Boyd and L. Vandenberghe, *Convex Optimization*, vol. 25, no. 3. 2010.

[82] G. S. Georgiou, P. Christodoulides, and S. A. Kalogirou, "Real-time Energy
      Convex Optimization, via electrical storage, in Buildings – A review," *Renew.
      Energy*, vol. 139, pp. 1355–1365, 2019, doi: 10.1016/j.renene.2019.03.003.

[83] R. H. Kwon, *Introduction to Linear optimization and extensions with MATLAB*.
      New York: Taylor and Francis Group, 2014.

[84] E. Rudié, A. Thornton, N. Rajendra, and S. Kerrigan, "System Advisor Model
      Performance Modeling Validation Report : Analysis of 100 sites," 2014.
      [Online]. Available: https://s3.amazonaws.com/locus-
      public/nrel/SAM_Validation_Report_final.pdf.

[85] J. Freeman, J. Whitmore, L. Kaffine, N. Blair, and A. P. Dobos, "System Advisor
      Model: Flat Plate Photovoltaic Performance Modeling Validation Report," 2013.
      [Online]. Available: http://www.nrel.gov/docs/fy14osti/60204.pdf.

[86] N. Diorio, "An Overview of the Automated Dispatch Controller Algorithms in
      the System Advisor Model," 2017. [Online]. Available:
      https://www.nrel.gov/docs/fy18osti/68614.pdf.

[87] N. Diorio *et al.*, "Technoeconomic Modeling of Battery Energy Storage in
      SAM," 2015. [Online]. Available: http://www.nrel.gov/docs/fy15osti/64641.pdf.

[88] J. Freeman, J. Whitmore, N. Blair, and A. P. Dobos, "Validation of multiple tools
      for flat plate photovoltaic modeling against measured data," 2014. doi:
      10.1109/PVSC.2014.6925304.

[89] N. Blair, A. Dobos, and N. Sather, "Case studies comparing system advisor
      model (SAM) results to real performance data," in *World Renewable Energy
      Forum, WREF 2012, Including World Renewable Energy Congress XII and
      Colorado Renewable Energy Society (CRES) Annual Conferen*, 2012, vol. 4, pp.
      2698–2703.

[90] W. Luo and Y. Li, "Benchmarking heuristic search and optimisation algorithms
      in Matlab," *2016 22nd Int. Conf. Autom. Comput. ICAC 2016 Tackling New*

Challenges Autom. Comput., pp. 250–255, 2016, doi: 10.1109/IConAC.2016.7604927.

[91] M. Mitchell, *An Introduction to Generic Algorithms*, First. London: The MIT Press, 1996.

[92] S. K. Garg, P. Konugurthi, and R. Buyya, "A linear programming-driven genetic algorithm for meta-scheduling on utility grids," *Int. J. Parallel, Emergent Distrib. Syst.*, vol. 26, no. 6, pp. 493–517, 2011, doi: 10.1080/17445760.2010.530002.

[93] P. K. Konugurthi, K. Ramakrishnan, and R. Buyya, "A Heuristic Genetic Algorithm based Scheduler for ' Clearing House Grid Broker ,'" in *Grid Computing and Distributed Systems Laboratory*, 2007, pp. 1–9.

[94] FLOGAS, "Gas conversions | Flogas." https://www.flogas.co.uk/frequently-asked-questions/gas-conversions (accessed Oct. 31, 2020).

[95] Cyprus Ministry of Energy Commerce and Industry, "Technical Guidance for buildings with nearly zero energy consumption," Nicosia, 2015. [Online]. Available: https://energy.gov.cy/assets/entipo-iliko/Τεχνικός Οδηγός ΚΣΜΚΕ_FINAL_low res single page.pdf.

[96] U. S. D. of E. (DOE) and US Department of Energy (DOE), "A Common Definition for Zero Energy Buildings," no. September, 2015, [Online]. Available: http://energy.gov/sites/prod/files/2015/09/f26/bto_common_definition_zero_energy_buildings_093015.pdf%5Cnhttp://energy.gov/eere/buildings/downloads/common-definition-zero-energy-buildings.

[97] A. J. Marszal *et al.*, "Zero Energy Building - A review of definitions and calculation methodologies," *Energy Build.*, vol. 43, no. 4, pp. 971–979, 2011, doi: 10.1016/j.enbuild.2010.12.022.

[98] J. Zuo and Z. Y. Zhao, "Green building research-current status and future agenda: A review," *Renew. Sustain. Energy Rev.*, vol. 30, pp. 271–281, 2014, doi: 10.1016/j.rser.2013.10.021.

[99] A. J. Marszal and P. Heiselberg, "Zero Energy Building (ZEB) definitions – A literature review," *Aalborg Univ.*, 2009, [Online]. Available: http://gin.confex.com/gin/2009/webprogram/Manuscript/Paper2784/Zero%5CnE

nergy%5CnBuilding%5Cndefinitions.pdf?q=project-profile-riverdale-netzero-projectedmonton-alberta.

[100] P. Torcellini, S. Pless, and M. Deru, "Zero Energy Buildings : A Critical Look at the Definition Preprint," *ACEE Summer study*, vol. 2, p. 15, 2006, doi: 10.1016/S1471-0846(02)80045-2.

[101] I. Sartori, A. Napolitano, and K. Voss, "Net zero energy buildings: A consistent definition framework," *Energy Build.*, vol. 48, pp. 220–232, 2012, doi: 10.1016/j.enbuild.2012.01.032.

[102] S. Kilkis, "A New Metric for Net-Zero Carbon Buildings," *ASME 2007 Energy Sustain. Conf.*, no. January 2007, pp. 219–224, 2007, doi: 10.1115/ES2007-36263.

[103] J. Kurnitski *et al.*, "How to define nearly net zero energy buildings nZEB," *REHVA J.*, no. May 2011, pp. 6–12, 2012.

[104] EU, "Directive 2010/31/EU of the European Parliament and of the Council of 19 May 2010 on the energy performance of buildings (recast)," *Off. J. Eur. Union*, pp. 13–35, 2010, doi: doi:10.3000/17252555.L_2010.153.eng.

[105] "Republic of Cyprus: Ministry of Energy, Commerce Industry & Tourism." Nicosia, 2020, [Online]. Available: http://www.mcit.gov.cy/mcit/mcit.nsf/dmlindex_en/dmlindex_en?OpenDocument.

[106] M. Hamdy, A. Hasan, and K. Siren, "A multi-stage optimization method for cost-optimal and nearly-zero-energy building solutions in line with the EPBD-recast 2010," *Energy Build.*, vol. 56, pp. 189–203, 2013, doi: 10.1016/j.enbuild.2012.08.023.

[107] J. Kurnitski, A. Saari, T. Kalamees, M. Vuolle, J. Niemel??, and T. Tark, "Cost optimal and nearly zero (nZEB) energy performance calculations for residential buildings with REHVA definition for nZEB national implementation," *Energy Build.*, vol. 43, no. 11, pp. 3279–3288, 2011, doi: 10.1016/j.enbuild.2011.08.033.

[108] E. Pikas, M. Thalfeldt, and J. Kurnitski, "Cost optimal and nearly zero energy building solutions for office buildings," *Energy Build.*, vol. 74, pp. 30–42, 2014, doi: 10.1016/j.enbuild.2014.01.039.

[109] P. C. P. Silva, M. Almeida, L. Bragança, and V. Mesquita, "Development of prefabricated retrofit module towards nearly zero energy buildings," *Energy Build.*, vol. 56, pp. 115–125, 2013, doi: 10.1016/j.enbuild.2012.09.034.

[110] X. Cao, X. Dai, and J. Liu, "Building energy-consumption status worldwide and the state-of-the-art technologies for zero-energy buildings during the past decade," *Energy Build.*, vol. 128, pp. 198–213, 2016, doi: 10.1016/j.enbuild.2016.06.089.

[111] S. S. Rao, *Engineering Optimization: Theory and Practice*, 4th ed. New Jersey: Wiley, 2009.

[112] P. H. Shaikh, N. B. M. Nor, P. Nallagownden, I. Elamvazuthi, and T. Ibrahim, "A review on optimized control systems for building energy and comfort management of smart sustainable buildings," *Renew. Sustain. Energy Rev.*, vol. 34, pp. 409–429, 2014, doi: 10.1016/j.rser.2014.03.027.

[113] Y. Cui, Z. Geng, Q. Zhu, and Y. Han, "Review: Multi-objective optimization methods and application in energy saving," *Energy*, vol. 125, pp. 681–704, 2017, doi: 10.1016/j.energy.2017.02.174.

[114] R. Baños, F. Manzano-Agugliaro, F. G. Montoya, C. Gil, a. Alcayde, and J. Gómez, "Optimization methods applied to renewable and sustainable energy: A review," *Renew. Sustain. Energy Rev.*, vol. 15, no. 4, pp. 1753–1766, 2011, doi: 10.1016/j.rser.2010.12.008.

[115] The MathWorks Inc., "What Is Global Optimization? - MATLAB & Simulink." 2016, [Online]. Available: http://www.mathworks.com/help/gads/what-is-global-optimization.html.

[116] W. S. Mcculloch and W. Pitts, "A logical calculus nervous activity*," *Bull. Mothemnticnl Biol.*, vol. 5, no. 4, pp. 115–133, 1943.

[117] D. Kriesel, *A Brief Introduction to Neural Networks*. 2013.

[118] S. Ding, H. Li, C. Su, J. Yu, and F. Jin, "Evolutionary artificial neural networks: A review," *Artif. Intell. Rev.*, vol. 39, no. 3, pp. 251–260, 2013, doi: 10.1007/s10462-011-9270-6.

[119] A. Mellit and S. A. Kalogirou, "Artificial intelligence techniques for photovoltaic applications: A review," *Prog. Energy Combust. Sci.*, vol. 34, no. 5, pp. 574–632,

2008, doi: 10.1016/j.pecs.2008.01.001.

[120] S. A. Kalogirou, G. A. Florides, P. D. Pouloupatis, P. Christodoulides, and J. Joseph-Stylianou, "Artificial neural networks for the generation of a conductivity map of the ground," *Renew. Energy*, vol. 77, pp. 400–407, 2015, doi: 10.1016/j.renene.2014.12.033.

[121] S. Samarasinghe, *Neural Networks for Applied Sciences and Engineering: From Fundamentals to Complex Pattern Recognition*, 1st ed. New York: Taylor and Francis Group, 2007.

[122] A. K. Jain, J. Mao, and K. M. Mohiuddin, "Artificial neural networks: A tutorial," *Computer (Long. Beach. Calif).*, vol. 29, no. 3, pp. 31–44, 1996, doi: 10.1109/2.485891.

[123] A. Mellit, A. S. Kalogirou, L. Hontoria, and S. Shaari, "Artificial intelligence techniques for sizing photovoltaic systems: A review," *Renew. Sustain. Energy Rev.*, vol. 13, pp. 406–419, 2009, doi: 10.1016/j.rser.2008.01.006.

[124] S. a Kalogirou, "Artificial neural networks in renewable energy systems applications: a review," *Renew. Sustain. Energy Rev.*, vol. 5, pp. 373–401, 2001, doi: 10.1016/S1364-0321(01)00006-5.

[125] D. Rajan and L. Kaur, "Applications of Artificial Neural Networks: A Review," *Indian J. Sci. Technol.*, vol. 9, no. 47, 2016, doi: 10.17485/ijst/2016/v9i47/106807.

[126] J. Liang and D. Ruxu, "Thermal comfort control based on neural network for HVAC application," in *Proceedings of 2005 IEEE Conference on Control Applications, 2005. CCA 2005.*, 2005, pp. 819–824, doi: 10.1109/CCA.2005.1507230.

[127] A. A. Argiriou, I. Bellas-Velidis, M. Kummert, and P. André, "A neural network controller for hydronic heating systems of solar buildings," *Neural Networks*, vol. 17, no. 3, pp. 427–440, 2004, doi: 10.1016/j.neunet.2003.07.001.

[128] E. Matallanas *et al.*, "Neural network controller for Active Demand-Side Management with PV energy in the residential sector," *Appl. Energy*, vol. 91, no. 1, pp. 90–97, 2012, doi: 10.1016/j.apenergy.2011.09.004.

[129] A. Tascikaraoglu, A. R. Boynuegri, and M. Uzunoglu, "A demand side

management strategy based on forecasting of residential renewable sources: A smart home system in Turkey," *Energy Build.*, vol. 80, pp. 309–320, 2014, doi: 10.1016/j.enbuild.2014.05.042.

[130] J. J. Cárdenas, L. Romeral, A. Garcia, and F. Andrade, "Load forecasting framework of electricity consumptions for an Intelligent Energy Management System in the user-side," *Expert Syst. Appl.*, vol. 39, no. 5, pp. 5557–5565, 2012, doi: 10.1016/j.eswa.2011.11.062.

[131] L. Magnier and F. Haghighat, "Multiobjective optimization of building design using TRNSYS simulations, genetic algorithm, and Artificial Neural Network," *Build. Environ.*, vol. 45, no. 3, pp. 739–746, 2010, doi: 10.1016/j.buildenv.2009.08.016.

[132] B. B. Ekici and U. T. Aksoy, "Prediction of building energy consumption by using artificial neural networks," *Adv. Eng. Softw.*, vol. 40, no. 5, pp. 356–362, 2009, doi: 10.1016/j.advengsoft.2008.05.003.

[133] D. Gossard, B. Lartigue, and F. Thellier, "Multi-objective optimization of a building envelope for thermal performance using genetic algorithms and artificial neural network," *Energy Build.*, vol. 67, pp. 253–260, 2013, doi: 10.1016/j.enbuild.2013.08.026.

[134] P. M. Ferreira, A. E. Ruano, S. Silva, and E. Z. E. Conceic, "Neural networks based predictive control for thermal comfort and energy savings in public buildings," *Energy Build.*, vol. 55, pp. 238–251, 2012, doi: 10.1016/j.enbuild.2012.08.002.

[135] K. Amarasinghe, D. Wijayasekara, M. Manic, D. He, and W. Chen, "Artificial Neural Networks based Thermal Energy Storage Control for Buildings," in *IECON 2015 - 41st Annual Conference of the IEEE Industrial Electronics Society*, 2015, pp. 5421–5426.

[136] A. E. Ben-Nakhi and M. A. Mahmoud, "Energy conservation in buildings through efficient A/C control using neural networks," *Appl. Energy*, vol. 73, no. 1, pp. 5–23, 2002.

[137] P. A. Gonzalez and J. M. Zamarreno, "Prediction of hourly energy consumption in buildings based on a feedback artificial neural network," *Energy Build.*, vol.

37, no. 6, pp. 595–601, 2005, doi: 10.1016/j.enbuild.2004.09.006.

[138] A. Mellit and A. M. Pavan, "A 24-h forecast of solar irradiance using artificial neural network: Application for performance prediction of a grid-connected PV plant at Trieste, Italy," *Sol. Energy*, vol. 84, no. 5, pp. 807–821, 2010, doi: 10.1016/j.solener.2010.02.006.

[139] S. Leva, A. Dolara, F. Grimaccia, M. Mussetta, and E. Ogliari, "Analysis and validation of 24 hours ahead neural network forecasting of photovoltaic output power," *Math. Comput. Simul.*, vol. 131, no. 2017, pp. 88–100, 2015, doi: 10.1016/j.matcom.2015.05.010.

[140] F. Almonacid, P. J. Pérez-Higueras, E. F. Fernández, and L. Hontoria, "A methodology based on dynamic artificial neural network for short-term forecasting of the power output of a PV generator," *Energy Convers. Manag.*, vol. 85, pp. 389–398, 2014, doi: 10.1016/j.enconman.2014.05.090.

[141] E. Izgi, A. Öztopal, B. Yerli, M. K. Kaymak, and A. D. Şahin, "Short-mid-term solar power prediction by using artificial neural networks," *Sol. Energy*, vol. 86, no. 2, pp. 725–733, 2012, doi: 10.1016/j.solener.2011.11.013.

[142] N. Al-Messabi, Yun Li, I. El-Amin, and C. Goh, "Forecasting of photovoltaic power yield using dynamic neural networks," in *The 2012 International Joint Conference on Neural Networks (IJCNN)*, 2012, pp. 1–5, doi: 10.1109/IJCNN.2012.6252406.

[143] G. Capizzi, C. Napoli, and F. Bonanno, "Innovative second-generation wavelets construction with recurrent neural networks for solar radiation forecasting," *IEEE Trans. Neural Networks Learn. Syst.*, vol. 23, no. 11, pp. 1805–1815, 2012, doi: 10.1109/TNNLS.2012.2216546.

[144] G. S. Georgiou, P. Christodoulides, and S. A. Kalogirou, "Optimizing the energy storage schedule of a battery in a PV grid-connected nZEB using linear programming," *Energy*, vol. 208, p. 118177, 2020, doi: https://doi.org/10.1016/j.energy.2020.118177.

[145] G. S. Georgiou, P. Christodoulides, and S. A. Kalogirou, "Implementing artificial neural networks in energy building applications - A review," 2018, doi: 10.1109/ENERGYCON.2018.8398847.

[146] G. S. Georgiou, P. Christodoulides, and S. A. Kalogirou, "A Neural Network Approach for short-term forecasting of PV Generation in Dwellings," 2018, doi: 10.1109/UPEC.2018.8541925.

APPENDIX I – Supportive Material

I.1 Zero Energy Buildings

I.1.1 General definitions

In 2015, the US Department of Energy published a guide titled as "*A Common Definition for Zero Energy Buildings*" stating that a ZEB is "*an energy-efficient building where, on a source energy basis, the actual annual delivered energy is less than or equal to the on-site renewable exported energy*" [96]. However, discussions and debates on how a ZEB should be and how the energy boundaries of the buildings are defined, makes the understanding and the development of such buildings more challenging [97]–[99]. For this reason, most of studies are suggesting and proposing new definitions for ZEBs and different calculation methodologies for the balance of both the energy and the carbon emissions associated with the building itself.

Even with the variety of definitions found in literature, the main concept of a ZEB, which is the reduction of the energy needs – via energy efficiency – and the balance of the energy demanded from the different grids with the energy supplied by either local or nearby RES, remains common. Yet, what mainly differs in each study is the calculation methodology for achieving these balances in a low energy building.

Torcellini et al. [100] stated that the general concept of a ZEB is the balance or the negative difference of the net sum between its annual grid energy and the energy supplied by local RES. Hence, the authors defined a Net ZEB (NZEB) as a building of high energy efficiency with low energy needs, so that the balance mentioned above can be achieved with the aid of RES. The authors expanded the term ZEB further and suggested definitions such as site ZEB, source ZEB, emissions ZEB and cost ZEB, depending on the climate, energy cost, greenhouse gas emissions, the investor and the project. The concept of a NZEB is the main interest in the study published by Sartori et al. [101], since the term ZEB may be more general and may also refer to standalone buildings. Another crucial point stated in this study, is the lack of an official characterization of a NZEB, which does not allow countries to define their own definition for a NZEB correctly, since these types of buildings solely depend on the energy targets-policies, climate conditions and so forth. Thus, the authors propose the term NZEB as a building connected to the grid and simultaneously balancing its energy

needs, but this energy balance needs to be addressed by different means such as defining the energy balance boundaries of the building, the physical boundary of the building, the metrics used and other parameters necessary towards a NZEB. Their main methodology is concentrated on a weighting system measuring and calculating different factors for reaching the so called Net ZEB Balance, which is simply the equality (or even negative value) of the difference between the weighted demand and the weighted supply within a period of time – usually a year. To this extent, they used different calculations and usable definitions necessary for achieving that balance.

Kilkis [102] proved that a NZEB is not necessarily an environmental-friendly building, as it actually emits greenhouse gases even if its metric energy is balanced with on-site RES. The author suggests and proposes a new definition for ZEB called Net-Zero Exergy Building (NZEXB), since the exergies of the heat energy along with the electrical energy are not balanced even if their energy balance is achieved. Hence, through the new metric method, it is possible to rate the real environmental impact of the building by also considering the balance between the exergies of the building and the carbon emissions. The definition of the NZEXB is stated as a building, which "*has a total annual sum of zero exergy transfer across the building-district boundary in a district energy system, during all electric and any other energy transfer that is taking place in a certain period of time*" [102].

Kurnitski et al. [103] proposed a framework for helping experts in EU member states to clearly understand the concept of a NZEB and a nZEB. They proposed the definition of a nearly net ZEB (nnZEB) based on the Energy Performance of Buildings Directive (EPBD) and related EU standards. They stated that a nnZEB is a building consuming a "*national cost optimal energy greater than 0 kWh/m^2/year of its primary energy*". Of course the minimum value for the primary energy shall be specified by each member state [104]. They defined primary energy as the difference between the delivered energy and the exported energy (RES) multiplied with the primary energy factor (final to primary) specified by the regulations of each member state. The authors also stated that the identification of the system's boundary is very important, as it determines which types of energy flows are to be integrated into the problem. Finally, the system's defined boundary should always take into account, as they mentioned, the energy flows related to the delivered energy for district heating, district cooling, electricity and renewable and non-renewable fuels and to the exported energy such as local RES.

In contrast with ZEB, whose definition is still under a wide discussion, the 2010/31/EU directive clearly defines a nZEB as a building of high energy efficiency with a significant portion of its very low energy needs to be supplied by either local or nearby RES. The main parameter set in this Directive, for quantifying the definition of nZEBs, was the building's primary energy consumption measured in kWh/m^2 per year. This parameter must remain as low as possible, depending on the EU member state energy needs, climate and so on. Hence, EU member states were obliged on proposing their own limits on the building's primary energy consumption and on developing their own methodology for calculating the building's primary energy consumption, according to EU standards and guidance provided within the EPBD.

The Directive defines primary energy as the *"energy from renewable and non-renewable sources, which has not undergone any conversion or transformation process,"* and demands energy needs for heating, cooling, ventilation, hot water and lighting to constitute the main parameters for calculating the building's primary energy consumption. Moreover, it is also required that the positive effect of RES, electricity produced by cogeneration, district or block heating and cooling systems and natural lighting must be considered, when the primary energy is calculated.

As aforementioned, each EU member state should define any requirements necessary for limiting the building's primary energy needs. For instance, The Republic of Cyprus issued the latest nZEB requirements Decree 121/2020, which is in force from 1st of July 2020 and requires each new building to comply with the requirements shown in Table 9. Furthermore, technical guides, examples and information related to nZEB are also published on the official website of Cyprus Ministry of Energy, Commerce and Industry, mainly for enabling the easier understanding, adoption and implementation of nZEBs. As it may be seen, such requirements compose passive measures and cannot manage the building's primary energy consumption affected by the stochasticity of the users' behaviour and renewable generation.

Based on the definitions presented in literature, it is clear that a *green* building – i.e., a building of high energy efficiency with low energy needs (e.g. ZEB, NZEB, nZEB, and so on) – is a means for reducing its primary energy needs and, simultaneously, increase its share of renewable energy in an interconnected energy grid. However, maintaining the nZEB's minimum requirements, daily, remains challenging, since the total primary energy of each building highly depends on the users' behaviour.

Table 9: Minimum requirements for new buildings in Cyprus

Requirements	
Energy efficiency on the energy certificate of the building	A
Maximum primary energy consumption for residential buildings	100 kWh/m^2/year
Maximum primary energy consumption for non-residential buildings, excluding hotels	125 kWh/m^2/year
Maximum primary energy consumption for hotels	220 kWh/m^2/year
Maximum average thermal permeability U for walls and elements of the construction (columns, beams and walls) contributing part of the building's shell. The increase of the thermal permeability U (beyond this value) is only allowed in cases when passive solar systems are used (e.g. Trombe walls, walls with high thermal storage)	0.4 W/m^2/K
Maximum average thermal permeability U for horizontal structural elements (floors, floors in cantilever, inclined roofs) and any other roofs being part of the building's shell.	0.4 W/m^2/K
Maximum average thermal permeability U for doors and windows, excluding shop showcases	2.25 W/m^2/K
The increase of the above thermal permeability values is only allowed when the total maximum average thermal permeability of the building's shell is not greater than: Shop showcases are excluded	0.65 W/m^2/K
Maximum average shading factor for windows being part of the building's shell, excluding shop showcases	0.63
Maximum energy consumption for heating in residential buildings	15 kWh/m^2/year
Average maximum lighting power installed for office buildings	10 W/m^2
It is allowed to increase the above maximum lighting power installed in case of:	The building is equipped with an automated management system, which allows:

Requirements	
	i) The continuous monitoring, recording, analysis and the ability of adapting the lighting energy consumption
	ii) The comparative analysis of the building's energy performance, locating any losses in building's lighting efficiency and informing the technical manager or department regarding ways for improving the energy efficiency
Least value of the total primary energy consumption coming from RES.	
RES systems installed shall consider the estimated consumption profile of the building, so as the energy generated being consumed by the building itself, where this is technically and economically feasible.	9% for hotels and 25% for all other building types
For residential buildings having solar systems for domestic hot water needs, the installation must be in accordance with the Technical Guidance of Solar Systems and the terms of the competent Urban Planning Authority	

Source: [105]

I.1.2 Moving toward ZEBs and some calculation methodologies

As it has been presented in the previous sub-section, the implementation of a ZEB or a very low-energy building (e.g. nZEB) is quite challenging, due to the different factors affecting the energy performance of the building. Despite the energy performance problem, energy and investment costs are also becoming a challenge for such buildings. This section reviews studies found in literature related to the concept towards a ZEB. This includes, the different calculation methodologies at the design phase, the different methodologies for the energy management within a building and the different techniques for the maximum utilization of the renewable energy supplied by local RES in buildings. Obviously, a combination of the above may be necessary towards ZEB – especially for the balance or the reduction of the total primary energy, which is influenced by the building's location, construction materials, weather conditions, user's behaviour, building efficiency, energy and installation costs and so forth.

Sartori et al. [101] presented different approaches towards a NZEB based on different selection criteria tools and on the type of balance selected according to the available data at the design phase. The core calculation of their methodology is the Net ZEB Balance shown in Figure 30.
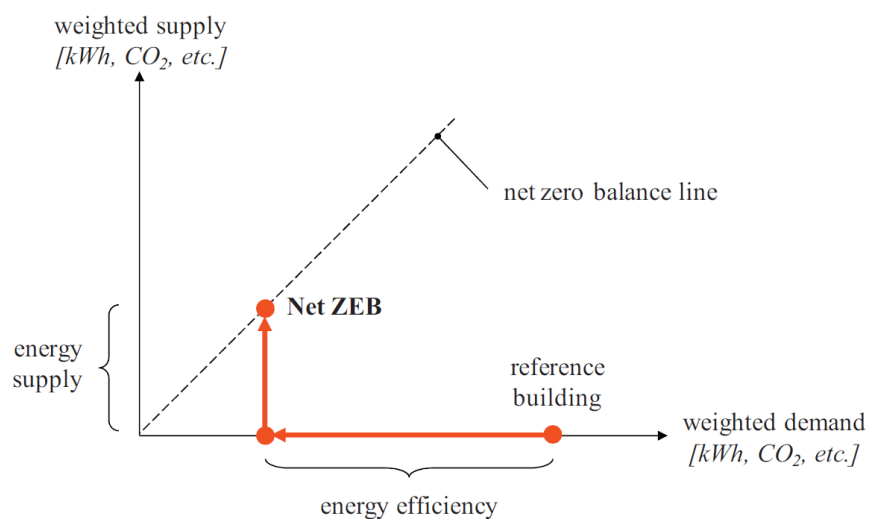

Figure 30: The net ZEB balance concept [101]

Kurnitski et al. [103] proposed a simplified method towards a nnZEB. The main target was to help experts in each EU member state to have a clear idea of the general concept of a ZEB and of the official definitions of a nZEB given in 2010/31/EU Directive [104]. Further to the different official definitions presented in the fields of delivered energy, exported energy, net delivered energy, system boundary, CO_2 emission coefficient, primary energy and energy performance of the building, the authors propose the diagram shown in Figure 31 as the main driver towards a nnZEB.
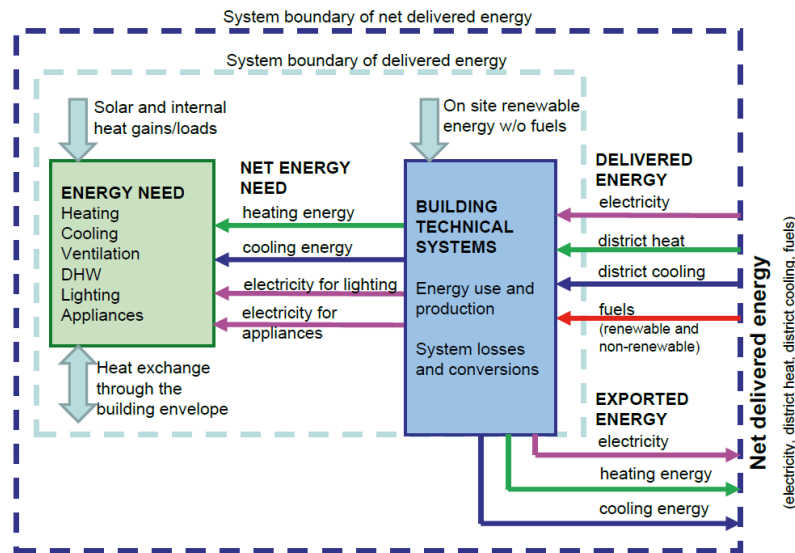

Figure 31: Energy boundary of net delivered energy [103]

Hamdy et al. [106] developed a method in compliance with the 2010/31/EU Directive for selecting the optimum variables for a nZEB, such as wall insulation, roof insulation, floor insulation, types of windows, RES, heating system and so forth, under a cost optimum solution considering both the building's primary energy consumption and investments. The method is based on minimizing two objective functions regarding the primary energy and the lifecycle cost of the building, through GA. The authors considered, among other technical service systems, the total energy needs of the building including heating, cooling, ventilation, lighting, pumps and fans, domestic hot water, cooking, appliances and the energy provided by RES. The defined solution is processed in three stages. The first stage is used to find the optimum variables for the building's envelope affecting the thermal performance of the building (insulations,

window type, building tightness). The second stage is used for assessing the primary energy and the lifecycle cost of the optimal combinations derived from stage 1 and suggests the optimum heating options such as electrical heating, oil boiler, district heating or ground source heat pump. The third and final stage is used for further reducing the primary energy consumption and the lifecycle cost by finding the optimal sizes of the RES (solar-thermal and PV). Among their many conclusions, they found that the cost optimum primary energy consumption for a nZEB should lay in the range of 93 and 103 kWh/m^2/year, the cost optimal size of the PVs – in buildings having high electrical demands (electrical heating and A/C units) – should be between 15–20m^2 and 5m^2 for buildings having fuelled based heating systems and for a nZEB, the solar-thermal collectors could be up to 15m^2. Obviously, such conclusions may not be valid for every region or EU member state; nevertheless, application of this method could lead to analogous results.

Model calculations for determining energy related cost optimal levels for a nZEB were proposed by Kurnitski et al. [107]. The authors propose the maximum primary energy requirement for a nZEB leading to a minimum life-cycle cost, without the need of using iterations or an optimization tool. The methodology is based on the calculation of the building's envelope construction concept and the calculation of the NPV . Once the energy profiles of each building were known, the authors could estimate the global energy related cost. They concluded that, for a detached house in Estonia, a 110 or 140 kWh/m^2/year of primary energy was the cost optimum solution, when specific insulation levels and technical systems sizes (solar thermal collectors, ground source heat pumps, etc.) are adopted. Among different combinations of the technical systems it was shown that the cost optimum primary energy is reached using either systems, a ground source heat pump or a gas heating system. Finally, the authors stated that installing PVs the primary energy could be further reduced; however, this would increase the construction costs.

Pikas et al. [108] used a similar approach as Kurnitski et al. [107] for finding the cost optimal primary energy consumption of an office building. The obtained results were based on data taken by [107] and on insulation levels as well as the window to wall ratio. With a 3-step procedure (1-optimal wall insulation thickness, 2-Cost optimal windows size and 3-Energy analysis with and without PV), the authors found that a 20-year cost optimal primary energy consumption – for an office building in Estonia – is

between 100 and 130 kWh/m^2/year using a smaller window to wall ratio, triple glazing and argon filled windows along with a wall insulation of 200 mm thickness.

Silva et al. [109] presented a methodology for the transformation of existing buildings into nZEBs. A novel modification of the buildings' façade under a multi-step procedure was introduced with the main target of optimizing the buildings' performance at the lowest cost possible. The study took place in Portugal in compliance with the Portuguese building regulations and in line with the EPBD recast. The authors developed a low cost prefabricated retrofit module able to be attached on the existing walls of the building in order to improve its energy performance. The steps followed in the study were the optimization of the design module installation, the calculation of the optimum insulation thickness of the module with the aid of the NPV and Modified Internal Rate of Return and the application of other energy efficiency measures such as building envelope improvements, replacement of existing mechanical systems with new of a higher efficiency and the installation of local RES, as required by the EPBD recast. The authors were able to calculate the cost optimum solution regarding the transformation of an existing building to a nZEB, by simply attaching a special (low-cost) material to the walls in addition to the standard energy efficiency measures (RES, window replacement, roof insulation, etc.). Finally, it was stated that the climate conditions are highly correlated with the results, as the climate conditions affect the buildings' energy performance. Nevertheless, their proposed method can be used everywhere and for that reason they also suggest other solutions, such as variation of the retrofit module insulation thickness and construction material (Aluminium composite finishing, Rock wool insulation, etc.) that would give different U-values, heat flux and temperature distribution across its surface.

Through this review on ZEBs, the main target of reducing the building's primary energy remains unchanged across all the proposed definitions and methodologies towards nZEBs. Despite the variety and high number of proposals, the transition from the current low adoption case towards a high adoption case, so the defined energy target levels are met, is still challenging. Taking into account both the nZEB low adoption rate and the rising trend of electrification in building energy sectors (e.g., the transition from traditional heating systems to heat pumps) [4], [110], electrical storage may significantly contribute to the nZEB target, if it is seen as a BEM medium instead of an investment of high economic cost.

I.2 Convex Optimization

This section explains, in brief, the relevant background theory of convex and linear optimization, as this Thesis utilizes LP. The main aim is to show how mathematical optimization is defined, how an optimization problem is mathematically expressed and how a non-linear (convex) problem may be transformed into an equivalent linear problem.

Mathematical optimization, in general, is the topic in mathematics that is concerned with finding a solution, which minimizes or maximizes a function either locally or globally, with respect to certain criteria. In other words, finding the optimum x^* that minimizes a function $f(x)$ and satisfying the constraints, then there is no z such that $f(z) < f(x^*)$. Similarly, finding the optimum x^* that maximizes a function $f(x)$, then there is no z such that $f(z) > f(x^*)$ [81], [111]; where, z is an arbitrary value in the domain of $f(x)$.

The standard form of a mathematical optimization problem may be presented by equations (88) and (89) below.

$$\text{minimise } f_o(x) \tag{88}$$

$$\text{subject to } f_i(x) \leq b_i, \quad i = 1, \ldots, m \tag{89}$$

where:

- x is the vector containing the variables to be optimized

- f_o is the objective function (aka cost function) to be minimized or maximized

- f_i is the equality/inequality constraint functions

- b is the vector containing the limits or boundaries of the constraint functions or problem

According to Stephen Boyd and Lieven Vandenberghe [81], the above problem is linear if the objective function f_o and the constraint functions f_i are both linear. On the other hand, if the objective function f_o and the constraint functions f_i are convex, then the problem is said to be convex; for more information regarding linear and convex functions it is recommended for the reader to refer to [81].

Convex Programming (CP) refers to convex problem optimization, while LP refers to linear problem optimization and, mathematically, a convex optimization problem along

with a linear optimization problem need to satisfy the conditions shown by equations (90) and (91), respectively.

$$f_i(\alpha x + \beta y) \leq \alpha f_i(x) + \alpha \beta_i(y), \quad \forall \{x, y\} \in \mathbb{R}^n \ \& \ \forall \ \{\alpha, \beta\} \in \mathbb{R} \qquad (90)$$

$$f_i(\alpha x + \beta y) = \alpha f_i(x) + \alpha \beta_i(y), \quad \forall \{x, y\} \in \mathbb{R}^n \ \& \ \forall \{\alpha, \beta\} \in \mathrm{R} \mid a + b = 1, a \geq 0, b \geq 0 \quad (91)$$

where:

- α, β are constants

- x and y are the optimization matrices

- $\mathbb{R}$ is the set of real numbers. In bold, it is meant that it is a vector of real numbers of length n

It can be clearly seen from the above conditions that a linear optimization problem is also a convex optimization problem and it is generally said that LP is a special case of CP.

Furthermore, a multi-objective non-linear optimization problem may be described as follows [112]:

$$\text{minimize} \, f_i(x), \, (i = 1, 2, \ldots, m) \qquad (92)$$

subject to

$$h_j(x), \, (j = 1, 2, \ldots, J) \qquad (93)$$

$$g_k(x) \leq 0, \, (k = 1, 2, \ldots, K) \qquad (94)$$

where:

- $f_i(x)$ is, in general, a nonlinear function

- $h_j(x)$ and $g_k(x)$ are, in general, the non-linear boundaries and the non-linear equality/inequality constraint functions, of function $f_i(x)$, respectively.

In most relevant Engineering studies, instead of running an algorithm with concurrent objective functions (aka multi-objective optimization), it is common to observe a lamped version of equation (92) and thus, the problem may be transformed into a single-objective problem, expressed in the following form [112].

$$\min_{x \in X} \sum_{i=1}^{m} w_i f_i(x) \qquad (95)$$

where:

- w is a weight factor representing the weighting (or significance) of each objective function $f_i(x)$. Boundaries and constraints remain the same as equations (93) and (94)

The most common convex optimization techniques used and proposed for solving the problem represented by equations (95), (93) and (94) are LP, Mixed-Integer Linear Optimization or Programming (MILP), Quadratic Optimization or Programming (QP), Non-Linear Optimization or Programming (NLP) and Mixed-Integer Non-Linear Optimization or Programming (MINLP), among which MILP dominates, due to its simplicity and convexity, which guarantees global solutions [82]. AI in some studies is also integrated for improving the model performance and reducing computational time, as Rahmani and Shen [11] proposed. In contrast, different heuristic optimization methods (e.g. PSO and GA) are now increasing their sharing in energy saving optimization applications, due to the increase of the problem's complexities and non-convex nature, as well as the need of solving multiple non-linear objective functions simultaneously, with high accuracy and performance [113]. Finally, AI such as ANN, fuzzy logic and GA are also integrated for improving model performance and reducing computational time [114].

Global optimization is necessary, in BEM applications, as it always guarantees energy related costs reduction in both the short term and the long term. Such scheme refers to the optimization running within a specified time horizon – say 24 hours – in which the algorithm searches for a value (global minimum) that minimizes the objective function (aka cost function) and with respect to all other feasible points [115]. By slightly modifying equation (95), the algorithm for optimizing a cost function globally may be represented as follows.

$$\min_{x \in X} J = \sum_{m=1}^{M} \sum_{t=1}^{T} w_{i,t} f_i(x, t) \qquad (96)$$

where:

- *t*, *T*, *m* and *M* refer to current timestep, optimization horizon (period), current iteration (e.g. day, month and so on) and total number of iterations (e.g. days, months, years and so on), respectively. Note that the objective function *f* becomes time dependent.

Since each objective function *f* changes over time instant *t* and all values are known *a priori*, equation (96) ensures that the total value of *J*, within the whole period, is minimized in a global manner. Nevertheless, this model assumes perfect conditions and does not account for any variations in the objective functions and other proper tools (e.g. MPC) are required for addressing such an issue.

For better understanding a convex optimization problem, an example, presented in Figure 32, shows a non-linear function along with its boundaries presented by the red lines. Clearly, the optimal point that minimizes the above function is at $x^* = 0$, showing that the optimum value is $f(x^*) = 0$. As there is no other point giving a lower value, then it is said that at $x^* = 0$ global optimization is achieved.

According to the definition given in [81], the function $f(x) = x^2$ is convex and since the constraints $x \geq -3 \equiv -x \leq 3$ & $x \leq 3$ are affine, then the problem it is said to be convex. This problem may also be solved using LP, but first, it is necessary to express function $f(x)$ with an equivalent objective function able to be linearized, which is of course its absolute value – i.e., $f(x) = |x|$, see Figure 33.
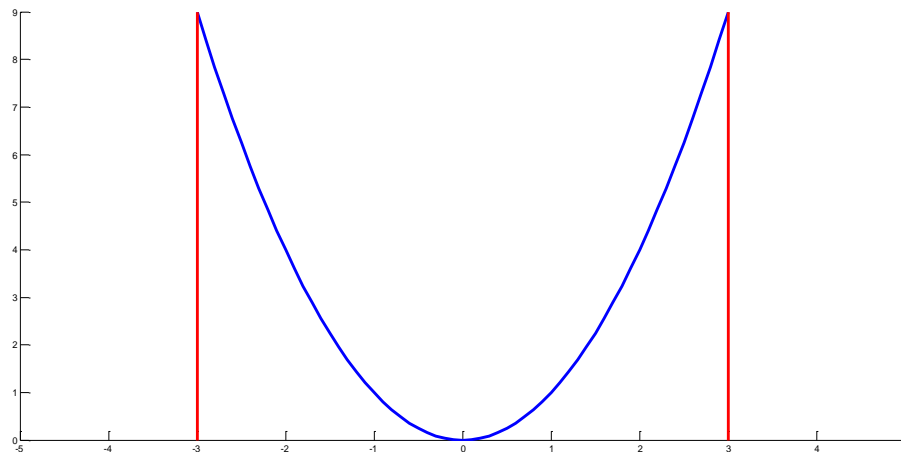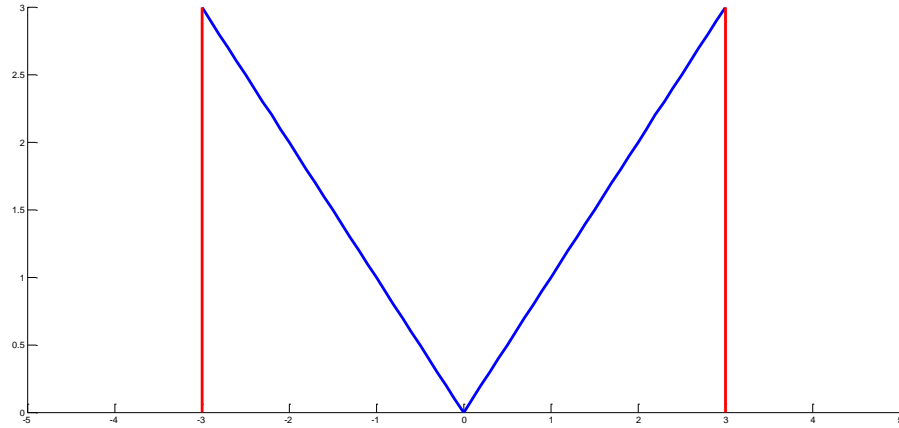

Figure 32: Objective Function $f = x^2$

Figure 33: Objective Function $f = |x|$

By expressing x as the difference of two slack variables x^+ and x^-, where $x^+, x^- \geq 0$, then the original problem can be linearized as below [81].

$$f(x^+, x^-) = |x^+ - x^-| \tag{97}$$

$$\Leftrightarrow f(x^+, x^-) = x^+ + x^-$$

subject to

$$x^+, x^- \geq 0 \tag{98}$$

$$-3 \leq x^+ - x^- \leq 3 \tag{99}$$

Note that the absolute term may be eliminated due to equation (98) and obviously by reversing the minus sign within the absolute term, since such a condition keeps the function always positive. Problem (97) is not the same as before, however it is an equivalent representation of the original problem $f(x) = x^2 \,|\, -3 \leq x \leq 3$, which describes a non-negative function having an optimum solution at $x^* = 0$. The linearization of the proposed model shown and discussed in this Thesis is based on the above principle − i.e., linearizing the absolute term of a cost function.

I.3 Simulation Data and Methodology for assessing a building base study with LP[7]

PV measurements were taken from a residential 5 kWp PV system located in Nicosia, Cyprus, in 10-minute intervals, between the 1st of March 2015 and the 29th of February 2016, as shown in Table 10. Load measurements were taken from the same dwelling, for the same period. PV data consists of different variables such as date and time, PV inverter energy output, PV inverter ac power output, utility grid voltage, PV inverter ac current output, PV inverter dc input voltage, PV inverter dc input current, PV inverter ac output current, ambient temperature, irradiance and wind speed. The parameters related to voltage, current, power and energy are directly measured from the inverter, with the weather-related parameters measured from an integrated weather station. All the parameters though are provided by the inverter's integrated software platform and can be accessed and downloaded by the user. Load measurements were taken from the same dwelling through a digital energy meter installed at the building's main circuit breaker. The measurements downloaded from the meter correspond to the hourly cumulative energy, as shown in the column "Meter reading [kWh]" in Table 10 and the hourly energy is simply calculated by subtracting the measurements between two consecutive hours. For instance, the grid energy imported (load consumption) between hours 01:00 and 02:00 is 686.6 kWh – 686.4 kWh = 0.2 kWh.

A small fraction of the original PV and load data used in this study are shown in Table 10. The complete PV and load profiles, for the whole year, are presented and discussed in the sub-sections. It should be noted here that the proposed approach uses parameters such as energy at the ac output of the PV inverter and the load consumption, which correspond to the "Energy [Wh]" and "Consumption [kWh]" columns in Table 10.

---

[7] Material from published paper [144]

Table 10: Small fraction of the real PV and load data

PV DATA									
Date	Energy [Wh]	ac Power [kW]	Grid Voltage [V]	ac Current [A]	dc Voltage [V]	dc Current [A]	Ambient Temp. [ºC]	Solar Irradiance [W/m^2]	Wind speed [m/s]
31/12/2015 06:30	1.64	9.86	242	0.04	300	0.03	7	11	3
31/12/2015 06:40	11.73	60.84	242	0.25	255	0.26	8	17	2
31/12/2015 06:50	26.23	87.42	242	0.36	263	0.37	8	29	3

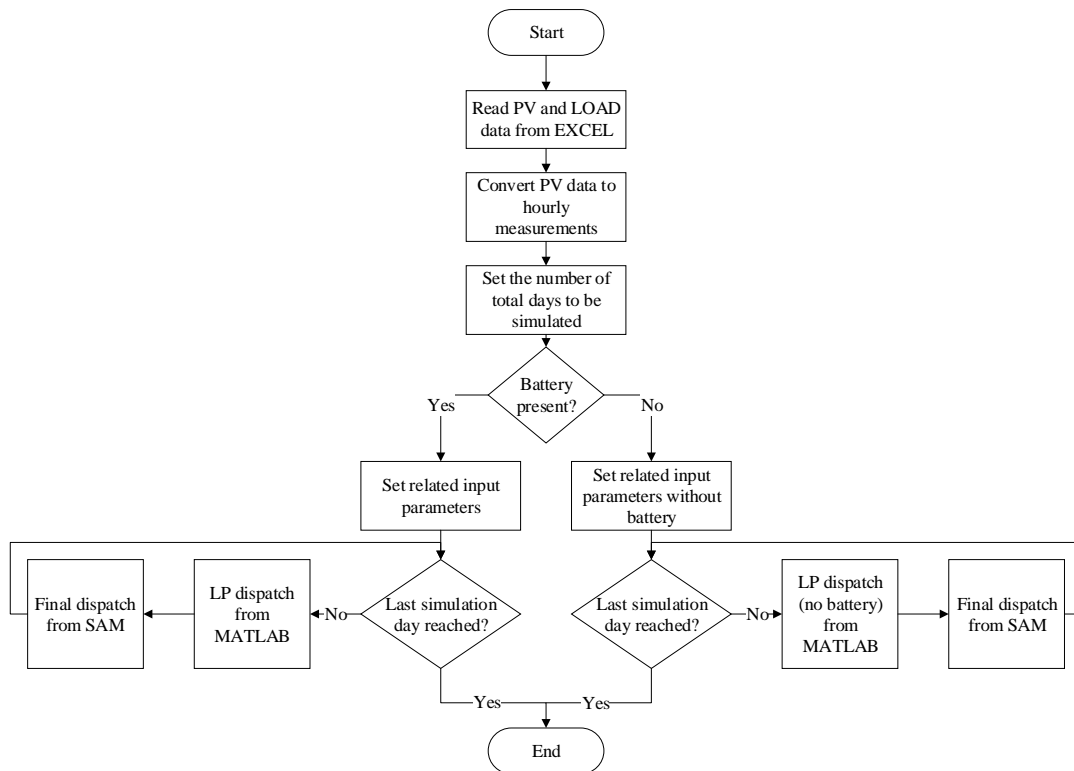| LOAD DATA			
Date	Time [h]	Consumption [kWh]	Meter reading [kWh]
31/12/2015	1:00:00	0.0	686.4
31/12/2015	2:00:00	0.2	686.6
31/12/2015	3:00:00	0.2	686.8

Figure 34: Simulation algorithm flowchart

The main task of the algorithm shown in Figure 34 is to read the PV and Load measurements and based on this information provide the forecasted battery dispatch, aiming the minimization of the net grid energy usage. Below, each stage of the algorithm presented is listed and explained.

- *Read PV and LOAD from Excel (Import stage):* The PV data downloaded from the PV inverter and the load data downloaded from the energy meter are stored in Excel and then imported in MATLAB.

- *Convert PV data to hourly measurements (Data pre-processing stage):* Once the data is imported in MATLAB, the PV measurements from 10-min intervals are converted to one-hour intervals, in order to match the hourly resolution of the load data. Specifically, the recorded ac power, based on a 10-min sampling rate, is multiplied with the time interval – i.e., 10 min / 60 min – for representing the 10-min energy flow. Then, the hourly energy is simply the sum of the 10-min energy delivered in each hour. For instance, the hourly energy delivered at 07:00 am is the sum of the energy delivered at 07:00, 07:10, 07:20, 07:30, 07:40 and 07:50 and so on.

- *Battery Present (Battery presence check stage):* At this stage, the algorithm checks if a battery is present or not with the aid of a binary variable entered by the user.

- *Set related Input parameters (Pre-defined parameters stage):* The user predefined parameters, such as battery initial storage, battery maximum and minimum charging and discharging energies, battery capacity, weight values and desired number of simulated days are set. In case a battery is not present, then all battery related parameters are set to zero.

- *Last simulation day reached:* At this stage, the algorithm enters a loop and repeatedly checks if the current day of simulation is the last one. Otherwise, the algorithm moves to the next stage.

- *LP dispatch from MATLAB (LP optimization run):* The algorithm runs, for each iteration (i.e., each simulation day) the LP model and gives the hourly optimum battery dispatch (charge/discharge) for the whole 24-hour period, based on the related PV generation and load consumption of the current day.

- *Final dispatch from SAM (Final dispatch run):* Once the LP dispatch is obtained from MATLAB, then the PV, load and the desired battery optimum dispatch are imported in SAM. Here, the whole dispatch is recalculated by SAM, following the given PV load and the desired LP dispatch obtained in MATLAB. In case the desired LP dispatch requires the battery to operate beyond its physical limits, then SAM recalculates the correct battery charge/discharge and the net grid energy, based on the energy balance equation and the available energy storage level of the battery at the current timestep.

The last three stages run in a repetitive manner, once per simulation day, with the total number of iterations being equal to the total number of simulation days predefined by the user.
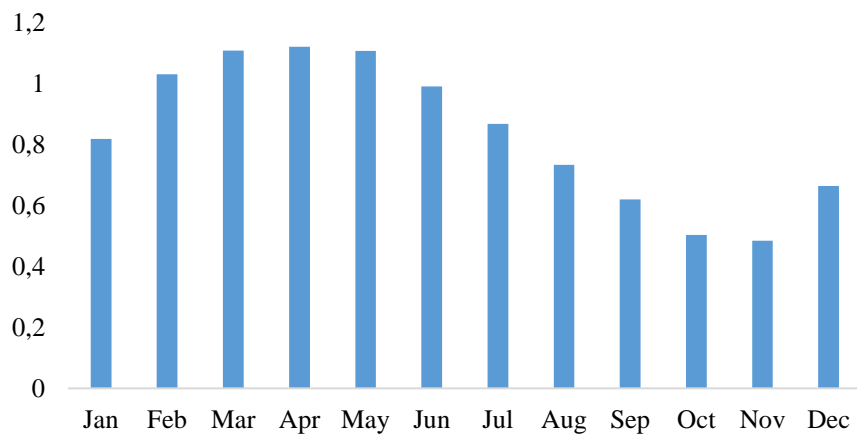
I.3.1 PV Profile

The recorded Plane of Array (PoA) irradiance (irradiance at the PV module's surface), the ac exported power, in 10-minute intervals, the monthly average ac power, the monthly total ac energy generated and the average 24-hour ac power output between the 1st of January 2015 and the 31st of December 2015 are shown in Figure 35.
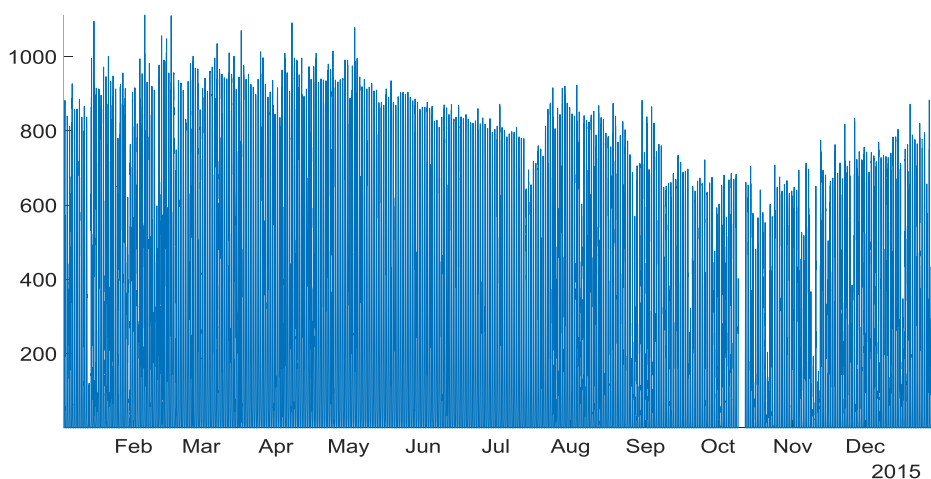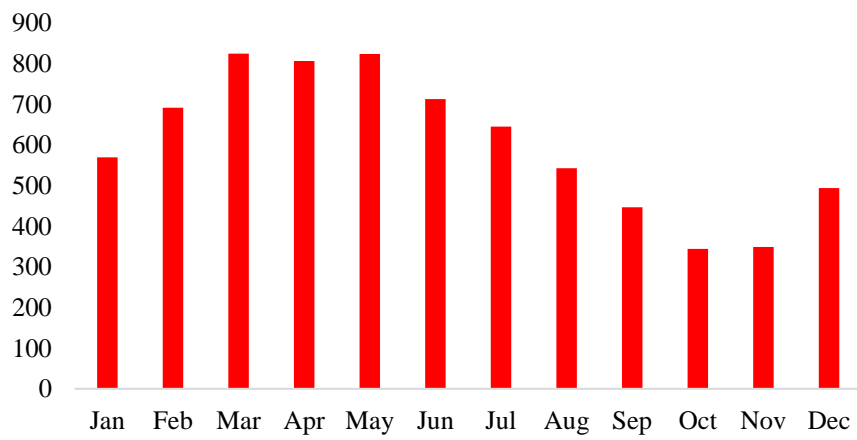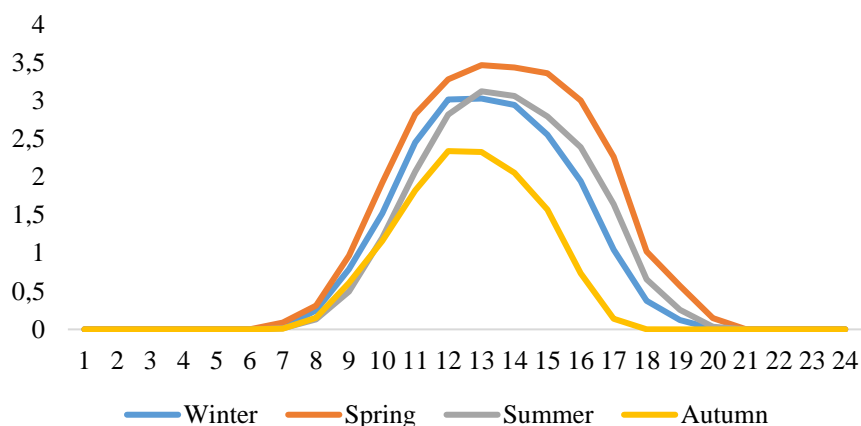

(a)
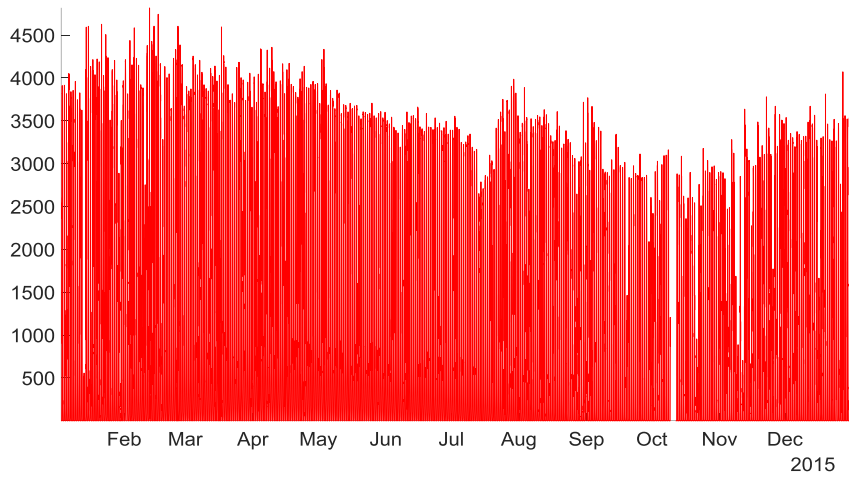
(b)

(c)

(d)

(e)

Figure 35: (a) PoA Irradiance, in W/m², 03/01–31/12/2015; (b) PV ac power output, in Watts, 03/01–31/12/2015; (c) Monthly PV average ac power output, in kW, 03/01–31/12/2015; (d) Monthly total PV energy output, in kWh, 03/01–31/12/2015; (e) Seasonal 24-hour PV average ac output, in kW, 03/01–31/12/2015

As may be observed, the highest energy levels are gained in the period of March and May. On the other hand, October and November are the months with the lowest production. As shown in Figure 35(e), the highest production occurs during Spring, as the conditions of the high irradiance and low temperatures yield a higher generation. In contrast, autumn has the lowest production, due to the increased number of the cloudy days. Finally, Winter and Summer share a similar profile. It is worth mentioning that in Summer, the generation is not as high as in Spring, due to the increased temperatures and soiling, yielding a lower production. Finally, this profile is very similar to a typical Cyprus PV generation profile, as one can observe through PVGIS (EU's official online tool) in line with a trusted PV simulation software such as SAM from NREL.
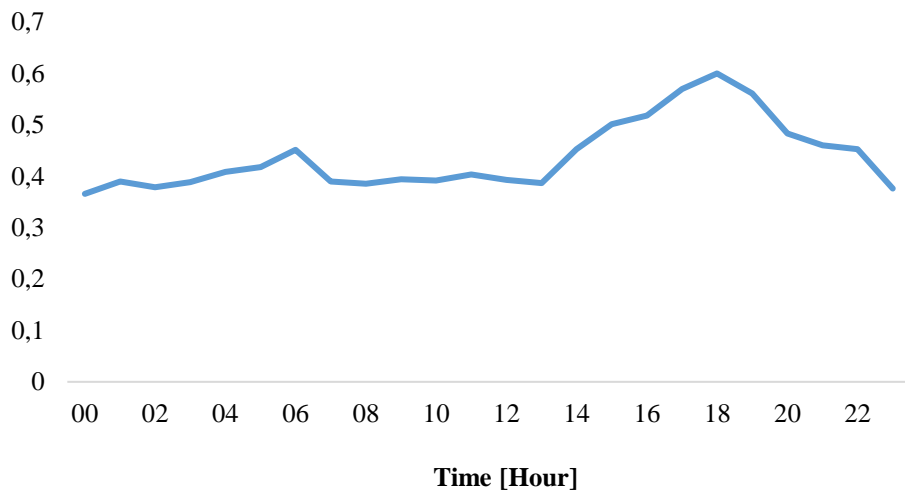
I.3.2 Load Profile

The total electrical energy consumption for 2015 was 3839.3 kWh, and the consumption profile is shown in Figure 36.
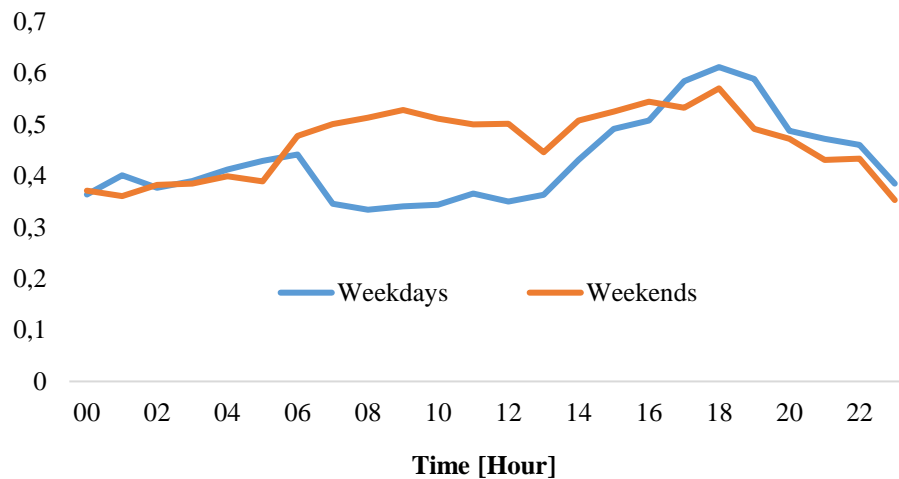
(a)

(b)

Time [Hour]
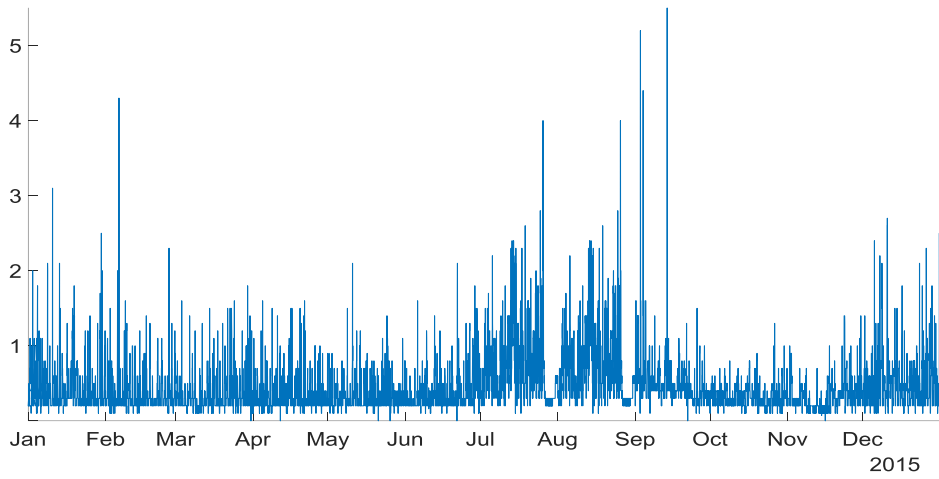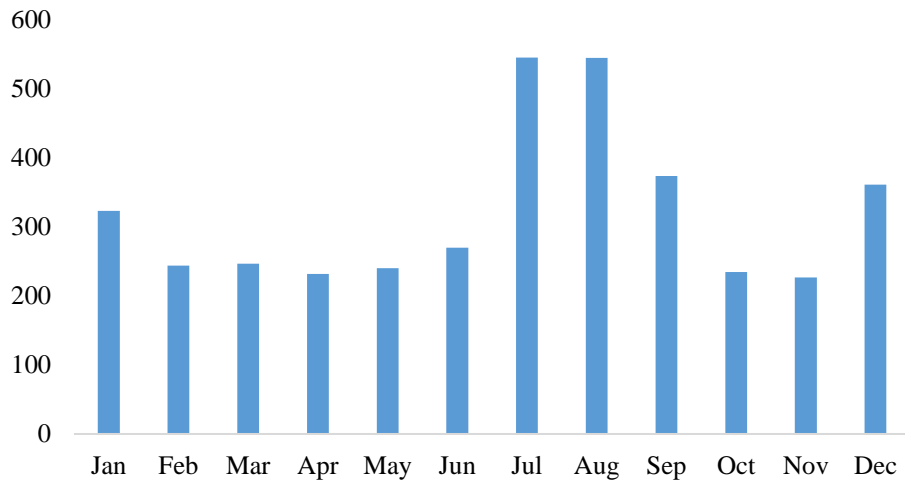
(c)

(d)
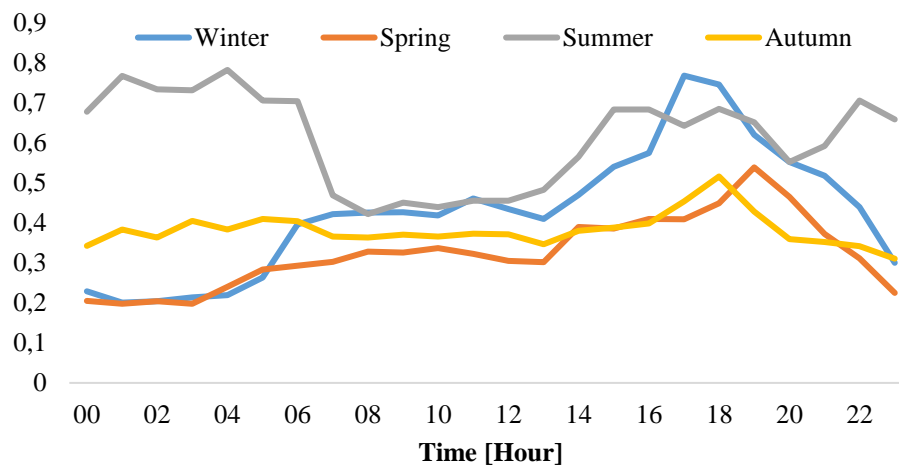
(e)

Figure 36: (a) Hourly load, in kWh, 03/01–31/12/2015; (b) Total monthly load, in kWh, 03/01–31/12/2015; (c) Annual average 24-hour load, in kWh, 03/01–31/12/2015; (d) Weekdays and Weekends annual average 24-hour load, 03/01–31/12/2015; (e) Seasonal average 24-hour Load 03/01–31/12/2015

According to Figure 36(a), the peak load occurred in September; however, the highest consumption occurred during July and August, due to the hot summer days, resulting to the increased cooling demand, as verified by Figure 36(b). The annual average 24-hour load shown in Figure 36(c) indicates that two peaks occur within the day, with the highest one taking place at around 6:00 pm, as the residents usually return home from work and begin their routine activities such as cooking, water heating, heating/cooling and so on. A smaller peak of the day occurs at 6:00 am, as the residents wake up and

135

begin their morning activities, such as using the kettle and so on. Figure 36(d) shows the average consumption profile on a 24-hour basis for both Weekdays and Weekends. As it may be observed, the Weekday profile is similar to the profile shown in Figure 36(c), whereas in weekends the high load is maintained between 9:00 am and 8:00 pm. The seasonal load is presented in Figure 36(e), showing that the annual 24-hour average load, as shown in Figure 36(c), exhibits similar patterns with the Winter, Spring and Autumn loads. On the other hand, Summer load is high during early morning, evening and late-night, due to the increased cooling needs, and low during the morning and noon. Such a profile may result to grid instability issues, due to the high PV generation and the low demand. Finally, peak loads for Winter, Spring and Autumn, occur roughly at the same time within the day, but with different magnitudes. The highest mismatch between PV generation and load demand is observed in the Spring, where the large energy exports to the utility grid, due to the high PV generation for a low demand, can lead to instability issues. Hence, the building's self-consumption via storage dispatch can help improve such a situation.

Finally, it is worth mentioning that the total annual load of ~3839 kWh is much lower than the total annual PV production of ~7245 kWh, showing that there is a high generation and load mismatch, resulting to the increased grid export energy. Of course, the correct sizing of the PV system, which is beyond the scope of this work, can be addressed during the design phase, minimizing the levels of such a high surplus energy.

I.4 Artificial Neural Networks[8]

This section mainly focuses on three pillars, concerning ANNs. At the beginning, the basic idea and theory behind ANNs is briefly summarized, followed by a brief explanation of the ANN structure in its simplest form, as well as the different types of ANNs found in literature. Applications of ANNs in concepts such as RES and energy optimization in buildings are presented and discussed along with some related studies found in literature. It is worth mentioning that as the basic theory is not covered in detail, the reader is encouraged to refer in literature for a better and deeper understanding.

I.4.1 History and Basic Background Theory

Artificial Intelligence (AI) constitutes a research area of high interest, for both practitioners and academics, as it is found very useful for solving complex problems that are difficult to solve using known and well developed conventional mathematical methods. Particularly, it can handle problems with large and complex data and provide meaningful results with a very good accuracy at relatively high computational speeds. Simplicity is a valuable feature of AI as it, due to its nature, does not require much information *a priori*, especially in ANNs, to predict the output.

The main idea of ANNs raised from the prototype Mcculloch and Pitts model first published in 1943 [116]. Their study first introduced mathematical models of neurological networks, based on threshold functions. As a result, the calculation of any logic or arithmetic function was made possible [117]. Soon after, researchers proposed different ANN models, each designed for specific applications, resulting to the variety of different ANN types. Nevertheless, the common share between the different ANNs is the calculation of either an arithmetic or a logic value, based on some criteria (aka thresholds).

In general, ANNs try – at a certain extent – to mimic the human brain, as they can learn from real examples. They can handle large and incomplete datasets, which could contain random noise, and after a learning process they can generalise well – especially in non-linear problems. This means that ANNs can learn from example data and

---

[8] Material from published paper [145]

estimate or predict the output from an input never seen before. According to Ding et al. [118], ANNs are non-linear systems and can be characterised as self-adapting, self-organising and real-time learning networks, whose architecture is defined by the connections between the neurons and their transfer functions. Moreover, ANNs are characterised by their fast convergence and fault tolerance as reported by Kalogirou and collaborators [119], [120].

The main idea of ANN rises from two basic functions of a human brain, as those were firstly discovered and identified by William James, an American psychologist, during the 20th century. The first function is when the connection between two neurons grows or strengthens during their simultaneous activation and the second is the action of the neuron itself, which is in turn the sum of its incoming signals that are proportional to the connection strength in which each of the signal travels through. These two important clues were the main reasons for the beginning of the ANN era [121].

ANNs are a branch of AI and are mainly used, but not limited to, for pattern recognition, data clustering, function approximation, data classification, optimisation and time-series forecasting [119], [121], [122]. An ANN is a set of interconnected artificial neurons found in groups (or layers) with the main task to process input data in a feed-forward or recurrent manner and exchange the data between them through the different interconnections, known as weights.

Figure 37 represents the mathematical model of an artificial neuron. Here, x_i (usually real number) represents the i-th input of the input vector x, w_i (real number) is the i-th weight amount of the connection in which the information travels from other neurons connected to this neuron, and θ is constant representing the bias of the neuron, that is the minimum threshold point at which the neuron becomes active. The weights are optimally adjusted during the training (or learning) process to best describe the 'importance' of each connection path between two neurons and, once trained, they remain fixed. The product of each signal along with its weight (i.e. $x_i w_i$) is summed for all inputs x to account for every contribution of the neurons connected to that neuron. Finally, the sum of products is passed to the activation function so as the output becomes $y = f(z)$; where $z = \sum_{i}^{N} x_i w_i + \theta$ and N is the total number of inputs.
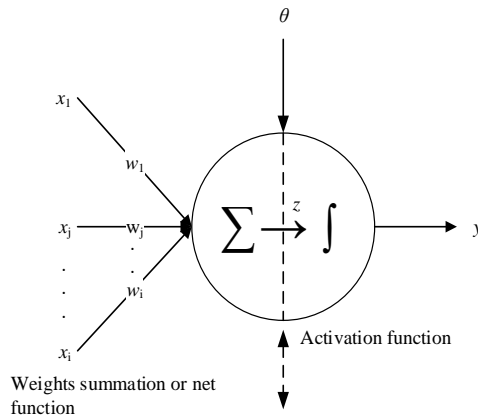
Figure 37: The basic neuron (modified from [8])

There are six continuous activation functions *f* that are commonly used, namely Sigmoid, Hyperbolic Tangent, Inverse Tangent, Threshold, Gaussian Radial basis, Linear and Step/Binary function; for more details and examples see [121], [123]–[125]. Step functions may also be used for problems dealing with binary variables. In such a case, the neuron is called perceptron and is mainly used for data classification problems. The selection of the right activation function clearly depends on the type and complexity of the problem.
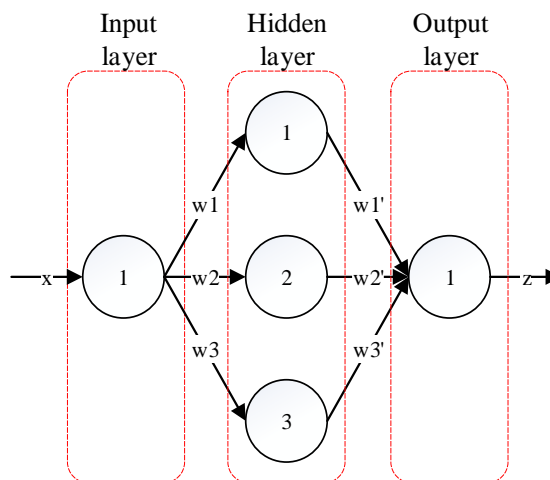

Figure 38: Single input, single output feed-forward ANN network

A simple feed-forward network consisting of one input layer, one hidden layer and one output layer is shown in Figure 38. In this case, the data flows from the input layer towards the output layer, through the available paths, as shown. One can derive the mathematical expression of the example network shown in the figure.

The main goal is to achieve an output value as close as possible to the targeted (desired) one – presented to the network during training – as well as to minimize the error function [123]. Shown in equations (100)–(101) are $E(k)$, the difference (error) between the output value of the k-th neuron and the targeted one, and E, the mean squared error, an assessment of the performance of the network.

$$E(k) = \sum_{k=1}^{N} (t_k - y_k)^2 \tag{100}$$

$$E = \frac{1}{N} \sum_{k=1}^{N} E(k) \tag{101}$$

where:

- t is the target value of the k-th element in the target vector

- y is the output value of the k-th neuron

- N is the total number of inputs presented in the network

With already many algorithms existing, ongoing research is highly focused in developing evolutionary algorithms for minimising the above function E and, thus, improving the overall performance of the network [118], [121]. The minimization of the error is usually based on gradient descent algorithms such as back propagation algorithm, batch learning, online learning and momentum. The latter is used for improving the stability of the learning process, as the weights – during learning – may experience unstable oscillations around the optimisation point and take values far from the optimum ones [121]. Learning of ANNs is a process where the ANN adjusts its weights until the error function E reaches a predefined tolerance. Learning algorithms and techniques of ANNs and types of ANNs are not discussed here.

I.4.2 ANNs for Energy Management and Prediction in Buildings

Various applications for Energy Sources Management, using ANNs exist, since they are used for optimum dispatch schemes in hybrid systems (RES with non-RES) as well as in other non-linear problems of high complexity. Nevertheless, ANNs may also be used for Energy Management in buildings for reducing energy demand, increasing user comfort level and also simplifying/improving non-linear conventional models used in this sector so far. The studies presented in this section, related to the Energy Management in buildings, underline the potential of ANNs.

Liang and Ruxu [126] adopted a direct neural network in their proposed model for thermal comfort and temperature control of a building having a HVAC system. One of the main targets of the authors was to simplify the process and hence use an ANN instead, for controlling the HVAC unit and at the same time keeping both the thermal comfort and the temperature at the desired levels. As a result, the learning rate was the only parameter to be tuned, instead of the many needed when the non-linear analytical model is used. Using a back-propagation algorithm the two-layer network was trained and showed good and similar performance compared to the common PI controller.

Argiriou et al. [127] developed a feed-forward back propagated ANN to control the temperature output of a hydronic heating plant. Their model had forecasting capabilities such as ambient temperature, solar irradiance prediction, indoor temperature prediction and supply temperature predictor, and showed good agreement with the actual readings. The proposed model's main aim was to optimally control the operation of the heating system by using the building's occupancy behaviour, thus avoiding any overheating or underheating of the building during occupancy hours. The authors tested the model in real office conditions and found that – in comparison to a conventional PID controller – the ANN could reduce the energy consumption by an average of 15%, while keeping the user comfort level high. The only problem faced with the ANN was its slow response to changes of the set point temperature defined by the user. This was solved using a trained boost module to overcome the discomfort occurred in the morning hours.

Matallanas et al. [128] proposed an Active Demand Side Management scheme, in a building, with the aid of an intelligent controller using ANNs. The controller was tuned and adjusted by a GA. The building itself had integrated PVs and the main objective of the study was to maximize the consumption of the local PV energy and to reduce both

the energy imported from the grid and the PV energy exported to the grid. At the same time, the user's preferences were respected. The novelty of this system was the interaction of the user with the controller. The user was able to provide the controller with the favoured operation period of each controlled appliance for the next day and, based on the prediction of the PV generation, a decision was made regarding the optimum action of the appliances. Finally, the controller was able to maximize the PV self-consumption by intelligently operate the appliances within the generation period.

Tascikaraoglu et al. [129] used solar radiation and wind speed forecasting along with DSM in a grid-connected Smart Home, in Turkey, with integrated PVs, a wind turbine and a storage system (batteries & electric vehicle). An AI model was developed, capable for predicting wind speed and solar radiation. Their AI model combined the Empirical Mode Decomposition method along with the Cascade-Forward Neural Network. The authors proved that their Home Energy Management System with prediction was capable for reducing electricity bills, shifting the operation of the appliances to off-peak times and also reducing the total shifting time of the controlled appliances for a whole year.

An Adaptative Neural Network Inference System (ANFIS) was proposed by Cardenas et al. [130], mainly for supporting an integrated Energy Management System in industrial plants. The model was capable for predicting the electrical energy consumption and used in an intelligent BEM System for supporting the decision making taken by the BEM system and thus optimizing the energy consumption even further. Due to the complex task of designing and configuring an ANFIS, the authors used a Multi-Objective Genetic Algorithm (MOGA) for the automatic development of the network and the selection and configuration of the various parameters. The authors achieved a very good performance with their proposed model.

Magnier and Haghighat [131] used a GA along with ANN for optimising the energy consumption and the thermal comfort within a building. Feed-forward ANN was used as a Response Surface Approximation model to evaluate the building's performance, and then Non-dominated-and-crowding Sorting Genetic Algorithm II (NSGA-II) was used for finding the optimal solutions, based on the predictions provided by the ANN. Variables such as heating and cooling consumption and PMV were continually predicted by the ANN. The ANN showed a good and accurate performance, resulting to

the significant reduction of the energy consumption within the building. Furthermore, the ANN dramatically reduced the computational time needed for simulations.

Ekici and Aksoy [132] used a back-propagation ANN for predicting the heating energy of three different dwellings. The ANN used three main input parameters of the building in order to predict the heating needs. The average prediction accuracy of the ANN was approximately 98%, which is well within the acceptable levels. The authors mentioned that their proposed model can easily predict the energy needs of any building in different cities.

Gossard et al. [133] used multi-objective optimisation for obtaining the optimum values of thermal conductivity and volumetric specific heat of the external walls. The optimisation target was achieved by minimising both the annual energy consumption and the summer comfort degree, using NSGA-II and a multi-layered feed-forward ANN. The ANN was used for evaluating the cost functions at high speed. A comparison between the ANN predicted results with analytical results showed that ANNs are superior. Finally, the authors could provide the optimum values of the building's envelope in a very efficient way with fast convergence.

Ferreira et al. [134] used Radial Basis Function (RBF) ANNs for controlling the operation of the HVAC systems at the University of Algarve. One RBF ANN was designed for estimating the PMV index and three Model Based Predictive Controllers (MBPC) based on the RBF ANNs were constructed for predicting the air temperature, humidity and global solar radiation. The selection of the parameters of the MBPC networks was based on the MOGA approach. The authors showed that the ANNs were able to accurately predict the required parameters, resulting to an efficient HVAC control, a reduction of the energy consumed as well as the preservation of the PMV at desired levels. A comparison to standard control methods was made showing that energy savings could be even higher than 50%.

Amarasinghe et al. [135] used a feed-forward ANN to control the cooling of a building through a Thermal Storage Tank (TES). The ANN controlled the amount of water extracted from the TES, which was then cooled down by a chiller and was distributed within the building. The inputs provided to the ANN were the building's predicted load of the next time step, the predicted utility load of the next time step, the power availability of the TES, the hour of the day, the day of the week, the ambient

temperature and the averaged room temperature. Using such inputs, the ANN could provide a control signal to the TES resulting to the increase of the energy savings compared to a traditional PD controller.

Ben-Nakhi and Mahmoud [136] used a General Regression ANN (GRNN) to predict the time of the end of thermostat setback of the A/C (HVAC) system in a building, so as to restore the building's temperature at the desired levels, just before the working hours of the building begin. The authors found that the use of a GRNN was superior in comparison to a software using analytical equations for calculating the Equation of State, since the software needed more inputs regarding weather information, resulting to a dropped efficiency. As stated by the authors, GRNN was much better for this case as it was not necessary to know the weather, *a priori*, for predicting the end of thermostat setback.

Gonzalez and Zamarreno [137] predicted the hourly electrical energy consumption in a building using an ANN structure, which used a part of its outputs as feedback, so as to improve learning and accuracy. Two parameters were used as inputs to the network, namely atmospheric temperature end electrical energy. The authors proved the robustness and accurate performance of their proposed model by achieving a Mean Bias Error of 0.0033.

Through the variety of applications reviewed, it is made obvious that ANNs can be applied in many energy related building scenarios such as RES generation prediction, maximisation of the RES self-consumption, DSM schemes, optimization of building design and retrofits, HVAC A/C heating and cooling control and so on, resulting to the reduction of the overall energy consumption of the building. It was shown that ANNs can easily be applied in such scenarios and thus improve the overall energy efficiency of a building leading to a significant reduction in energy consumption and energy bills.

Compared to other conventional methods, ANNs are superior with regard to speed and accuracy. As a result, they are found to be very attractive, especially in scenarios such as building energy prediction and management where many factors (e.g. user's behaviour, building type, building location, climate and so on) affect the prediction accuracy, making it difficult for conventional multivariate models to forecast accurately. Furthermore, ANNs – compared to other conventional models – help reduce the energy consumption due to their robustness, generalisation to scenarios never seen before and

fault tolerance. Finally, ANNs are found useful in building energy applications and applying them in nZEBs remains one of the core ideas of the current research.

I.4.3 A Preliminary Design for PV forecasting and a Base Study Results using ANNs[9]

In Engineering applications, especially in control and prediction, ANNs are mostly favoured due to their fault tolerance, robustness to data errors and noise. Furthermore, such networks converge fast and require less amount of computational effort [119].

A core application of ANNs is forecasting and various attempts have been made from different researchers. Mellit and Alessandro [138] used a multilayer perceptron ANN model to predict the solar radiation on a 24-hour basis. Inputs such as day of month, mean daily solar radiation and mean daily ambient temperature were used. The output layer of the network gave the 24-h forecast of solar radiation. A Cross validation technique was used for designing the optimal model for this case. The authors tested their model on a building having PVs and achieved a Mean Absolute Error of 3–4% approximately. Leva et al. [139] used a feed-forward ANN architecture to predict both the output of a PV plant as well as the solar radiation, using only given weather forecasting data as inputs to the network. The main focus of their study was to analyze and evaluate the effect of an accurate input dataset into the network. Using different error analysis techniques, the authors showed that the output of the network was significantly dependent on the input dataset accuracy as well as on whether the day was either sunny or cloudy. Finally, a real application was carried out and satisfactory results were obtained. Almonacid et al. [140] proposed a nonlinear autoregressive ANN for predicting the output of a PV generator on an hourly basis. Current values of both the global solar radiation and the air temperature were used as inputs to the network. Two separate ANN structures were used for predicting the next hour solar radiation and the ambient temperature. Once the forecasts of both the solar radiation and the ambient temperatures were obtained, another ANN was used to predict the output of the PV system. The model was satisfactorily accurate with an error of 3% approximately. Izgi et al. [141] used a feedforward ANN to determine the most representative time horizon for predicting the PV output of small scale PV systems. They showed that the length of

---

[9] Material from published paper [146]

the time horizon to be used as a forecasting period varied from 3 to 40 minutes, depending on the season. Messabi et al. [142] developed two dynamic ANNs; a Focused Time Delay ANN (FTDNN) and a Distributed Time Delay ANN for predicting the output of a PV system, for a short-term forecasting. The inputs to the network were past values of the output. The authors showed that for multistep prediction the FTDNN model performed better. Capizzi et al. [143] developed a Wavelet Recurrent ANN for predicting a two-day ahead solar radiation. The proposed model performed the prediction in the wavelet domain and then the output signal was obtained using the inverse wavelet transform. With this approach the authors achieved a very accurate result with a network being robust in errors appeared within the input data.

In the sequel of this Chapter, a preliminary ANN model, initially developed, is presented demonstrating the method of forecasting the next day 24-hour PV generation, in a building, using only historical inputs.

I.4.3.1 Methodology

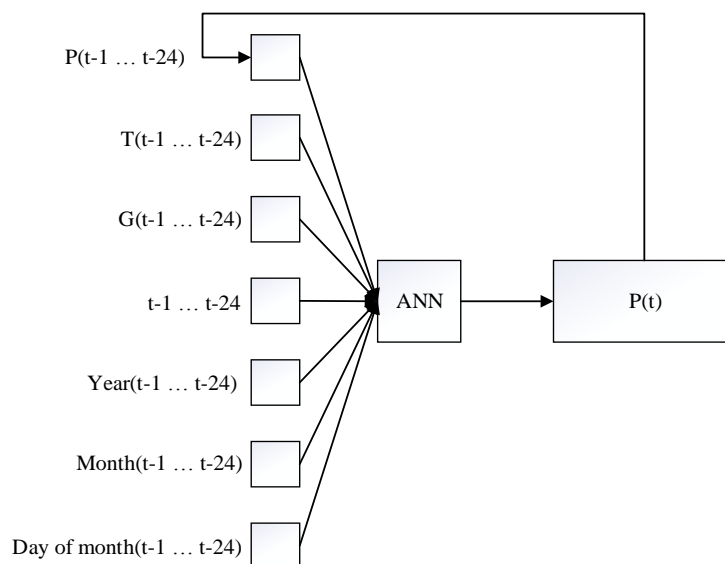A basic ANN model was initially developed, which is shown in Figure 39.

Figure 39: A preliminary design of a NARX Neural Network

This is a non-linear Autoregressive with exogenous inputs (NARX) ANN, which is suitable for time series forecasting. The data available for both training and validation of

the model were taken from a dwelling in Cyprus, having a 5 kWp PV system installed. Hourly measurements for irradiance (G), wind speed (W), ambient temperature (T) and power output of the PV system (P) are used from 1st of March 2015 – 2nd of March 2016, with the 2nd of March 2016 not included in the learning process. This allows testing the network with unseen data. Excel used for storing the data and MATLAB imports it for pre-processing. Specifically, the inputs to the network were the previous daily samples of G, T and P as well as the hour (t), the year, the month and the day of month. The reason of this input dataset selection will be explained in the next sub-section. The targeted outputs were the measured PV power output at the current time t. Thus, the prediction matrix gives the PV power output for the next 24 hours. For instance, when the 2nd of March needs to be predicted, then at time t, the data of the 1st of March will be presented to the network, and so on.

During this preliminary design phase, the main aim was to identify from the given dataset which inputs make the network perform best. For this reason, the default network topology of MATLAB's ANN toolbox was used. Cross-correlation and autocorrelation analysis were performed on the input variables to find which of them correlate with the output and how many previous days from each input variable should be provided to the model.

The data is normalized in the range of [0, 1] and during the learning process, the network receives an input matrix of 7 rows and 8808 columns (367 days x 24 hours) with each row representing an input variable and each column representing the hour of the day. From this data 70% was used for training, 15% for validation and 15% for testing, which is the default of MATLAB's ANN toolbox. An ANN with 1 input layer consisting of total 7 inputs, a hidden layer consisting of 18 neurons having a sigmoid activation function and an output layer with 1 neuron having a linear activation function is used. The training uses the Levenberg-Marquardt back-propagation algorithm and takes less than a minute for the learning process to finish on an Intel i7-7700HQ 2.8 Hz PC with 16 GB of RAM PC.

Before building the input matrix, a cross-correlation analysis along with autocorrelation analysis were performed on the given dataset. This allowed, at a certain extent, to determine the statistically relevant inputs and discard any irrelevant inputs that may worsen the performance of the network. Nevertheless, for the final selection different

combinations of the input variables were contacted. The combination giving the smallest error was selected as will be shown later in this Chapter.

I.4.3.2 Base Study Results

I.4.3.2.1 Cross-Correlation Analysis

Cross-Correlation is a statistical method defining the mathematical relationship between two variables. The more linear the relationship the higher the correlation. MATLAB's built-in function *corrcoef* was used for this analysis with the analysis used mainly for identifying the relationship (correlation) between inputs G, T and W and output P. Since only historical input data are fed to the network, the cross-correlation between previous days of G and T and current P day was also conducted.

Figure 40 shows the cross-correlation between each individual input variable T, G, W and P. As can be seen, P has the highest correlation with G and the lowest correlation with W. The relationship between G and P is (nearly) linear since the correlation between these two variables is 99.05%. On the other hand, T and W have lower correlations and a further error analysis using the trial and error approach was conducted, as it will be shown in a later sub-section of this Chapter.
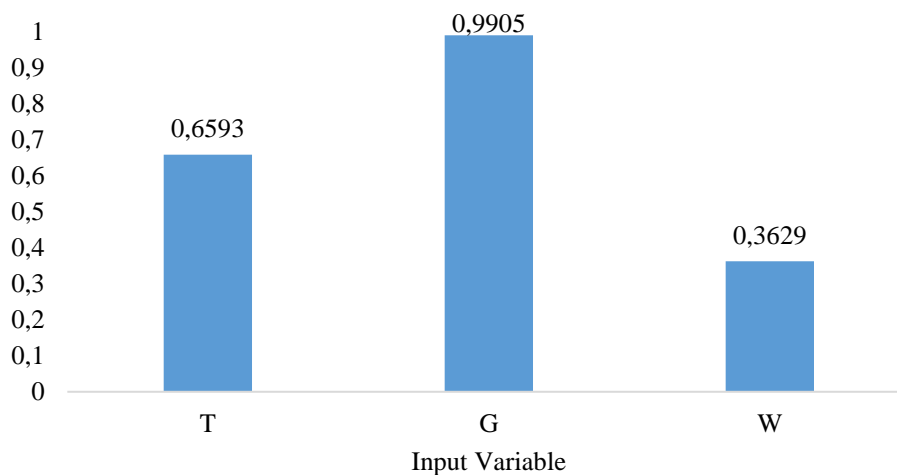

Figure 40: Correlation of P with T, G and W

Finally, the cross-correlation between the historical values of each input variable (e.g. $G(t - n)$) with the current values of PV power output (i.e., $P(t)$) was conducted, so as to

see how the current P values are correlated with historical values of the input variables but also with itself. Again, this was also cross-validated with the aid of the trial and error approach as it is shown later using the Autocorrelation Analysis. The correlation between the historical values for each input variable and P is illustrated in Figure 41. Note that wind speed (W) is not included as its correlation with the PV output is very low (36.29%). As can be seen in the figure, for the three cases of P, T and G the correlation slightly drops with the number of historical days increasing. That is, even if we include the last 10 days within the input matrix (e.g. $P(t-1) \ldots P(t-240)$), there will be no significant change in the ANN output, as the correlation between historical days and the present day slightly drops.
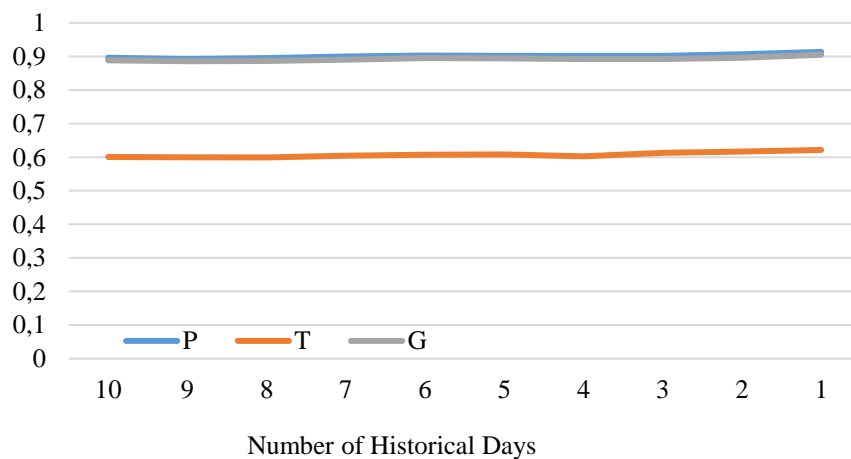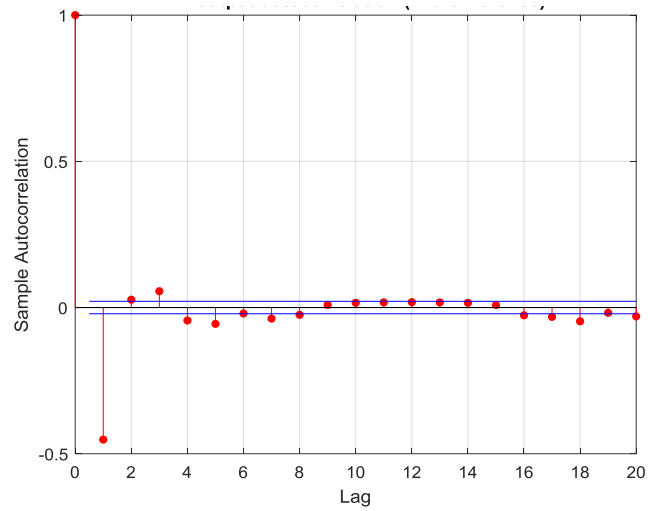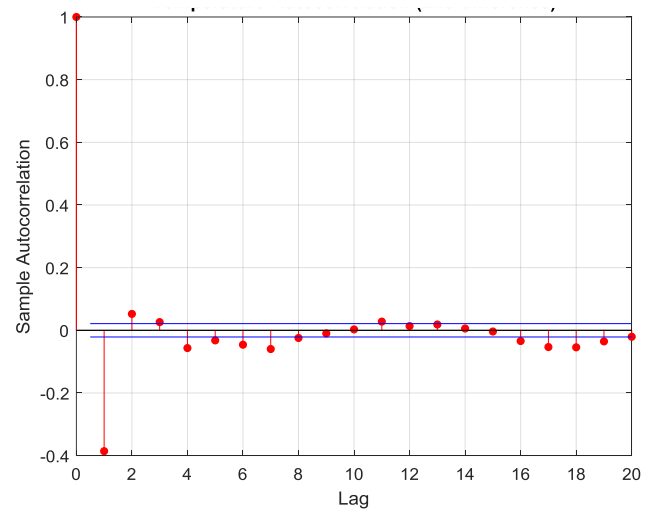

Figure 41: Correlation vs Historical Days

I.4.3.2.2 *Autocorrelation Analysis*

Autocorrelation analysis is another statistical method able to determine the correlation of a variable with its previous values when this variable changes in time. This analysis is similar to the approach shown in Figure 41 and is commonly used in time-series analysis. MATLAB's built-in function *autocorr* was used for this analysis. Applying autocorrelation in this case, allows the determination of the number of historical days to be included in the ANN input matrix.

(a)

(b)

Figure 42 shows the sample autocorrelations for P, T and G, respectively. Each lag, except lag 0, corresponds to a previous value – i.e., a historical day. Obviously, the highest correlation is obtained at Lag = 0, as this is the correlation between the 1st entry and the 1st entry – i.e., the present day with itself. As the number of Lag increases the correlation decreases. For instance, at Lag = 1 (i.e., the previous day) the second highest correlation occurs, meaning Lag 1 is highly correlated to Lag 0. After Lag 1 the correlation dumps, in an oscillatory manner, to the value of 0. This indicates that, for the three variables, there is no need to use more historical days than the previous day. This was also confirmed with Figure 41 in the Cross-Correlation Analysis.
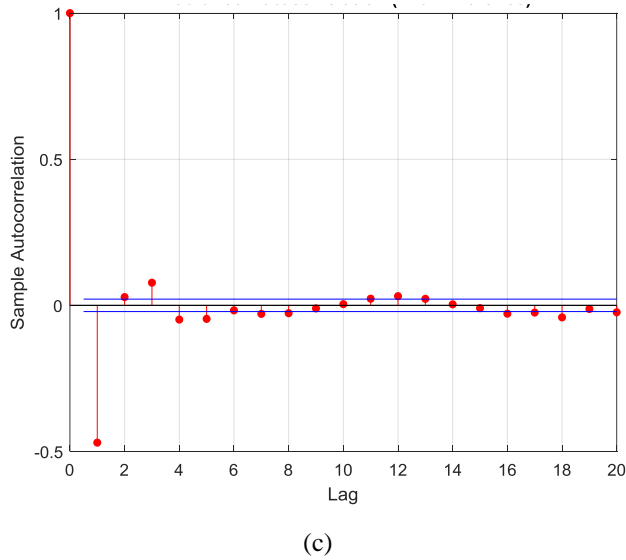
(c)

Figure 42: (a) PV power output (P) autocorrelation**,** (b) Temperature (T) autocorrelation, (c) Irradiance (G) Autocorrelation

I.4.3.2.3 Trial and Error Approach

A trial and error approach was conducted for different case scenarios, so as to find which combination of the input variables gives the best performance for the ANN. The selection criterion used here was based on the Mean Squared error (MSE), which is defined as:

$$E = \frac{1}{N} \sum_{t=1}^{N} \left[P(t)_a - P(t)_p \right]^2 \tag{102}$$

where:

- N is the number of hours

- t is the current hour

- P_a is the actual (measured) PV power output at time t and P_p is the predicted PV power output at time t.

The actual data used in this case was the 24 different measured values of the PV power output for the 2nd March 2016. As a first approach, 7 past days were included in the input matrix with 9 different scenarios been attempted, as shown in Table 11. This table

shows how the most appropriate inputs were selected, based on the performance of an ANN with 1 input neuron, 10 hidden neurons and 1 output neuron.

Table 11: Different scenarios attempted for selecting input variables

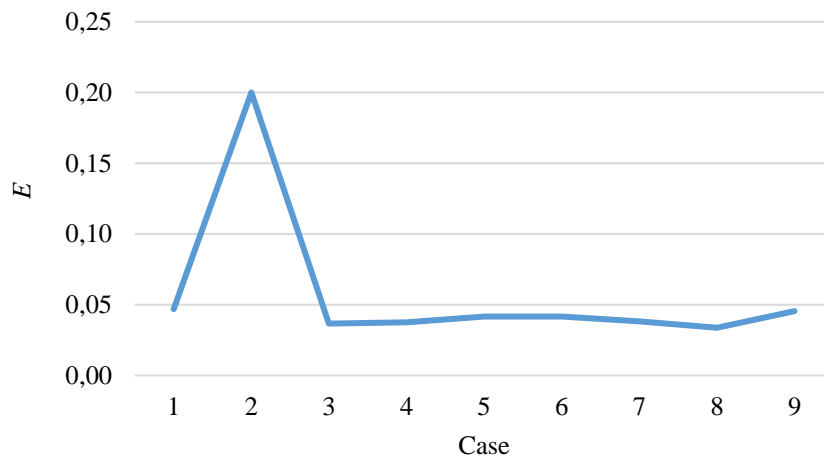| Case	Historical Days	Inputs								Number Of Neurons	E
		P	T	G	W	Year	Month	Day	Hour		
1	7	✓				✓				10	0.0468
2	7	✓				✓				10	0.2000
3	7	✓				✓	✓			10	0.0366
4	7	✓				✓	✓	✓		10	0.0375
5	7	✓				✓	✓	✓	✓	10	0.0417
6	7	✓				✓	✓	✓	✓	10	0.0416
7	7	✓				✓	✓	✓	✓	10	0.0383
8	7	✓		✓		✓	✓	✓	✓	10	0.0337
9	7	✓	✓	✓	✓	✓	✓	✓	✓	10	0.0455

Figure 43: Error minimization based on input variable selection (7 days used as historical data for P, G and T)

The error reduction can be seen in Figure 43. The most appropriate inputs were selected based on the combination with the lowest error value obtained from the table and figure

above. Obviously, it is scenario 8 that should be selected, with the input variables to the network being P, G, Year, Month, Day and Hour (t). It should be noted that the results are indicative as for each training process the numbers are different, due to the different network behaviour. Nevertheless, the error reduces in a similar manner, if the same trial and error approach is followed.

Similarly, a second approach was attempted for selecting the number of the previous days that give the lowest error and which will be included in the input matrix. Ten different scenarios with the same ANN as in the previous approach were used – 1 input neuron, 10 hidden neurons and 1 output neuron. The results are shown in Figure 44. As can be seen, Scenario 1 gives the best performance, meaning that only the previous day of P and G should be included in the input matrix.
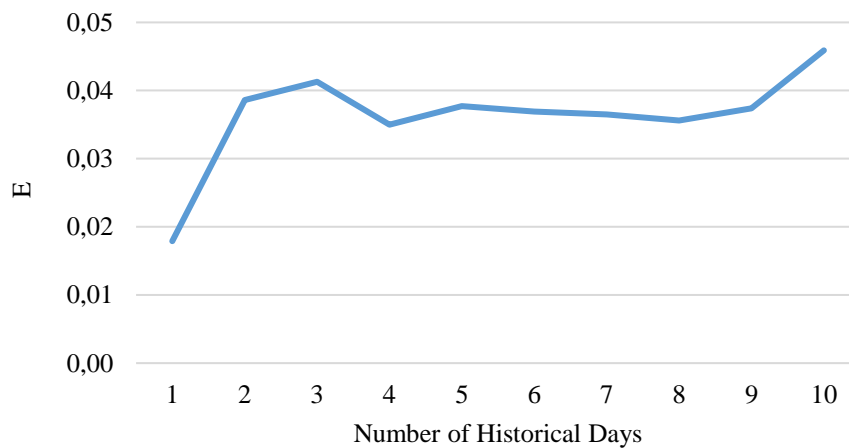

Figure 44: Error minimization based on number of previous days (P, G, Year, Month, Day and Hour as inputs)

A third and final approach, similar to the two shown before, was attempted for selecting the most appropriate number of neurons, giving the best performance. It was found that the error is minimized with the increase in the number of hidden neurons. However, from a certain number and above the error increases again. The minimal error was achieved with 18 neurons with the results shown in Figure 45.
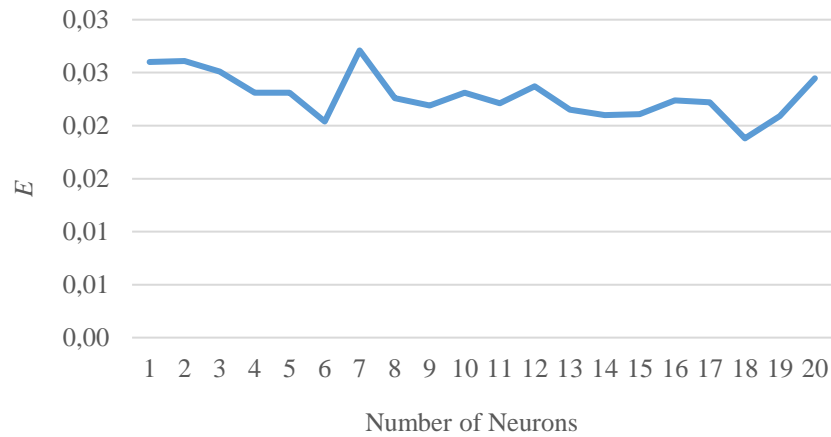
Figure 45: Error minimization based on number of neurons (1 day used as historical data for P and G along with Year, Month, Day and Hour as inputs)

Using this methodology, the final input matrix was built, and the most appropriate number of hidden neurons was selected. Using these results, the final ANN structure (NARX model) can be seen in Figure 39 with 7 input neurons, 18 hidden neurons with a sigmoid activation function and 1 output neuron with a linear activation function. The overall performance of the network gives a (normalized) MSE of 1.4% approximately. for a cloudy day and an overall correlation of 99%. The prediction of the ANN for the 2nd March of 2016 can be seen in Figure 46.
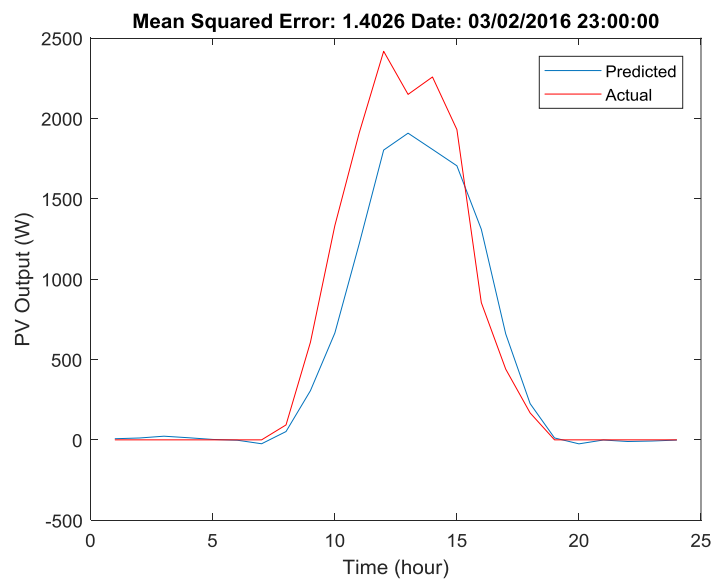

Figure 46: 24-hour forecasting of PV power output on 2nd March 2016

As mentioned at the beginning of section I.4.3.1, this preliminary design phase of the project had the main target of finding the input variables giving the best network performance, so as less complicated datasets can be used. This will result in the use of a reduced instrumentation for weather monitoring such us humidity, temperature, wind speed measuring, and so on. Using as fewer external input variables as possible allows the maximum utilization of a standard and less complicated dataset (e.g. P and G) resulting to a reduced computational effort and total cost reduction. Obviously, this result can be improved for reducing the MSE and increasing the overall correlation between the predicted and actual data.

APPENDIX II – Publications

1. Georgiou, G. S., Nikolaidis, P., Christodoulides, P., & Kalogirou, S. A. (2020). A hybrid optimization approach for autonomy enhancement of nearly Zero Energy Buildings based on battery performance and Artificial Neural Networks. *Energies*, 13(14)

2. G. S. Georgiou, P. Christodoulides, and S. A. Kalogirou. (2020), "Optimizing the energy storage schedule of a battery in a PV grid-connected nZEB using linear programming," *Energy*, vol. 208, p. 118177, 2020, doi: https://doi.org/10.1016/j.energy.2020.118177.

3. Georgiou, G. S., Christodoulides, P., & Kalogirou, S. A. (2019). Real-time energy convex optimization, via electrical storage, in buildings–A review. *Renewable Energy*, *139*, 1355-1365

4. Agathokleous, R., Bianchi, G., Panayiotou, G., Aresti, L., Argyrou, M. C., Georgiou, G. S., ... & Christodoulides, P. (2019). Waste Heat Recovery in the EU industry and proposed new technologies. *Energy Procedia*, *161*, 489-496

5. Georgiou, G. S., Nikolaidis, P., Lazari, L., & Christodoulides, P. (2019). A Genetic Algorithm Driven Linear Programming for Battery Optimal Scheduling in nearly Zero Energy Buildings. In *2019 54th International Universities Power Engineering Conference (UPEC)* (pp. 1-6). IEEE

6. Georgiou, G. S., Christodoulides, P., & Kalogirou, S. A. (2018). A Neural Network Approach for short-term forecasting of PV Generation in Dwellings. In *2018 53rd International Universities Power Engineering Conference (UPEC)* (pp. 1-6). IEEE

7. Georgiou, G. S., Christodoulides, P., & Kalogirou, S. A. (2018). Implementing artificial neural networks in energy building applications—A review. In *2018 IEEE International Energy Conference (ENERGYCON)* (pp. 1-6). IEEE

8. Panayiotou, G. P., Bianchi, G., Georgiou, G., Aresti, L., Argyrou, M., Agathokleous, R., ... & Christodoulides, P. (2017). Preliminary assessment of waste heat potential in major European industries. *Energy Procedia*, *123*, 335-345

9. Georgiou, G. S., Christodoulides, P., Georgiou, A., & Kalogirou, S. A. (2017). A linear programming approach to the optimal utilization of renewable energy sources

in buildings. In *2017 52nd International Universities Power Engineering Conference (UPEC)* (pp. 1-6). IEEE

10. Georgiou, G. S., Christodoulides, P., Kalogirou, S. A., & Florides, G. A. (2016). Optimal utilization of Renewable Energy Sources in nearly Zero Energy Buildings– A review, In *The 5th International Conference on RES&EE - New Challenges*, Nicosia, Cyprus

11. Georgiou, G. S., Christodoulides, P., Kalogirou, S. A., Florides, G. A., & Lazari, L. (2016). A preliminary design of an intelligent system for the optimal utilization of renewable energy sources in buildings. In *The 26th International Ocean and Polar Engineering Conference*. International Society of Offshore and Polar Engineers